Università degli Studi di Napoli “Federico II”

Scuola Politecnica e delle Scienze di Base
Area Didattica di Scienze Matematiche Fisiche e Naturali

Dipartimento di Fisica “Ettore Pancini”

Laurea Magistrale in Fisica

Leggett-Garg’s inequalities and quantum annealing

Relatori:
Prof. Giulio De Filippis
Dott. Procolo Lucignano
Prof. Arturo Tagliacozzo

Candidato:
Vittorio Vitale
Matricola N94/350

A.A. 2016/2017

Contents

List of Figures

Introduction

Adiabatic quantum computing relies on the idea of embedding a hard optimization problem into a physical system, whose ground state contains its solution. In principle any quantum algorithm can be run on a adiabatic quantum computer, however the interest of the scientific community is focused on optimization problems which are very difficult to handle on classical computers. It can be shown that hard optimization problems can be mapped onto complex many body hamiltonians, thus they are also of interest from the point of view of fundamental physics. Recent experimental progress has resulted in quantum annealers operating on hundreds of qubits. Studying the quantum properties of these devices has renewed dramatic interest and debate in this rapidly growing area. Our work is placed in this context and has been driven mainly by two questions:

- Since quantum devices are influenced by their environment, do commercial quantum annealers exploit quantum features? To what extent one can ignore the decoherence and thermalization process due to the environment?
- How is it possible to check the *quantumness* of a system that performs quantum annealing?

In order to answer to these questions, we will introduce the study of the *Leggett-Garg's inequalities*, which Leggett and Garg developed in 1985, interested in how one could demonstrate the presence of the quantum coherence of a macroscopic quantum system. Leggett-Garg's inequalities are Bell's-like inequalities in time and predict anomalous values for some correlation functions that are only possible if the system behaves according to quantum mechanics. They also provide sharp bounds for classical correlation functions.
In this work we will not focus on the multiple features of quantum annealing, but we are going to introduce its concept and its main properties and discuss the adiabatic evolution of a single two-level system in interaction with its environment. We are motivated to study this simple system by the difficulty of calculating

the Leggett-Garg's inequalities during the annealing dynamics, which cannot be done by projective measurements due to the fact that they destroy the adiabatic evolution of the system. Indeed, since the solution of the optimization problem is stored in the lowest energy configuration of the system, any projective measurement is detrimental for the adiabatic quantum computation. For this reason, we will introduce the problem of the *weak measurements* and we will look for a method to evaluate the Leggett-Garg's inequalities during the adiabatic quantum dynamics without causing a lost in the reliability of the outcome. Finally we will show an approach to take into account the presence of a dissipative environment and analyse the case of a single qubit performing quantum annealing.
The outline of the work is the following:

In the first chapter we will provide to the reader a summary of the whole work in order to describe the main result obtained and how we got them. Here we will introduce only the fundamental notions of the tools used throughout our work and we will keep trace of the different topics reminding the reader to a deeper explanation in the other chapters.

In the second chapter we will introduce the concept of quantum computation making a comparison between the circuit model and the adiabatic quantum computation. Then, we will describe the idea of the quantum annealing and the problems it may arise.

In the third chapter we will derive the Leggett-Garg's inequalities starting from the assumptions of Leggett and Garg, that point out our understanding of how macroscopic world works. Then we will describe the useful example of a single qubit and discuss the problem of the projective measurements from the point of view of the quantum annealing.

In the fourth chapter we will focus on weak measurements and on a method to evaluate the correlation function with repeated measurements which do not modify the system dynamics.

In the fifth chapter we will derive an approach for solving the dynamics of a system coupled to a thermal bath, which we will suppose to be an ensemble of harmonic oscillators (phonons), and we will obtain a master equation for the density matrix in the Lindblad form.

In the sixth chapter we will, finally, discuss the problem of a single qubit in the presence of dissipation. We will check the *quantumness* of the system making use of the Leggett-Garg's inequalities and discuss the result obtained.

Chapter 1

Motivations and results

The research about quantum computing, and particularly about adiabatic quantum computation (ADQ), has received a strong boost due to the official presentation of the first commercial quantum annealer produced by the D-WAVE company [8]. Since the realization of the D-WAVE annealer, many physicists questioned themselves about whether or not the system was actually performing quantum computing, inquiring about the presence of entanglement and the role of decoherence during the annealing.
Stimulated by the latter point, we started our work to understand whether one could test the "quantumness" of the evolution of a system and what estimators could be used as witness of quantum coherence.
In this thesis we study the quantumness of the evolution of a simple qubit in interaction with a dissipative environment during the annealing dynamics.
In order to provide to the reader an extended summary of our research, in this chapter we are going to illustrate the whole work in a few steps recalling the main observations and results obtained. With this in mind, we will show only the fundamental notions of the concepts that we will use in the following and we remind the reader to a deeper reading of the whole thesis for a more comprehensive explanation.

1.1 Quantum annealing

Quantum annealing (QA) is a technique for solving optimization problems which is the quantum counterpart of the classical *thermal annealing* [5]. It is a lively topic of study partly because the AQC is considered a valide alternative to the standard circuit model of quantum computation (described in sec 2.1) and partly because, in the last years, commercial devices are claimed to work exploiting the principles of QA.

The idea of QA and, then, of AQC is to perform a slow evolution of a system from the ground state of a simple Hamiltonian, of which we have complete knowledge, to the ground state of an Hamiltonian which encodes our optimization problem. Optimization and decision problems are hard task for classical computers because their computation time grows exponentially with the number of elementary units that constitute the system under investigation. Final Hamiltonians are themselves difficult to be solved. Typically, they are Ising Hamiltonians that, due to frustration effects, are very hard to handle. Therefore QA is relevant also from the point of view of fundamental physics.
The slow variation from a Hamiltonian to the other, can be done using any annealing schedule, namely changing the functional dependence on time of the time-dependent Hamiltonian which describes the system. The simplest one uses a linear schedule like

$$H(s) = (1-s)H_0 + sH_I \tag{1.1}$$

where $s = t/t_f, s \in [0,1]$ and t_f is called *annealing time*, H_0 is the starting Hamiltonian and H_I is the Hamiltonian which encodes our optimization problem. This is, also, the one that we will use throughout this work.
The adiabatic theorem (described in appendix D) guarantees that the system will remain in the ground state of the Hamiltonian $H(s)$ at each given time if the, so called, adiabatic condition is satisfied:

$$\max_{s\in[0,1]} \frac{|\langle k(s)| \partial_s H |k'(s)\rangle|}{t_f \Delta_{kk'}^2} \ll 1, \tag{1.2}$$

where $|k(s)\rangle$ are the eigenvectors of the Hamiltonian $H(s)$ corresponding to the eigenvalues $E_k(s)$, and $\Delta_{kk'} = E_k(s) - E_{k'}(s)$. This condition constraints the choice of the speed of the evolution and, practically, the choice of the annealing time t_f. Anyway, especially for large spin ensembles, the energy gap between the ground state and the first excited state can become quite small during the evolution, and non adiabatic energy level transitions called *Landau-Zener transitions* can happen [10].
Different control parameters can be defined in order to evaluate the distance of the final result from the exact one. For example, in this work, we consider the *residual energy* which is the difference from the energy of the system at the annealing time t_f and the one of the ground state of H_I: of course in the case of $t_f \to \infty$ it tends to zero.

$$\epsilon_{\text{res}}(t_f) = \frac{1}{N}(\langle\psi| H(t_f) |\psi\rangle - E_0(t_f)). \tag{1.3}$$

Even if the adiabatic condition is satisfied, a number of problems may arise in practical implementation of a quantum annealer. For instance, the detrimental

effect of the environment may cause loss of coherence and the thermalization of the system may populate the energy eigenstates according to the classical Boltzman distribution.
Thus a fundamental issue is how to define if the annealing is quantum or classical. With this in mind, in order to perform a test of the quantumness of the evolution of a system during the quantum annealing we developed the formalism of the Leggett-Garg's inequalities (LGIs) which are Bell's-like inequalities in time.

1.2 LGIs and weak measurements

For briefness we recall here the postulates at the base of the LGIs, Ref.[13]:

A: **Macroscopic realism per se**. A macroscopic object which has available to it two or more macroscopically dinstinct states is, at any given time, in a definite one of those states.

B: **Non-invasive measurability**. It is possible in principle to determine which of these states the system is in, without any effect on the state itself or on the subsequent system dynamics.

C: **Induction**. The properties of ensembles are determined exclusively by intial conditions (and in particular not by final conditions).

Starting from these points, encoding how we expect macroscopic objects to behave, one can demonstrate that some classical correlation functions of the system must satisfy certain constraints. These constraints may be written as inequalities that depend on the number of measurements perfomed on the system during its evolution. We will take into account only the *third-order Leggett-Garg's inequalities* which means that we will suppose to perform only 2 measurements during the evolution.
Denoting with Q a dichotomic variable of the system which can assume value $+1$ or -1, we can define a two points correlation function as

$$C_{ij} = \sum_{Q_i, Q_j = +,-1} Q_i Q_j P_{ij}(Q_i, Q_j), \tag{1.4}$$

where $Q_i = Q(t_i)$ stands for the measured value of the observable Q at time t_i, $P(Q_i, Q_j)$ is the probability of obtaining the results Q_i and Q_j and its subscripts remind us the times at which the measurements are perfomed.
Following Ref.[14], assumptions A and B help us to simplify the expression of C_{ij} as $C_{ij} = \langle Q_i Q_j \rangle$ (see chapter 3) so that we can derive the third-order LGIs:

$$-3 \leq K_3 \leq 1; \quad K_3' \equiv C_{12} + C_{23} - C_{13}, \tag{1.5a}$$

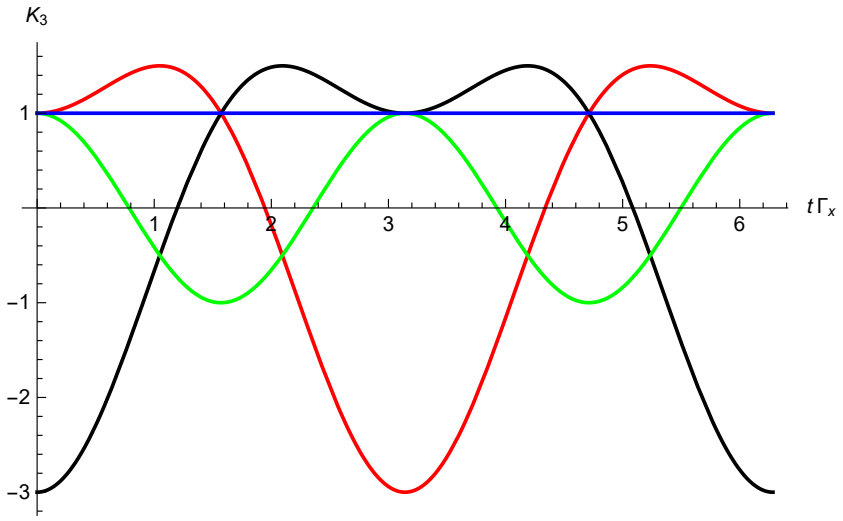

Figure 1.1: Plot of the third-order Leggett-Garg's functions in function of the time difference between two subsequent measurements. The curve in red shows the quantity K_3 , the black and green ones show the quantities K_3' and K_{3perm}, respectively. A violation of the Leggett-Garg's inequalities occurs when one of the functions take values greater than 1. The bound is enlightened by the blue line.

$$-3 \leq K_3' \leq 1; \quad K_3' \equiv -C_{12} - C_{23} - C_{13}, \tag{1.5b}$$

$$-3 \leq K_{3perm} \leq 1; \quad K_{3perm} \equiv -C_{12} + C_{23} + C_{13}. \tag{1.5c}$$

The functions K_3,K_3' and $K_{3\text{perm}}$ are usually called Leggett-Garg's functions. In order to give a quantitative understanding of how LGIs work we here describe a simple case of a single $1/2$-spin evolving under the Hamiltonian $H = \Gamma_x S_x$. In this case, considering the choice $\hat{Q} = \sigma_z$ as dichotomic observable, the correlation function C_{ij} assumes a simple analytical expression

$$C_{ij} = \cos\Gamma_x(t_j - t_i). \tag{1.6}$$

where $\hbar = 1$. Since C_{ij} depends only on the difference between the times at which the measurements are performed, in Fig.1.1 we plot the functions K_3, K_3' and $K_{3\text{perm}}$ with respect to $t = t_j - t_i$. It is evident that the evolution of the system is quantum because at least one inequality is violated at any given time. Since a LG's violation at any time is not verified for every choice of the Hamiltonian H, one usually takes into account only the function K_3 and studies its behavior. In the absence of decoherence, indeed, it must periodically exceed 1 during the evolution providing a way to assess the quantum behavior of the system.

However, if we want to analyse a system which is evolving adiabatically, correlation functions and average values cannot be taken using projective measurements

because they strongly perturb the system projecting the state of the system onto the subspace of the measured observable.
In order to circumvent this problem, first of all, one could think about measuring just a small part of the entire system. We may build the LGIs function starting from the correlation function of an observable of the subset, which encodes the behavior of the whole ensemble. Anyway this may not leave unchanged the evolution of the system, if it is small in size.
On the other hand considering a large system is a hard challenge from a computational point of view, because the dimension of the Hilbert space grows as 2^N where N is the number of bits (or spins) which constitute the system. Altough it could be useful in order to make "less relevant" the measurements on a single qubit, this approach is impossibile to manage except for cases with particular symmetries.
If we think about weakening the interaction between a spin and the rest of the ensemble to uncouple the two subsets we may incur in another problem. Taking into account very weak couplings, the calculation of the LGIs might become useless. Indeed we cannot be fairly sure that the LGIs provide a comprehensive description of the entire ensemble.
Another idea, could be performing ideal negative measurements: unfortunately one can demonstrate that, altough it seems non-invasive, because it does not change the eigenstates populations, it is detrimental for the coherences between the eigenstates. This is shown in section 3.3.2.

In this work we present a new way to calculate the LGIs, generalising a method described in Ref.[36], based on weak measurements.
Let us consider a two-level system (qubit), realized by a double quantum dot (DQD). An electron in the DQD can occupy the dot number 1 or number 2. We describe this possibility by a spin degree of freedom, saying that if $\sigma_z = 1$ the electron is in the dot 1 and if $\sigma_z = -1$ it is in the dot 2. As shown in Fig.1.2, we assume that the DQD is capacitively coupled to a quantum point contact (QPC). The current flowing through the QPC depends on the position of the electron in the DQD and assumes different values, say I_1 or I_2, whether the electron resides in the first or in the second quantum dot, respectively. It is then a dichotomic variable and it can be used to measure the state of the qubit and to evaluate the Leggett-Garg's inequalities. Indeed, it can be mapped onto a dimensionless variable x, which assumes only values ± 1, considering the relation

$$I = \frac{I_1 + I_2}{2} + x\frac{(I_1 - I_2)}{2}. \tag{1.7}$$

To keep trace that we are measuring the current, in the following we will use I instead of x and we will consider the possible outcome of I the values $I_1 = 1$

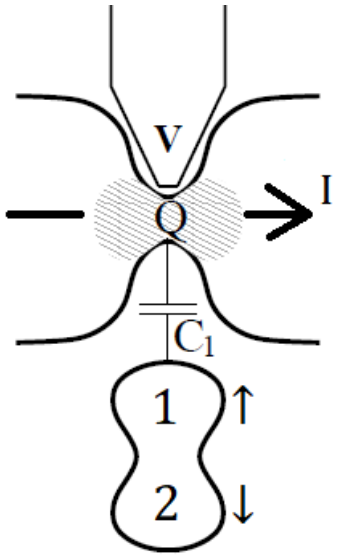

Figure 1.2: Diagram of the measurement apparatus. A double quantum dot is capacitively coupled to a quantum point contact (QPC). The current flowing through the quantum point contact depends on the position of the electron in the double quantum dot. The current across the QPC is switched on and off with the help of a gate voltage V [34].

and $I_2 = -1$. As in Ref.[37], we propose to measure the current flowing through the QPC sending short voltage pulses and recording the outcoming current. If the pulses last less than the typical time of measurement needed to distinguish between the two outcomes I_1 and I_2 (which is the time for which the signal-to-noise ratio is close to unity [38]), one cannot establish with certainty which is the state of the system, namely the position of the electron in the DQD. Therefore if the interaction between the measuring set-up (QPC) and the system (DQD) is very short or weak, one has to consider the value of the current as distributed according to a certain probability distribution

$$P(I) = \rho_{11} P_1(I) + \rho_{22} P_2(I). \tag{1.8}$$

Here we have imposed that I is normally distributed, centered around the two values it could assume in the case of projective measurements (-1,1), with a variance D inversely proportional to the pulse lenght τ_v. The quantities ρ_{11} and ρ_{22} are the diagonal elements of the density matrix ρ of the DQD.
If one takes into account this approach, it is possible to calculate analitically how the measurement of the QPC influences the DQD. Indeed, the update rule of the density matrix describing the DQD becomes very simple and it is evident that the shorter is the pulse, the less the system is perturbed, as explained in chapter

4. The density matrix ρ' after the measurement is related to the one before the measurement ρ by the following equation:

$$\rho' = \frac{1}{\rho_{11}e^{\gamma} + \rho_{22}e^{-\gamma}} \begin{pmatrix} \rho_{11}e^{\gamma} & \rho_{12} \\ \rho_{12}^{*} & \rho_{22}e^{-\gamma} \end{pmatrix}, \tag{1.9}$$

where $\gamma = I/D$.
In order to extract meaningful information on the qubit, one must repeat the same measurement multiple times and evaluate the current as the average of the different results.
To check the validity of our adiabatic evolution, we can study the residual energy. We remind the reader that considering a simple qubit schematised by a DQD and measuring the current flowing through the QPC is equivalent to measure the dichotomic variable σ_z of a spin $1/2$, because the flowing current depends only on the position of the electron in the double quantum dot.
In Fig.1.3 we see the behaviour of the residual energy of the system in the case of the annealing dynamics of a single qubit described by the Hamiltonian

$$H(s) = (1-s)\frac{\Gamma_x}{2}\sigma_x + s\frac{\Gamma_z}{2}\sigma_z. \tag{1.10}$$

We set $\Gamma_x = \Gamma_z = 1$GHz, as in Ref.[39], and express all the energies in units of Γ_x and the times in units of $1/\Gamma_x$ ($\hbar = 1$). The value of the residual energy at $t_f = 10\sqrt{2}$, when no measurement is perfomed, is approximately $\epsilon_{\text{res}} = 5 \cdot 10^{-4}$. This result is in agreement with Ref.[39]. When we perfom a measurement, the residual energy approaches the unperturbed case by weakening the interaction, that is increasing the variance D.
For each choice of the variance D the simulation is repeated for different values of the time at which the measurements are perfomed. The results are derived repeating the evolution 10^4 times and verifying that increasing the number of repetitions does not affect the outcomes.
In Fig.1.4 we show the uncertainty on ϵ_{res} (curve in blue) normalized by the value of ϵ_{res} obtained for $N = 10^5$. D is D=50 and the time at which the measurement is performed is $t = 3.3$ in units of $1/\Gamma_x$.
The plot shows that the points follow the curve $1/\sqrt{N}$. Already for $N = 10^4$ the error is very small and we may be fairly sure that the value of the residual energy obtained is reliable. In the same plot there is also a curve in red which shows the error on the function K_3 of which we will talk later.
As shown in Fig.1.3, ϵ_{res} is small enough to guarantee the right convergence of the system energy to the target ground state, already for $D \approx 20$. Hence we choose D=50 for all the following simulations.

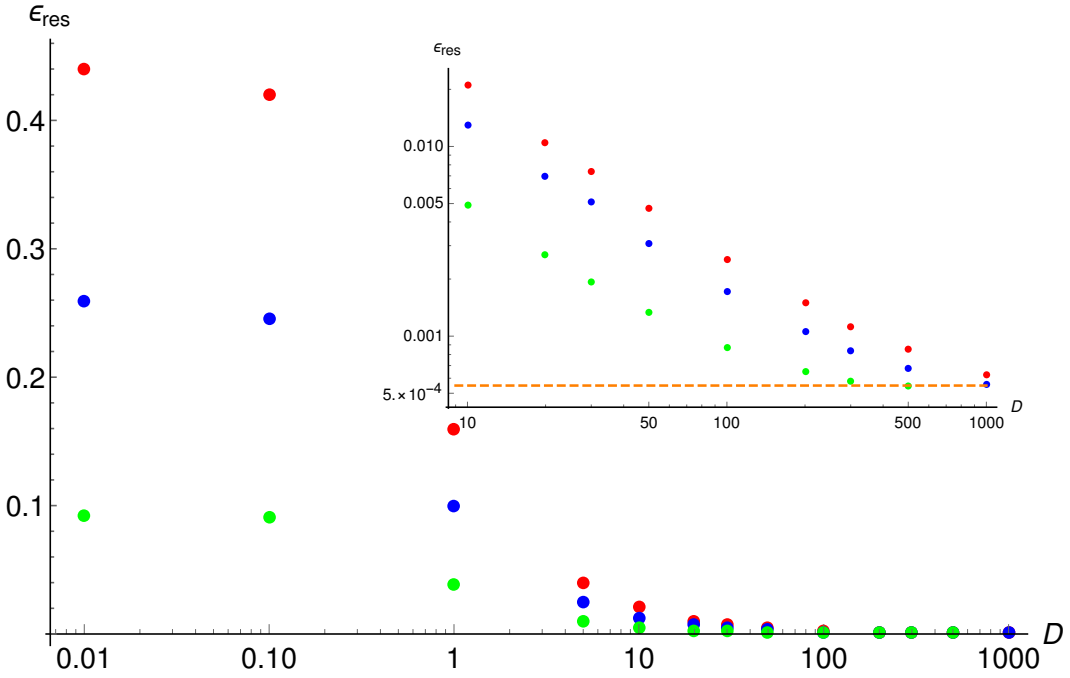

Figure 1.3: Log-linear plot of the residual energy of the system as a function of the variance D and of the measurement time t. We set $t_f = 10\sqrt{2}$; a single measurement has been performed per run at times 0.3 t_f, 0.5 t_f and 0.7 t_f (red, blue, green).

- Red, 0.3 t_f,
- Blue, 0.5 t_f,
- Green, 0.7 t_f.

We observe that the residual energy decreases eventually going to $5.49 \cdot 10^{-4}$ which is the residual energy of the system in the absence of interaction. The inset shows the trend in the interval $D \in [10, 10^3]$ in bilogarithmic scales highlighting the value $5.49 \cdot 10^{-4}$ with a dashed orange line.

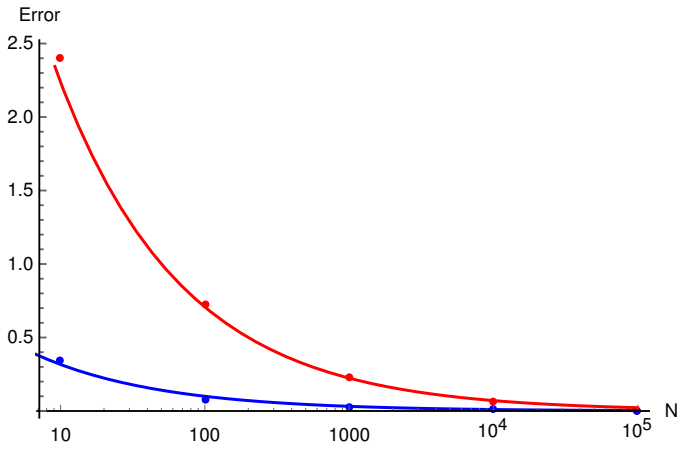

Figure 1.4: Log-linear plot of the errors on the residual energy and on K_3. We fix D=50 and evaluate σ_{K_3} and $\sigma_{\epsilon_{\text{res}}}$ for different values of N. The time difference t is fixed as $t = 3.3\ 1/\Gamma_x$. The errors obtained are normalized by the value of ϵ_{res} and K_3 obtained with $N = 10^5$. We show in red the error on K_3 and in blue the one on ϵ_{res}. The curves are guides for the eyes while the points are the ones simulated.

1.3 Results

First of all, let us simulate the evolution of the qubit in the case of a closed system, i.e. without interaction with the environment, and let us calculate the Leggett-Garg's functions during the annealing dynamics. This is important as starting point to demonstrate that the LGIs provide information about the quantum behavior of the system in the absence of interaction and to compare it with the outcomes in the case of coupling with a source of decoherence.
In Fig.1.5 we see that the function K_3 is above the unitary "classical" bound at the annealing time t_f. In the following we will consider only the function K_3 to assess the behavior of the system at $t \approx t_f$. The curves are guides for the eyes, while the points are the ones computationally simulated. The LGIs functions are plotted with respect to the difference time between two measurements, thus the value $t = 5\sqrt{2}$ corresponds to a final measurement at time $t = t_f = 10\sqrt{2}$.
We have taken into account $t_f = 10\sqrt{2}$, because for this choice of the annealing time the qubit dynamics is adiabatic as shown by the ground state population, approximately equal to one, and by the residual energy $\epsilon_{\text{res}} \approx 5.4 \times 10^{-4}$ (see chapter 6). Our results are in agreemeent with Ref.[39].
In Fig.1.4 we depict in red the error on K_3 at a given time t=3.3, obtained considering the previous choice of t_f. It is calculated considering the standard deviation of the results of the different simulations and normalizing it dividing by the value of K_3 at t=3.3 in the case of $N = 10^5$ runs. We observe that for

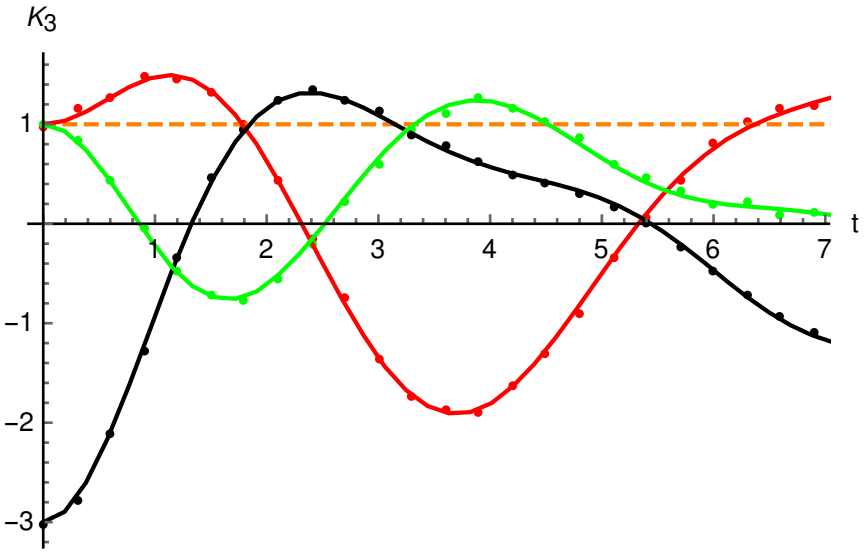

Figure 1.5: Plot of the Leggett-Garg's, without coupling to a thermal bath. The curves are the ones obtained performing projective measurements. The points are the values calculated with our method, considering D=50 and N=10^5. K_3 in red, K_3' in black and K_{perm} in green. The orange line highlights the bound of the LGI. Here $t = t_2 - t_1 = t_3 - t_2$, $t \in [0, t_f/2]$.

K_3 is necessary a greater number of repetitions to get the same confidence on the results with respect to ϵ_{res}. In the following we fix $N = 10^5$ which ensures us the convergence of the quantities calculated.
We consider the interaction with the external environment. We describe the environment in detail in chapter 5, where we derive a master equation in Lindblad form. This is a differential equation for the reduced density matrix of the system whose form is the following

$$\frac{d\rho_S}{dt} = -i[H, \rho_S(t)] + \mathcal{D}(t)[\rho_S(t)]. \tag{1.11}$$

where $H = H_S + H_{LS}$, H_S is the hamiltonian describing the qubit alone and $\mathcal{D}$ and H_{LS} given by

$$\mathcal{D}(t) = \sum_{\alpha,\beta,\omega} \gamma_{\alpha\beta}(\omega)\left[L_{\omega,\beta}(t)\rho_S(t)L^+_{\omega,\alpha}(t) - \frac{1}{2}\{L^+_{\omega,\alpha}(t)L_{-}\omega,\beta(t), \rho_S(t)\}\right] \tag{1.12a}$$

$$H_{LS} = \sum_{\alpha,\beta,\omega} S_{\alpha\beta}(\omega)L^+_{\omega,\alpha}(t)L_{\omega,\beta}(t), \tag{1.12b}$$

are the Dissipator and the Lamb-Shift Hamiltonian respectively. Here $S(\omega)$ and $\gamma(\omega)$ are related to the spectral density matrix of the bath by the relation

$$\Gamma_{\alpha\beta}(\omega) = \frac{1}{2}\gamma_{\alpha\beta}(\omega) + iS_{\alpha\beta}(\omega). \tag{1.13}$$

The environment is described by a thermal bath of harmonic oscillators (phonons):

$$H_B = \sum_{k=1}^{\infty} \omega_k b_k^+ b_k, \tag{1.14}$$

where b_k^+ and b_k are, respectively raising and lowering operators for the k-th oscillator with frequency ω_k. We express the interaction between system and bath as

$$H_I = \sum_{i=1}^{N} \sigma_z^i \otimes B_i \tag{1.15}$$

where N is, in general, the number of considered qubits. The operators B_i are defined by

$$B_i = \sum_k g_k^i (b_k^+ + b_k), \tag{1.16}$$

where g_k^i are the constants that couple the i-th spin with the k-th oscillator.
In this work we consider a single qubit, then all the coupling constants reduce to a single one, that is g, and we take into account a bath in thermal equilibrium at inverse temperature $\beta = 1/k_B T$ and described by an ohmic spectral density

$$\gamma(\omega) = 2\pi\eta \frac{g^2 \omega e^{-\frac{|\omega|}{\omega_c}}}{1 - e^{-\beta\omega}}. \tag{1.17}$$

Here we set a frequency cutoff ω_c and introduce η, a positive constant with dimensions of time squared.

First, using the tools of chapter 5, we consider the dynamics of the qubit in the presence of decoherence without calculating the LGIs. The differential equation is solved numerically using a fourth-order Runge-Kutta algorithm. In chap. 6 we prove that the bath is detrimental for the quantum annealing and, while the adiabatic theorem performs better increasing the annealing time, a long interaction between the system and the environment destroys the coherences of the system and brings it to thermalization.
Then we calculate the LGIs fixing D=50, $t_f = 10\sqrt{2}$, $\omega_c = 25$ and $\beta = 10$ and perfoming simulations for different values of the system-bath coupling. In Fig.1.5 we show our results. First of all, they demonstrate that our method reproduce the same correlations (points in the plot) obtained with projective measurements (curves) and, secondly, that the Leggett-Garg's inequalities may be used as witness of quantum coherence. They tell us that the system is not exhibiting quantum correlations at the end of the annealing time when the coupling is strong enough, because the curve K_3 is below the classical bound of the LGIs.

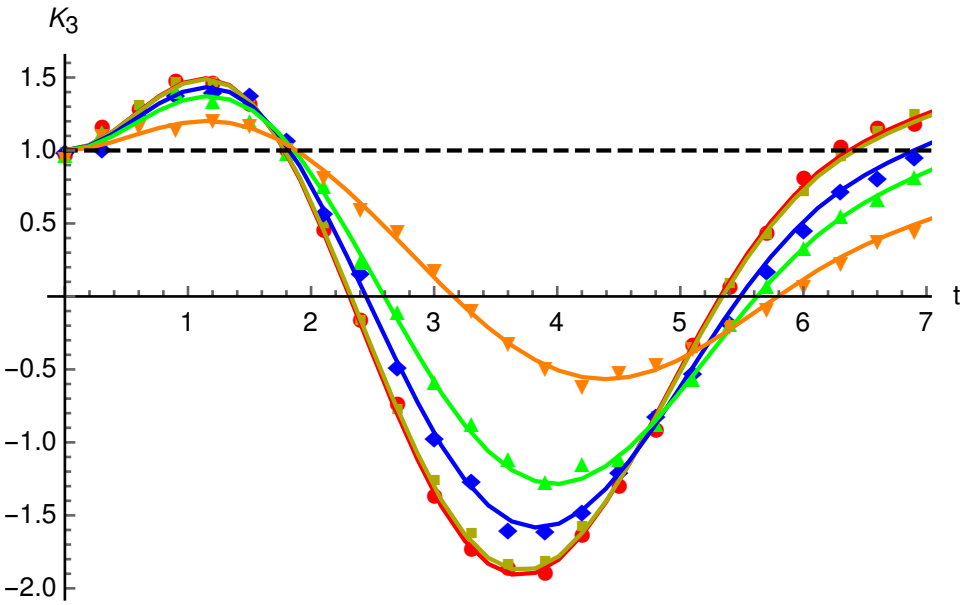

Figure 1.6: Plot of the Leggett-Garg's function K_3 during the annealing dynamics with different coupling constant to a thermal bath. The curves are guides for the eyes, being the ones obtained performing projective measurements. The points are the values calculated with our method, considering $\beta = 10$,D=50 and N=10^5.

- Red, $\eta g^2 = 0$,
- olive, $\eta g^2 = 10^{-3}$,
- blue, $\eta g^2 = 10^{-2}$,
- green, $\eta g^2 = 2 \times 10^{-2}$,
- orange, $\eta g^2 = 5 \times 10^{-2}$.

The black line highlights the bound of the LGIs. The LG's functions are plotted as function of the difference of the times at which the measurements have been perfomed: $t_2 - t_1 = t_3 - t_2 = t$. The time t goes from 0 to $t_f/2$ so that it scans the whole evolution.

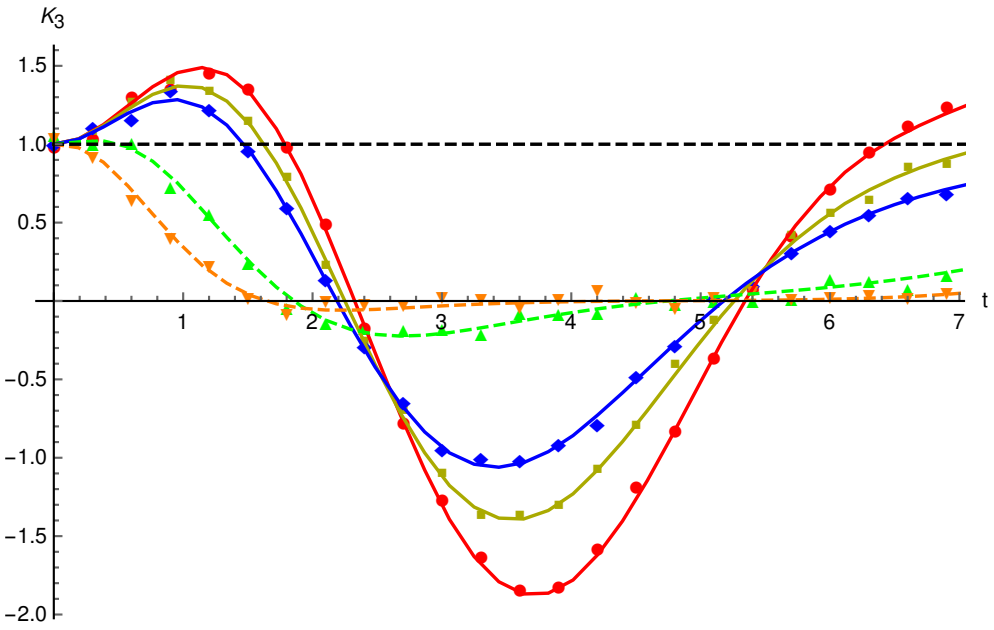

Figure 1.7: Plot of the Leggett-Garg's function K_s during the annealing dynamics with different coupling constant to a thermal bath. D=50 and N=10^5. $\beta = 10$ in red, $\beta = 0.05$ in blue, $\beta = 0.005$ in green. Here $t = t_2 - t_1 = t_3 - t_2$, $t \in [0, t_f/2]$.

Increasing the temperature reduces coherence times and quantum properties are expected to be destroyed faster, since the system is coupled to a "hot" environment. For this reason, in Fig.1.7, we show the behavior of the LG's function K_3 at fixed coupling but for different values of the inverse temperature β. We set $\eta g^2 = 10^{-3}$ so that, for $\beta = 10$, K_3 is over the bound at t=$t_f/2$, and we study the evolution of the system for different values of β. From Fig.1.7, it is evident that the temperature plays a key role in the detrimental effect of the thermal bath. For low temperatures the quantum behavior persists during the whole evolution even in the presence of coupling with the environment. However, increasing the temperature, the time during which the system shows quantum features decreases, eventually going to zero for very high temperatures.
Since we have used a master equation written in Lindblad form, we must consider that this approach guarantees reliable results only in the weak coupling limit. Therefore the results shown for very high temperatures might be beyond our approximation and have to be considered with care.

1.4 Conclusions

Adiabatic quantum computation is a modern topic of study and may be a fruitful field of research. The idea of this thesis is to explore this delicate subject and provide a contribution for a better understanding of the competition between the quantum dynamics and the interaction with a classical environment during the quantum annealing. With this in mind, we put ourselves into the discussion of whether or not the system evolves following a quantum dynamics during the annealing schedule, when the system is interacting with the environment. We came out with a new method to assess the quantumness of a system during its evolution. It is based on the LGIs evaluated in the framework of weak measurements, that allows us to measure correlations in times without perturbing the annealing dynamics. We showed that they hold information about the interaction with the environment and that they can be used as witness of quantum coherence.
Do our results allow us to answer the point raised at the beginning of this section? Namely: are commercial annealers, claimed to work performing adiabatic quantum computation, really quantum annealers? Are their outcomes macroscopic manifestations of quantum mechanics?
Our results show, for a very simple model, that if one measures the LGIs along the adiabatic dynamics, a possible, yet non trivial, outcome could be $K_3(t_f/2) < 1$ thus assessing that the final result of the computation was due to a non trivial occurrence of quantum and classical mechanisms. Hence, strictly speaking, we would not classify this machine as quantum.
However this approach is still at its infancy. Extending it to more complicated ensembles like a N spins Ising chain with periodic boundary conditions, with N> 1 of course, would be a fascinating way along which to proceed in order to provide a more powerful tool to whoever is interested in the study of adiabatic quantum computation and in the theoretical analysis of the newest devices which exploit the quantum annealing.

Chapter 2

Quantum computation and quantum annealing

Quantum computation has attracted much attention over the last decades, partly because classical computers will reach, eventually, their natural limits and partly for its promise of providing a speed-up of certain computationally hard problems compared to classical computing.
Let us consider, for instance, the problem of factoring an integer m of arbitrary size. A way to proceed is try to divide m for all the prime numbers starting from 2 to $\sqrt{m}$ since the rest is a prime number itself. This is, obviously, very uneffective and it takes $2^{\frac{n}{2}}$ trials to provide the factorization, if n is the number of digits of m.
Searching in the literature for an ingenious algorithm to face this problem, one could find that the number of attempts, whatever the method, cannot fall below $2^{cn^{1/3}}$, still increasing exponentially in n [1] (c is a constant).
Therefore, since in 1994 Shor [2] demonstrated that one can perform the same factorization in polynomial time using the properties of quantum mechanics, many people have started to think about quantum computation as a powerful alternative to the standard circuit model.

The building block of classical computation is the *bit* which assumes two values, namely 1 or 0. Quantum computation, instead, is built upon the concept of quantum bit or *qubit*. The difference among these two objects is substantial. Since a qubit is a quantum entity, we may find it in any possible superposition of the states $|0\rangle$, $|1\rangle$ which are the analogous of the states of the classical bit. This points out that a qubit may be at any time in the logic state 0 or 1 with

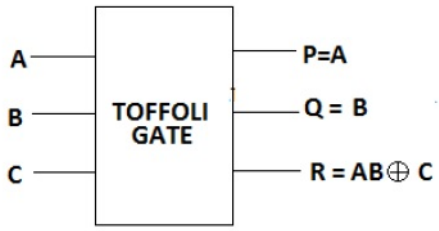

Figure 2.1: Toffoli gate. A,B,C are the inputs while P,Q and R are the outputs.

a certain probability. All the characteristics of the quantum computation rely on this property.
In the following we are going to describe how to realize quantum computation in terms of logic gates in analogy with the circuit model of the classical computation (sec.2.1). There are many different architectures for quantum computers based on different physical systems.
Recent quantum devices are based on iontrap, nuclear magnetic resonance, spin- and charge-based quantum dots and photonic systems; therefore we are not going to exhibit a specific implementation of the gates described but we remind the reader to Ref. [3].
On the other hand we will introduce the idea of the adiabatic quantum computation as an alternative to the previous implementations. We will discuss its equivalence with the circuit model and focus on some problems that are a hot topic of study today (sec.2.2).

2.1 The circuit model

Let us remind first some notion of classical computation. For a deeper look at this topic the reader could refer to Ref.[1].
If a *bit* is the fundamental concept of classical computation, *logic gates* are the basics dowels of the classical computers. Logic gates are physical structures that relate one or more outputs to the input bits. A logic gate is called a *universal gate* if one can build any other gate starting from it, and it is said *reversible* when maps the inputs to the outputs as a one-to-one function. The importance of the reversibility of a gate relies in the heat generation during the computing process which is of the order of the inverse temperature β for each irreversible function in the circuital set-up (Ref.[4]).
The most simple universal and reversible gate in classical computation is the *Toffoli gate* (Fig.2.1) named by Tommaso Toffoli and also known as *Controlled-Controlled Not*. It is described by the following input/output table, where according to Fig.2.1 A, B and C are the inputs and P,Q and R are the outputs.

A	B	C	P	Q	R
0	0	0	0	0	0
0	0	1	0	0	1
0	1	0	0	1	0
0	1	1	0	1	1
1	0	0	1	0	0
1	0	1	1	0	1
1	1	0	1	1	1
1	1	1	1	1	0

It leaves the bit C unchanged when A or B are in the logic state 0, while changes the state of C when A and B are 1. When the bit C is set equal to 1, the gate behaves as a NAND[1] which one can demonstrate to be a universal gate. This is a trivial observation that allow us to assert that the Toffoli gate is universal as well.
The circuit model of classical computation can be also transferred to quantum computation. The quantum computers may be tought of as classical computers dealing with n qubits instead of n bits. While the state of n bits is described in binary notation by an integer i $\in [0, 2^{\mathrm{n}} - 1]$:

$$i = i_{n-1}2^{n-1} + \dots i_1 2 + i_0 \tag{2.1}$$

where $i_0, \dots, i_{n-1}$ are single bit values, the state of n-qubit is a quantum state residing in the 2^n Hilbert space $\mathcal{H}_n$ tensor product of the single qubit spaces:

$$|\psi\rangle = \sum_{i=0}^{n-1} c_i |i\rangle = \sum_{i_{n-1}=0}^{1} \cdots \sum_{i_0=0}^{1} |i_{n-1}\rangle \otimes |i_0\rangle . \tag{2.2}$$

In order to realize quantum logic gates analogous to classical logic gates one has to perform unitary transformations on the state $|\psi\rangle$, that usually are denoted with U.
Even though the evolution of the n-qubit state is described by a 2^nx2^n matrix, according to the Schrödinger's equation, this matrix can always be decomposed into products of unitary operations acting only on one or two qubits. This operations are the above-mentioned quantum gates.
As in the case of classical computation a sequence of elementary operations allows one to build up arbitrarly complex computations. The generalization of the Toffoli gate is the, so called, *Deutsch gate*. The Deutsch gate is also known as Controlled-Controlled U because it works similarly to the Controlled-Controlled

[1] A NAND gate has two inputs and one output. It is not reversible but universal. It works as an AND (the output is 1 when A and B are 1) followed by a NOT (which inverts the logic input).

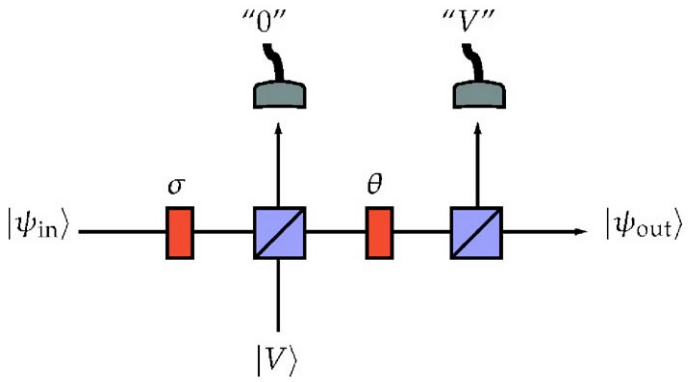

Figure 2.2: The NS gate by Rudolph and Pan. Based on a vacuum detection of the first output port and a single vertically polarized photon on the second output port, the sign of the quadratic term is changed. The success probability is $\eta = (3-\sqrt{2})/7$.

Not, where the Not gate is replaced by a unitary transformation. Hence, if $|A\rangle, |B\rangle, |C\rangle$ are the input qubits, the outputs $|P\rangle, |Q\rangle, |R\rangle$ of the gate are expressed by

$$|P\rangle |Q\rangle |R\rangle = |A\rangle |B\rangle U^{AB} |C\rangle ; \tag{2.3}$$

a unitary transformation U is applied to the qubit C if and only if A and B are in the state $|1\rangle$. When the transformation U is set as $\sigma_x = \begin{pmatrix} 0 & 1 \\ 1 & 0 \end{pmatrix}$ we get that the gate behaves as the Toffoli gate because it changes the state of the qubit C if and only if A and B are in the logic state 1. Taking into account that the Toffoli gate is reversible and universal one can assert that the Deutsch gate is reversible and universal as well; however unlike the classical case one can demonstrate that the Deutsch gate itself can be realized with reversible single- or double-qubit gates.
Set aside the theoretical features of quantum computation, another problem to discuss is the implementation of the described framework which rises many difficulties to deal with. First of all, as it follows from quantum mechanics, quantum gates return the right output only with certain probability. This implies that the more are the gates in play in the circuit, the less one can expect that the set-up yelds the right result.
For example we can take into account a gate realized with photonic qubits called *Non-linear sign* by Rudolph and Pan [29]. Looking at Fig.2.2, one observes that it consists of two plates (in red) that rotate the polarization of the input photons, two detectors (in grey) that count the photons incoming and two polarized beam splitters (in blue) that reflect the beam if it is vertically (V) polarized and transmit

it if it is horizontally (H) polarized. The generic input state of the gate is given by the following expression:

$$|\psi_{in}\rangle = (\alpha + \beta a_H^+ + \frac{\gamma^2}{\sqrt{2}} a_H^{+2}) b_V^+ |0\rangle \,, \tag{2.4}$$

where a_i^+ is the operator that creates a photon in the horizontally propagating mode with polarization i ($i = H, V$) and b_i^+ is the one that creates a photon in the vertically propagating mode. It must give in output the final state

$$|\psi_{out}\rangle = (\alpha + \beta a_H^+ - \frac{\gamma^2}{\sqrt{2}} a_H^{+2}) b_V^+ |0\rangle \,, \tag{2.5}$$

that is it must change the phase of the state if there are two photons incoming. This is possible only if the first detector does not count photons and the second counts one photon in the vertical propagating mode as shown in Ref.[29], after some algebra.
Since all the other cases must be rejected, the gate does not perform well every time one uses it and one can determine the probabilty of the gate operation η, which is $\eta = (3-\sqrt{2})/7$. This gate is used to build universals double-qubit gates as the CZ fate, see Ref.[29], then the latter and all the circuits built with it are not deterministic as well. If, for instance, one realizes a circuit constituted by N gates of this type, the success probability of the circuit scales approximately as η^N which means that one needs $1/\eta^N$ trials on average to provide the right outcome. It is evident that increasing the number of gates, the circuit becomes less efficient.
Of course the problem has been studied deeply and for a long time and there exist many protocols to mitigate the problem, for example the KLM protocol [27] in the case of photonic qubits, but since the problem is intrinsic in quantum mechanics it is impossible to realize a quantum gate which relates the outputs to the inputs with certainty.
Moreover, another problem one has to face in the realization of the circuit model is the undesired interaction of the quantum gates with the outside world. The unwanted influence of the environment shows up as noise in quantum computation processes, thus hampering the operation of the logic gates. Often, the errors will propagate during the computation and add up each other giving an unreliable output.
With these things in mind one might look for another way to pursue the same goals. This way is called *Adiabatic quantum computation* and is a lively topic of research and experimentation, although there are relevant problems to deal with, also in this case. In the following section we will introduce the concept of *Adiabatic Quantum Computation* and *Quantum Annealing*, that are closely related.

2.2 Adiabatic quantum computation

Adiabatic quantum computation started as an approach for solving optimization problems in analogy with the thermal annealing, introduced by Kirkpatrick, Gelatt and Vecchi [5]. However it fastly developed into an important and useful alternative to the circuit model. Indeed, it has been demonstrated both that the circuit model can efficiently simulate the adiabatic model [6] and that an adiabatic simulation of a circuit could be reliable with at most polynomial corrections [7].

The introduction of the AQC cannot get around a description of the thermal annealing before getting into the troubles of the quantum annealing, hence this is what we will discuss first in this section; then we will describe quantum annealing and its questions but we will not give a detailed account of an experimental realization for which the reader could refer to Ref.[8].
As written above, the *thermal* or *simulated annealing* was introduced as solution for optimization problems which has to do with finding the global minimum of a given function, usually called *cost function*.
In general, there are various tested alghoritms to solve certain optimization problems exactly, however they are small in number and too problem specific so that only approximate results can be found for harder problems. Hence one can take into account heuristic algorithms that are approximated and based on the iterative improvement of the gotten solutions, among which there is also the *thermal annealing*.
Let us remark that a cost function, in general, has a rugged cost-configuration landscape by which we mean that its behavior is extremely non monotonic and that the system can assume a lot of configurations with almost equals values of the cost function so that it is extremely difficult to find the global minimum: the importance of this remark will be clear soon.
The usual starting heuristic algorithm is the *local minimization* algorithm. Here one starts with a random configuration of the system C_0 and step by step makes local changes in the system accepting the new configuration if the cost function is lower than the preceeding and discarding it if not. This method reduces the cost function until a configuration is reached where it assumes a value corresponding to a minimum. Of course when the cost function has many local minima the system could remain trapped in one of them which is not the global one. Once there, there is no chance to improve the result but restarting from the beginning several times and choosing the best result from all the simulations. In 1983 Kirkpatrick et al. [5] suggested a brilliant method to avoid the trapping in the cost-configuration landscape which is what we called *classical* or *thermal annealing* (CA). One can introduce fluctuations in the above-described algorithm so

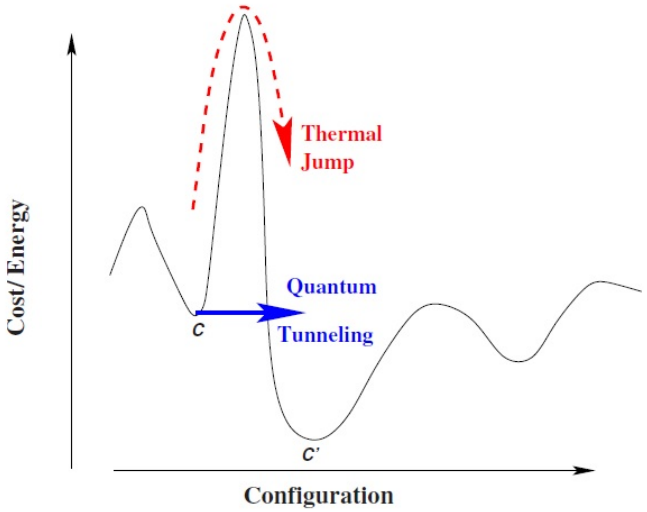

Figure 2.3: Giving a general Cost/Energy landscape, the system can get out a local minimum with thermal jumps in the case of the CA or with quantum tunneling in the case of the QA. The figure shows how in the case of high and narrow barriers, the second one is quite easy while jumping over the edge requires wide fluctuations in temperature. We denote with C and C' two configurations of the system corresponding to the local minima [9].

that the configuration change is not always to lower-cost configurations. With this craftiness the system can escape the local minima and explore the entire configuration space. In order to reach a minimum, the fluctuation, that Kirkpatrick et al. thought to introduce with an artificial temperature T, must decrease during the process, eventually going to zero. However, classical annealing can be unsatisfactory for a number of reasons. Firstly the cost-configuration landscape could be constitued by deep minima so that the thermal fluctuations are too weak to let the system cross the high barriers around them, furthermore the number of configuration of a system grows really fast increasing in size (exponentially for a Ising spin chain, for instance) hence CA cannot do much better than simple local minimization algorithms because cannot explore all the configurations space. Neverthless quantum mechanics has the solution to both these problems with its quantum tunneling, hence quantum annealing has been studied and developed till finding use in quantum computation.

The fundamental idea of the QA is going through the narrow barriers of the cost-function landscape by means of quantum tunneling, instead of jumping over the edges of the barries as in CA (Fig.2.3). Hence, it is apriori not obvious that CA should behave worse than QA, indeed they are strictly depending on the

configuration landscape. Furthermore, in practical realization of QA simulations on a classical computer one has to deal with a huge computational effort due to the Hilbert space dimensions.
The base of QA is encoding the result of an hard optimization problem in the fundamental state of a certain Hamiltonian H_I. As H_I belongs to the same complexity class of the optimization problem, H_I itself is difficult to manage. The system is prepared in the fundamental state of a simple Hamiltonian H_0, instead, of which we have complete knowledge. Then the system is made to flow adiabatically to the ground state of H_I, with an *annealing schedule* like:

$$H(t) = \left(1 - \frac{t}{t_f}\right) H_0 + \frac{t}{t_f} H_1. \tag{2.6}$$

Here we used a linear *annealing schedule*, the time t_f is called *annealing time*, and usually the Hamiltonian is expressed in terms of a dimensionless variable $s = t/t_f$:

$$H(s) = (1 - s)H_0 + sH_I. \tag{2.7}$$

While the concept is pretty simple, one has to face with different problems. First of all, this approach is based on the results of the *Adiabatic Theorem* which tell us that the annealing time must satisfy the following inequality to ensure that the system will always be in the ground state (app. D):

$$\max_{s\in[0,1]} \frac{|\langle k(s)| \, \partial_s H \, |k'(s)\rangle|}{\tau \Delta_{kk'}^2} \ll 1. \tag{2.8}$$

Since adiabatic theorem is the fundamental feature of the quantum annealing, this paradigm is also known as adiabatic quantum computation. For this reason, in the following we will use them interchangeably.
In the last equation, $|k(s)\rangle$ are the eigenvectors of the Hamiltoninan $H(s)$ corresponding to the eigenvalues $E_k(s)$, and $\Delta_{kk'} = E_k(s) - E_{k'}(s)$. Therefore for every k and k' the energy gap must not vanish, otherwise the annealing time diverges. This implies that many complicated Hamiltonian displaying first order phase transitions are hard to deal with. Furthermore, even if the minimum energy gap does not vanish one might have to deal with Landau-Zener transitions [10] if the energy gap becomes very small, which always happens increasing the system size. In order to take a control parameter over this problems, one usually introduces the, so called, *residual energy* or calculates the population of the ground state at the annealing time, namely the *fidelity*. The residual energy is defined as

$$\epsilon_{\text{res}}(t_f) = \frac{1}{N}(\langle\psi| \, H(t_f) \, |\psi\rangle - E_0(t_f)), \tag{2.9}$$

where N is the number of constituens (two-level systems/qubits) of the system, $|\psi\rangle$ is the state of the system and $E_0(t_f)$ is the ground state energy at the annealing time. One expects the optimal t_f to be the inverse square of the minimup energy gap and the residual energy to scale with a power-law ($\propto t_f^{-2}$) increasing time, neglecting transition problems [23].
In the practical implementation of the annealing, we have to observe that quantum systems are always interacting with their environment which influences their evolution. Therefore the evolution of the system, usually written as a differential equation for the density matrix, is no long unitary and relaxation and dephasing take place because of the interaction of the system with a thermal bath. The interaction is characterized by two time scales, the first one is usually denoted with T_1 and stands for the *relaxation time* which is the time a system needs to fill the energy levels following the classical Boltzmann distribution, the second is the time T_2 known as *dechoerence time* that is the time after which all the coherence term in the system state are vanished.
While adiabatic quantum computation seems to be more robust to thermal noise [33] with respect to circuit model, the decoherence is anyway a relevant problem that does not ensure us to find the right quantum state at the end of the annealing procedure neither that the system is evolving following complete quantum dynamics. The last one is the problem we want to face in this work assessing the "quantumness" of the qubit evolution during the quantum annealing. In particular we will make use of the Leggett-Garg's inequalities.

Chapter 3

Leggett-Garg's Inequalities

Since its formulation, quantum mechanics has rised manyfold fundamental questions that are still topic of study nowadays. Taking apart the debate about its different interpretations, for instance, one has to face the issue of the quantum violation of local realism, or the measurement problem. In this plethora of different open questions, another one, arises if we try to extrapolate the laws of quantum mechanics up to the macroscopic scale. The question is whether or not the laws of quantum mechanics hold for macroscopic objects. *Macroscopic coherence* has been introduced by Erwin Schrödinger with his famous cat-based thought experiment, in 1935 [11]. The experiment involves a cat which resides in a box with a sample of radioactive poison. The cat is clearly a macroscopic object, but whether it is alive or not depends entirely on a quantum system, namely which particular energy state the radioactive substance occupies. Schrödinger therefore argued that the system was in a superposition of states which described the cat being alive and dead, known as macroscopic coherence. Any attempt to check in the cat would collapse this wavefunction according to the Copenhagen interpretation of quantum mechanics, and one would find the cat either alive or dead. The idea of quantum mechanics operating in its usual bizarre way on a classical object runs counter to our intuitive understanding of how macroscopic world works. Therefore the bound between classical and quantum mechanics and how the latter arises from the first one increasing the system size are open problems and vivid topics of study.
Interested in whether macroscopic coherence could be realised in laboratory and how one could demonstrate its presence, Leggett and Garg developed and wrote their work in 1985. In contrast with spatial Bell's Inequalities that put constrains on the correlations of spatially separated systems, they wrote similiar inequalities

that test the correlation of the same system measured at different times.

The fundamental step of Legget and Garg's work was the encoding of how we expect macroscopic object to behave. They turned this behavior in a small set of principles or assumptions that, quoting directly from [12], read:

A: **Macroscopic realism per se**. A macroscopic object which has available to it two or more macroscopically dinstinct states is, at any given time, in a definite one of those states.

B: **Non-invasive measurability**. It is possible in principle to determine which of these states the system is in, without any effect on the state itself or on the subsequent system dynamics.

C: **Induction**. The properties of ensembles are determined exclusively by intial conditions (and in particular not by final conditions).

The whole properties define what has been called "classicity" or "macrorealism". The assumption C, also called "arrow of time", reflects our basic notions about causality, and it has been set aside from the discussion of the formulation of the Legget Garg inequalities (LGI). Assumptions A and B have been subject to vigorous discussions till nowadays. Regarding A, there is a plethora of definition of "macroscopic realism", for example it has been asserted even that macroscopicity is not necessary for the derivation of LGIs [15]. Since this problem is way too much wide than what we will need for the further discussion, the reader could refer to Ref.[14] and Ref.s therein for a deeper look at the formulation of the LGIs. Concerning assumption B, it seems counterfactual for a quantum system since it refers to a property that the system would have if it was macroscopic, which is not. Legget and Garg proposed, as a solution of this problem, the idea of performing "ideal negative measurements": in that case, the measurement process is constructed such that the measurement device interacts with the system if and only if the system has one particular value (i.e. double-slit experiment with a detector blocking one slit). The absence of signals from the detector means that the result of the measurement is the opposite it can measure; although the experimenter can know what is the value of the observable measured, the system will not be affected by the negative measure.

Based on the assumptions above, Leggett and Garg derived Bell's-like inequalities that any system in accord with "macrorealism", that is behaving classically, should obey [13]. Violations of these inequalities provide evidence of quantum behavior of a system if one accepts that the alternative to classical probabilities is quantum mechanics. Therefore these ones can be interpreted as

an indicator of the *quantumness* of a system. With this in mind, Leggett-Garg's inequalities have been used in a wide range of experiments. Their violation in an experimental set-up was first announced by Palacious-Laloy and coworkers in 2010 [16], then the topic flourished with a number of different experiments which witnessed the violation of Leggett-Garg's inequalities in a huge amount of different physical systems such as: photons [17], phosphorus impurities in silicon [18], superconducting devices [19], nuclear magnetic resonances [20] and nitrogen-vacancy centers [21].

3.1 Derivation of the LGIs

Following Ref.[14], in this section we briefly introduce the Leggett-Garg's inequalities and discuss their properties as witness of *quantumness*.
Let us begin with the definition of a dichotomic variable Q which can assume value $+1$ or -1: $Q(t_i) = Q_i$ stands for the measurement value of the observable at time t_i. We denote with $P_i(Q_i)$ the probability of obtaining the result Q_i. Therefore, the correlation function C_{ij} can be defined as follows:

$$C_{ij} = \sum_{Q_i, Q_j = +,-1} Q_i Q_j P_{ij}(Q_i, Q_j), \tag{3.1}$$

where the subscripts of P remind us of the times at which the measurements were performed. Assumption A, that is "Macrorealism per se", guarantees that P_{ij} can be obtained as the marginal probability of $P_{ij}(Q_i, Q_j, Q_k)$.

$$P_{ij} = \sum_{Q_k; k \neq i,j} P_{ij}(Q_i, Q_j, Q_k) \tag{3.2}$$

Withouth the assumption of "Non-invasive measurability" earlier measurements can affect the followings and the probabilities do not necessarily come from a joint probability distribution. With this assumption, instead, we can drop the subscripts of P_{ij} and use the $P(Q_i, Q_j, Q_k)$ alone to calculate the three correlation functions: C_{12}, C_{23}, C_{13}. Starting from the general expression

$$C_{ij} = \sum_{Q_i, Q_j = +,-1} Q_i Q_j P(Q_i, Q_j) = \langle Q_i Q_j \rangle, \tag{3.3}$$

we obtain

$$\begin{aligned}
C_{12} =& P(+,+,+) + P(+,+,-) + P(-,-,+) + P(-,-,-) \\
& - P(+,-,+) - P(+,-,-) - P(-,+,+) - P(-,+,-), \\
C_{13} =& P(+,+,+) + P(+,-,+) + P(-,+,-) + P(-,-,-) \\
& - P(+,+,-) - P(+,-,-) - P(-,+,+) - P(-,-,+), \\
C_{23} =& P(+,+,+) + P(-,+,+) + P(+,-,-) + P(-,-,-) \\
& - P(+,+,-) - P(-,+,+) - P(+,-,+) - P(-,-,+),
\end{aligned} \tag{3.4}$$

where we have considered $P(+,+,+) = P(+1,+1,+1)$, etc.
Using the completeness relation $\sum_{Q_i,Q_j,Q_k} P(Q_i,Q_j,Q_k) = 1$, we can obtain $K_3 = C_{12} + C_{23} - C_{13}$:

$$K_3 = 1 - 4[P(+,-,+) + P(-,+,-)]. \tag{3.5}$$

The upper bound of K_3 is given by $P(+,-,+) = P(-,+,-) = 0$ which is $K_3 = 1$; the lower bound, instead, is given by $P(+-,+) + P(-,+,-) = 1$, therefore $K_3 \geq -3$. Besides the above inequality, that is

$$-3 \leq K_3 \leq 1 \tag{3.6}$$

other inequalities exist, that can be found in the literature. Generalizing K_3 to higer order in n for example, $K_n = C_{12} + C_{23} + ... + C_{(n-1)n} - C_{1n}$, we have:

$$\begin{aligned} -n \leq & K_n \leq n-2 \quad n \geq 3,\ odd; \\ -(n-2) \leq & K_n \leq n-2 \quad n \geq 4,\ even. \end{aligned} \tag{3.7}$$

In addition, various simmetry properties can be used to derive further constrains on the correlations. Firstly, we can redefine the dichotomic variable $Q \to -Q$ at various time in K_n. Taking K_3 as example, this operation generetes the following inequality:

$$-3 \leq K_3' \leq 1; \quad K_3' \equiv -C_{12} - C_{23} - C_{13}. \tag{3.8}$$

In the end, the last, different, third order inequality can be obtained from the K_3, just changing a sign:

$$-3 \leq K_{3perm} \leq 1; \quad K_{3perm} \equiv -C_{12} + C_{23} + C_{13}. \tag{3.9}$$

In principle, one can derive others functions starting from the function K_3 and building all the quantities one can obtain permuting all the time indices. In our example (third order inequalities), the only three different cases are the inequalities proposed above.
Since most experimental tests of Leggett-Garg's inequalities up to date have been performed on two-level systems, it is interesting to examine in depth the violation for this system which we refer to as qubit. Therefore, in the following we will discuss the canonical example of a qubit evolving under the hamiltonian $H = \Gamma_x S_x$. In this paper, we do not take into account the higher orders inequalities: the reason will be clear later, in section 3.2 and in appendix A. Indeed, we are interested in some particular property which can help us to detect the quantum or classical behavior of the system at any time. It will be shown that the trivial case of a qubit can be a useful example to become familiar with the Leggett-Garg's inequalities and also to solve the above-mentioned problem.

3.2 LGIs for a qubit

We choose as dichotomic variable $\hat{Q} = \sigma_z$ which take value ± 1 if the z-component of the spin of the qubit is up/down. Classically, the correlation can be expressed as $C_{ij} = \langle Q_i Q_j \rangle$; for a quantum system, instead, this have not a unique analogue due to the problem of operators ordering. In [22] it is shown that the correlation function can be calculated as follows:

$$C_{ij} = \frac{1}{2}\langle\{\hat{Q}_i, \hat{Q}_j\}\rangle \tag{3.10}$$

that is considering the symmetrised combination of the observables.
Let us consider the Hamiltonian $H = \frac{\Gamma_x \sigma_x}{2}$. The evolution operator is a simple rotation around the x-axis and the correlation takes the simple analytical expression:

$$C_{ij} = \cos\Gamma_x(t_j - t_i) \tag{3.11}$$

where we have chosen $\hbar = 1$. If we set the first time $t_1 = \pi$ and $t_{i+1} - t_i = t$ we can express the Leggett-Garg's functions (K_3, K_3', K_{3perm}) in terms of the difference time between two measurements:

$$\begin{aligned} K_3 &= 2\cos\Gamma_x t - 2\cos 2\Gamma_x t \\ K_3' &= -2\cos\Gamma_x t + 2\cos 2\Gamma_x t \\ K_{3perm} &= \cos 2\Gamma_x t \end{aligned} \tag{3.12}$$

They are plotted in Fig 3.1. The K_3 oscillates as a function of the time t and violates the inequality only for certain values of t. However, owing the oscillatory nature of K_3, we observe that the system should follow a quantum dynamics even though the Leggett-Garg's inequality is not violated, because we are not taking into account the presence of sources of dechoerence. This observation tells us that the non-violation of the inequality can not be a sufficient condition for the macrorealism and can not define the behaviour of the system.
In this special case, the problem can be solved considering not just the violation provided by K_3 but also the one of K_3'. As shown in Fig.3.1 and observed, for the first time, in Ref.[24], indeed, K_3 and K_3' are complementary: one is violated when the other is not and vice-versa. Therefore, this intuition provide a complete detection of the non-classical properties of the two-level system. In appendix A we show that this property cannot be used for systems with a higher angular momentum, after defining a new pattern for the calculation of the time correlations functions of multi-qubit systems.
In addition to the previous analysis the violation of the Leggett-Garg's inequalities can be associated with the non commutativity of the observable $\hat{Q}(t)$ at different

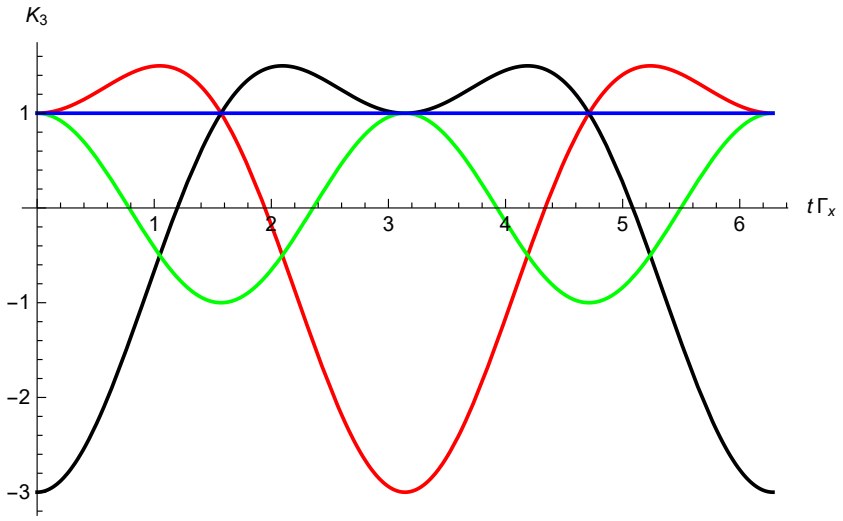

Figure 3.1: Plot of the third-order Leggett-Garg's functions in function of the time difference between two subsequent measurements. The curve in red shows the quantity K_3 , the black and green ones show the quantities K_3' and K_{3perm}, respectively. A violation of the Leggett-Garg's inequalities occurs when one of the functions take values greater than 1. The bound is enlightened by the blue line.

times. Parameterising the $\hat{Q}$ observable as $\hat{Q} = \vec{a}_i \cdot \vec{\sigma}$, where $\vec{\sigma}$ is the vector of the Pauli matrices, we can use the identity

$$(\vec{a}_2 \cdot \vec{\sigma})(\vec{a}_3 \cdot \vec{\sigma}) = \vec{a}_2 \cdot \vec{a}_3 \mathbb{1} + i\vec{\sigma} \cdot (\vec{a}_2 \times \vec{a}_3), \tag{3.13}$$

to simplify the expression of the commutator:

$$[\hat{Q}(t_i), \hat{Q}(t_j)] = 2i\vec{\sigma} \cdot (\vec{a}_i \times \vec{a}_j). \tag{3.14}$$

If we consider the example of a qubit with $\hat{Q} = \sigma_z$ and Hamiltonian $H = \frac{\Gamma_x \sigma_x}{2}$, that is evolving according to the evolution operator $U(t) = e^{-i\Gamma_x \frac{\sigma_x}{2} t}$, we can obtain:

$$[Q_i, Q_j] = 2i\sigma_x \sin \Gamma_x (t_j - t_i). \tag{3.15}$$

No violation occurs when all the commutators between the variable at different times vanish simultaneously, that are $\Gamma_x t = \frac{n}{2}\pi$, see Fig 3.1. Instead, maximum Leggett-Garg's violations occurr at times differences maximizing the commutators, i.e. at $\Gamma_x t = \pm\frac{\pi}{3}$.
However, also for a two-level system, we may consider a case where the LGIs are not always violated. Let us choose the Hamiltonian:

$$H = \Gamma_x \frac{\sigma_x}{2} + \Gamma_z \frac{\sigma_z}{2}, \tag{3.16}$$

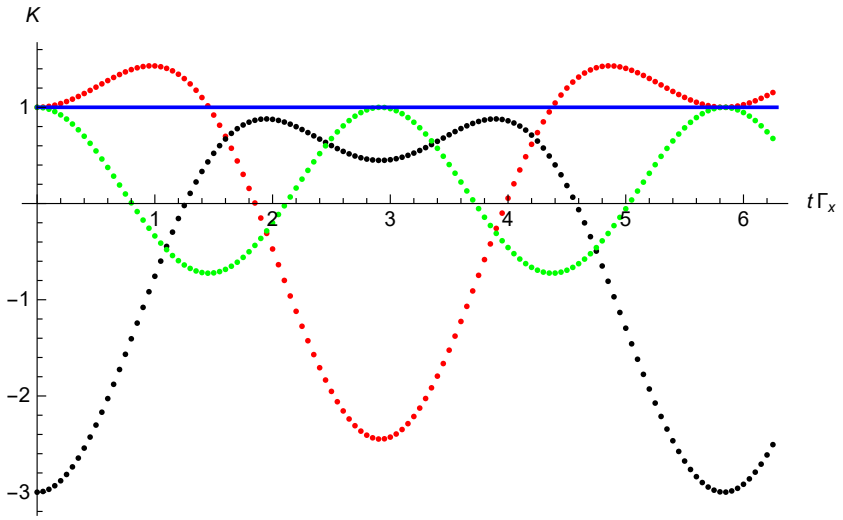

(a) Plot of the third-order Leggett-Garg's functions in function of the time difference between two subsequent measurements, with $\Gamma_x = 0.5$ and $\Gamma_z = 0.2$ and σ_z as dichotomus variable. The curves are calculated per points. The curve in red shows the quantity K_3 , the black and green ones show the quantities K_3' and K_{3perm}, respectively. A violation of the Leggett-Garg's inequalities occurs when one of the functions take value greater than 1. The bound is enlightened by the blue line.

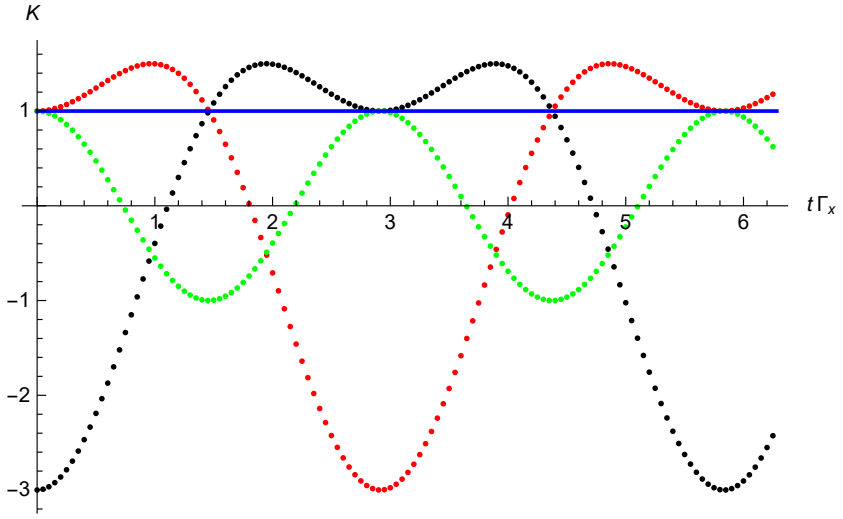

(b) Plot of the third-order Leggett-Garg's functions in function of the time difference between two subsequent measurements, with $\Gamma_x = 0.5$ and $\Gamma_z = 0.2$ and σ_y as dichotomus variable. The curves are calculated per points. The curve in red shows the quantity K_3 , the black and green ones show the quantities K_3' and K_{3perm}, respectively. A violation of the Leggett-Garg's inequalities occurs when one of the functions take value greater than 1. The bound is enlightened by the blue line.

Figure 3.2

the simple addition of the term $\Gamma_z \frac{\sigma_z}{2}$ changes drastically the property observed before. The evolution operator consists in a rotation around the axis given by the $\vec{n} = (\frac{\Gamma_x}{\sqrt{\Gamma_x^2+\Gamma_z^2}}, 0, \frac{\Gamma_z}{\sqrt{\Gamma_x^2+\Gamma_z^2}})$ versor. Due to the fact that the rotation now occurs around the $\vec{n}$-axis the correlation functions behave differently and this is shown in Fig.3.2a. If we consider as dichotomic variable the y-component of the spin σ_y, we can recover what we have seen before. In Fig.3.2b we see that the Leggett-Garg's functions are complementary. This means that at least one inequality is always violated and that they can be used as **witness of quantum coherence**. Of course it is not always possible to choose the y-component of the spin as dichotomic variable, because it requires a more relevant computational effort than performing measurement along the z direction. With this in mind, in the following we will consider as dichotomic variable $Q = \sigma_z$ and study K_3 alone. Indeed, in the absence of interaction with the environment, we know that the Leggett-Garg's function K_3 must return to exceed the bound $K_3 = 1$ during the evolution even if it is under $K_3 = 1$ for certain intervals, therefore it can provide sufficient information of the system behavior.

3.3 LGIs and Quantum Annealing

As we wrote before, our goal is to test the quantumness of a system evolution during an annealing dynamics. The system we take into account is described by the following Hamiltonian:

$$H(s) = s\frac{\Gamma_x}{2}\sum_{i=1}^{N}\sigma_x^i + (1-s)\frac{\Gamma_z}{2}\sum_{i=1}^{N}\sigma_z^i + (1-s)\frac{J}{2}\sum_{<i,j>=1}^{N}\sigma_z^i\sigma_z^j, \qquad (3.17)$$

where s$\in [0,1]$. In this expression we can dinstinguish a kinetic term that is the one that causes the flipping of the spins ($\Gamma_x \sum_i \sigma_x^i$), a potential energy contribution which forces the spins to align in the same direction ($\Gamma_z \sum_i \sigma_z^i$) and an interaction term that (with $J \geq 0$) provides an increase of energy if two spin are aligned in the same direction and a decrease if they are antiparallel ($\frac{J}{2N}\sum_{<i,j>}\sigma_z^i\sigma_z^j$); the sum runs only on the near-neighbours.
To evaluate the LGIs one has to perform at least two measurements during the evolution of the system to measure a dichotomic variable which can be chosen arbitrarly. However, these measurements influence the evolution of the system projecting the quantum state onto a subspace correspondent to the measured value. They break the annealing dynamics giving a final result which is not statisfying for our purposes.
With this in mind, we propose two different ways to approach the problem. Although in the end we proof that they cannot be used to test the quantumness

of our system, they are very instructive as they highlight our way of reasoning. In the next chapter we will introduce a scheme based on weak measurements that we will succesfully use in the rest of the thesis.

3.3.1 Single qubit measurement

The first idea to avoid the problem of the invasiveness of the measurements is to measure a simple qubit to assess the quantumness of the whole system, assuming that, the measurement process, interacting with a single qubit, does not influnce strongly the dynamics when the system is large enough. Using $C_{\alpha\beta}$ (Eq.3.1) we need to calculate the probabilty of getting the measurements Q_m and Q_l at the times t_α and t_β, respectively, where Q_m and Q_l are the values of the measurement of a dichotomic variable $\hat{Q}$ of a single spin. To obtain $C_{\alpha\beta}$ computationally, we can evolve the entire system and project on the subspace defined by the value of $\hat{Q}$ at a given istant; repeting this action twice we achieve the following expression:

$$|\psi\rangle = \Pi_l^1 U(t_\beta, t_\alpha)\Pi_m^1 U(t_\alpha, 0)\,|\psi_0\rangle\,. \tag{3.18}$$

Here $|\psi_0\rangle$ is the initial state of the system, $|\psi\rangle$ the final state, Π_m^1 represents the projector onto the subspace where only the state of the first qubit is fixed and U is the evolution operator. Equation 3.18 expresses the evolved state after two measurements, at times t_α and t_β, with outcomes Q_m and Q_l, on the chosen qubit. This means that the square of this quantity is what we were looking for: $P_{\alpha\beta}(Q_m, Q_l)$, where the subscripts α, β remind us the times when the measurements were performed. The correlation function at times t_α and t_β becomes:

$$C_{\alpha\beta} = \sum_{l,m} Q_m Q_l P_{\alpha\beta}(Q_m, Q_l). \tag{3.19}$$

In the special case we want to discuss, we consider as dichotomic variable the spin along a given direction $\vec{S}\cdot\vec{n}$. Therefore it is useful to write the qubit state as a superposition of the following eigenstates:

$$\begin{aligned}\left|\vec{S}\cdot\vec{n} = \frac{1}{2}\right\rangle &= \cos\frac{\theta}{2}\,|\uparrow\rangle + \sin\frac{\theta}{2}e^{i\phi}\,|\downarrow\rangle \\ \left|\vec{S}\cdot\vec{n} = -\frac{1}{2}\right\rangle &= \sin\frac{\theta}{2}\,|\uparrow\rangle - \cos\frac{\theta}{2}e^{i\phi}\,|\downarrow\rangle\,,\end{aligned} \tag{3.20}$$

and it is evident that the possible values of the dichotomic variable are $+1$, if the qubit is in the eigenstate $\left|\vec{S}\cdot\vec{n} = \frac{1}{2}\right\rangle$, and -1, if it is in the eigenstate $\left|\vec{S}\cdot\vec{n} = -\frac{1}{2}\right\rangle$. Hence, the choice of the dichotomic variable falls on the choice of the direction of the spin considered and so of the angles ϕ and θ.

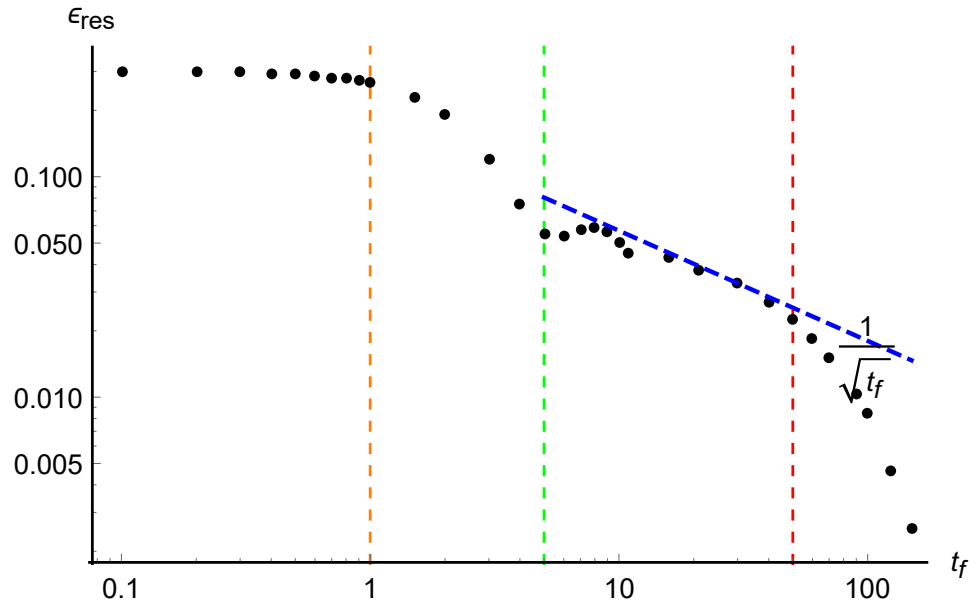

Figure 3.3: Plot of the residual energy of the system for different values of the annealing time t_f.

First of all, let us analyse the behavior of a system, composed by 8 spins, for instance. Let us consider the annealing dynamics without performing measurements and neglecting the interaction with a thermal bath. Let us fix the energy scale in 3.17 setting $\Gamma_x = 1$GHz and $\Gamma_z = 1$ GHz, $J = 0.6$ GHz, in the following the times will be expressed in units of $1/\Gamma_x$ while the energies in units of Γ_x . Calculating the residual energy of the system for different choices of t_f we obtain the behavior in Fig.3.3. We can recognize 4 regions. In the first one the residual energy is constant and far from zero because the system had not enough time to evolve ($t_f \in [0, 1]$). In the second ($t_f \in [1, 5]$) the behavior is exponential, due to the probability of Landau-Zener transitions [45]. In the third ($t_f \in [5, 50]$), it is evident a power-law scaling as $1/\sqrt{t_f}$ which would be the asymptotic behavior in the termodynamic limit. Since the system has finite size instead, in the last region ($t_f > 50$) we observe an exponential trend [30]. For $t_f \approx 20$ the system is in the region where it has reached its ideal asymptotic behavior and the annealing time scales with a power-law. We are fairly sure that the system is in its ground state at the end of the evolution and therefore that the annealing dynamics has been successful.
The residual energy at the end of the evolution, for $t_f = 20$, is $\epsilon_{\text{res}} = 3.93 \times 10^{-2}$ in units of Γ_x, according to Fig.3.3. It has been calculated numerically, solving

the equation for the density matrix

$$\frac{d\rho}{dt} = -i[H, \rho], \ \hbar = 1. \tag{3.21}$$

Performing a measurement at a given time during the evolution, influences the system and the residual energy is different at the end of the annealing dynamics, however if the measurement is performed on a subset of the whole system one might expect a lower variation of the residual energy. This observation is not true for the case we are studying, indeed measuring the z-component of the spin of one qubit at time $t_f/2$ we obtain $\epsilon_{\text{res}} = 1.21 \times 10^{-1}$. With this in mind, we might think about weakening the interaction between the qubit we want to measure and the ensemble so that the influence due to the perturbation is neglegible. Anyway this idea is detrimental if we want to construct the Leggett-Garg's inequalities. Indeed, if the qubit is strongly uncoupled from the ensemble, the LGIs cannot provide information about the whole system. Let us point out that one could increase the number of qubits of the ensemble, in order make less relevant the qubit measured with respect to the whole system; however, since increasing the system size means increasing the dimension of the Hilbert space which grows as 2^N it requires a huge and unmanageable computational effort.

3.3.2 Ideal negative measurement

Another way to perform non invasive measurements is to use ideal negative measurements (INM). In INM the apparatus is set-up so that it registers a 'click' if the systen is in one specific state, otherwise it does not interact with the system. If we consider a two level system as in Ref.[26] and an ancilla qubit, the scheme for perfoming the INM can based on considering the following operators to simulate the measurements of the total angular momentum:

$$\begin{aligned} CG_{-1} &= |-1\rangle\langle -1| \otimes \mathbb{1} + |0\rangle\langle 0| \otimes \sigma_x + |1\rangle\langle 1| \otimes \sigma_x, \\ CG_0 &= |-1\rangle\langle -1| \otimes \sigma_x + |0\rangle\langle 0| \otimes \mathbb{1} + |1\rangle\langle 1| \otimes \sigma_x, \\ CG_1 &= |-1\rangle\langle -1| \otimes \sigma_x + |0\rangle\langle 0| \otimes \sigma_x + |1\rangle\langle 1| \otimes \mathbb{1}. \end{aligned} \tag{3.22}$$

Here we denote with $|-1\rangle, |0\rangle$ and $|1\rangle$ the eigenvectors of J^2 and J_z with $J^2 = 2$ ($\hbar = 1$). The operators in Eq.3.22 correspond to the application of a rotation to the ancilla bit when the sistem is not in the state we want to measure and to the identity operator applied on the ancilla bit when the system is in the state we want to measure. Although it seems that this scheme is not invasive, it can be shown that the state population are preserved but some of the interaction terms vanish, so that during the annealing schedule this type of interaction still is too strong and invasive to be used to anaylize the system. Let us demonstrate

the assertion before: if we denote with ρ_S the density matrix of the system right before the measurement and we set the ancilla qubit in the state $|\uparrow\rangle$, we have that the total density matrix ρ_{tot} is given by the product of the density matrix of the system ρ_S and the one of the ancilla ρ_A:

$$\rho_{tot} = \rho_S \otimes \rho_A = \begin{pmatrix} P_{-1} & a & b \\ a^+ & P_0 & c \\ b^+ & c^+ & P_1 \end{pmatrix} \otimes \begin{pmatrix} 1 & 0 \\ 0 & 0 \end{pmatrix}. \tag{3.23}$$

Here we wrote a generic density matrix ρ_S in the J_z basis and the density matrix of the ancilla qubit as the pure state $|\uparrow\rangle\langle\uparrow|$. P_i (i=-1,0,1) are the probabilties that the angular momentum J_z get values $J_z = -1, 0, 1$, that are also the populations of the states $|-1\rangle, |0\rangle$ and $|1\rangle$, Let us study the action of the operator CG_{-1}, for instance, which is equal to

$$CG_{-1} = \begin{pmatrix} 1 & 0 & 0 & 0 & 0 & 0 \\ 0 & 1 & 0 & 0 & 0 & 0 \\ 0 & 0 & 0 & 1 & 0 & 0 \\ 0 & 0 & 1 & 0 & 0 & 0 \\ 0 & 0 & 0 & 0 & 0 & 1 \\ 0 & 0 & 0 & 0 & 1 & 0 \end{pmatrix} \tag{3.24}$$

Hence, we have that, after the measurement, the ancilla-system ensemble is described by

$$\rho'_{tot} = CG_{-1}\rho_{tot}CG_{-1} = \begin{pmatrix} P_{-1} & 0 & 0 & a & 0 & b \\ 0 & 0 & 0 & 0 & 0 & 0 \\ 0 & 0 & 0 & 0 & 0 & 0 \\ a^+ & 0 & 0 & P_0 & 0 & c \\ 0 & 0 & 0 & 0 & 0 & 0 \\ b^+ & 0 & 0 & c^+ & 0 & P_1 \end{pmatrix}. \tag{3.25}$$

We can trace over the ancilla (system) degrees of freedom to obtain the reduced density matrix of the system (ancilla) respectively. Doing so we obtain the following density matrices:

$$\rho'_S = \begin{pmatrix} P_{-1} & 0 & 0 \\ 0 & P_0 & c \\ 0 & c^+ & P_1 \end{pmatrix}, \tag{3.26a}$$

$$\rho'_A = \begin{pmatrix} P_{-1} & 0 \\ 0 & P_0 + P_1 \end{pmatrix}. \tag{3.26b}$$

It is evident that the ancilla contains the information about the state before the measurement, indeed the first diagonal element is the probability of obtaining the result -1 from a projective measurement, however the density matrix of the system is substantially altered by the measurement procedure. Indeed comparing $\rho_S^{'}$ with ρ_S we can note that while the diagonale part (hence the populations) have been preserved, all the interaction terms between the measured state and the others are null.

Chapter 4

Weak Measurements

Introductive textbooks to quantum mechanics describe the measurement process as projective but a more general description of the measurement can be worked out. As pointed out by Nielsen & Chuang [3] the reason most physicists do not learn the general formalism of measurement theory is because usually physical systems can only be measured in a very coarse manner. In quantum information or computation, instead, one could aim for a high level of control over the measurements. Hence a more comprehensive formalism for the description of the measurement process is demanded. Another reason to forsake the projection postulate is the, so called, *repeatability*. Performing a projective measurement and getting an outcome Q means that a subsequent measurement gives the same outcome and does not change or destroy the quantum state. This repeatability remind us that many important measurements in quantum mechanics are not projective measurements. Let us, for instance, think about measuring the position of a photon: it destroys the photon itself and certainly make it impossibile to repeat the measurement. Many other physical systems are not repeatable in the sense of the projective measurements and adopting the formalism developed by Nielsen & Chuang should be a better choice to approach to their study.
On the other hand, all physical processes last for a finite time and also physical measurements should have a finite duration and run for a sufficiently long time to acquire the information needed. Hence, the measurements are not instantaneous, and are rather continuous, hence we need a more general formalism. Indeed it is necessary to describe the gradual evolution caused by the interaction between the system being measured and the measuring apparatus. Continuous quantum measurement is object of intensive study and, during the last decades, have been developed firm theories which mostly use differential Langevin equations.

In the previous chapters we have pointed out that we want to measure an observable without perturbing the system under investigation, nor destroying its quantum state. In order to deal with this problem we must develop a different approach to the measurement process. A possible route is to perform quantum non demolition (QND) measurements, among which we consider the Kicked-QND measurement that we will discuss later. They present a lot of advantages that recommend them both from a theoretical and from an experimental point of view.
By contrast with respect to continuous measurement, analysis that uses conditional differential Langevin equations, they can be described with a non-unitary (discrete in time) quantum-map. Secondly, the kicking mechanism allows the experimentalist to tune the measurement strenght and perform less invasive measurements. Finally the kicking mechanism can be implemented, in general, in the experimental set-up quite simply. We will take into account the example of a quantum point contact kicked by a voltage pulse generator.

In the following we are going to consider the case of measurements on a two-level system following mostly Ref.[35], [36] and [38].
First, we derive the, so called, *Quantum Bayesian formalism* as done in [35], then we reformulate the approach to adapt it for measuring the Leggett-Garg's Inequalities of a single qubit. The choice of taking into account a single qubit is due to the computational effort needed to implement the method we are going to describe. This does not rule out the possibilty of generalising our approach to a multi-qubit system.

4.1 Derivation of the quantum Bayesian formalism

The most comprehensive quantum measurement postulate can be formulated as follows [3]: Quantum measurements are described by a collection $\{M_Q\}$ of measurements operators. These are operators acting on the state space of the system being measured. The index Q refers to the measurements outcomes that may occur in the experiment. If the state of the quantum system is $|\psi\rangle$ immediately before the measurement then the probability that the result Q occurs is given by

$$P(Q) = \langle\psi| M_Q^+ M_Q |\psi\rangle . \tag{4.1}$$

After the measurement the state changes satisfying the rule

$$|\psi'\rangle = \frac{M_Q |\psi\rangle}{\sqrt{\langle\psi| M_Q^+ M_Q |\psi\rangle}}. \tag{4.2}$$

Obviously the probabilities must sum to one and this yelds to the completeness equation:

$$\sum_Q M_Q^+ M_Q = \mathbb{1}. \tag{4.3}$$

These rules describe a, so called, *strong measurement* in the more general case. The projective measurements are just special cases as it is shown in [3].
We are interested in weak measurements, because we do not want to perturb the evolution of the system. Let us take into account a bipartite ensemble composed of an *ancilla* A and the system under investigation S. We want to show how one can extract information about the system performing measurements on the ancilla.
Let us denote with $|Q\rangle_A$ the orthonormal basis in the ancilla Hilbert space $\mathcal{H}_A$, and with M_Q the measurement operators that act in the space $\mathcal{H}_S$ and are indexed by the states of A. These operator satisfy the completeness relation and the probability of finding the result Q is given by

$$P(Q) = Tr(\rho_S M_Q^+ M_Q), \tag{4.4}$$

where ρ_S is the density matrix of the system S. The density matrix is updated similarly to as written before

$$\rho'_S = \frac{M_Q \rho_S M_Q^+}{Tr(M_Q^+ M_Q \rho_S)}. \tag{4.5}$$

This equation define a non-unitary map from density operators to density operators. To show how this scheme works, let us describe a physical example taking into account a quantum point contact (QPC) coupled to a double quantum dot (DQD). In a double quantum dot the electron can occupy one site at every given time. We denote the sites with a number, say 1,2. In Fig.4.1 we see a diagram which describes the measurement apparatus. The experimental set-up works in this manner: the QPC transport properties, i.e. the flowing current, are influenced by the DQD in the sense that measuring the current across the QPC one can infer which quantum dot the electron of the DQD occupies. This is possible because the QPC is capacitively coupled to the DQD. The voltage denoted by V is a voltage gate that helps to stop the current flowing. Let us suppose the DQD be in the general two-level state $\psi_S = \alpha |1\rangle_S + \beta |2\rangle_S$ and that we send a current from the left-side of the DQD. If $|L\rangle_A$ is the state of an incident electron we can write the initial state as

$$|\psi\rangle_{\text{in}} = |L\rangle_A (\alpha |1\rangle_S + \beta |2\rangle_S). \tag{4.6}$$

Within Landauer-Buttiker's approach, in the ballistic limit, we can calculate the currents via the scattering matrix approach. Such scattering matrices depend on

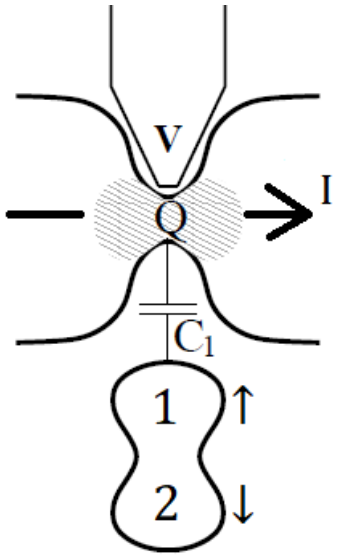

Figure 4.1: Diagram of the measurement apparatus. A double quantum dot is capacitively coupled with a quantum point contact. The current flowing through the quantum point contact depends on the position oof the electron in the double quantum dot (Courtesy of Ref.[34]).

whether the electron is in the first or in the second quantum dot:

$$S_j = \begin{pmatrix} r_j & \bar{t}_j \\ t_j & \bar{r}_j \end{pmatrix} \tag{4.7}$$

where $j = 1, 2$. Taking into account that $|L\rangle_A = \begin{pmatrix} 1 \\ 0 \end{pmatrix}$ we get

$$|\psi\rangle_{out} = \alpha(r_1 |L\rangle_A + t_1 |R\rangle_A) |1\rangle_S + \beta(r_2 |L\rangle_A + t_2 |R\rangle_A) |2\rangle_S . \tag{4.8}$$

In this framework, one performs a measurement of the current and get $I = 0(\neq 0)$ whether the electron is reflected(transmitted); the corresponding measurement operators are

$$M_R = \begin{pmatrix} t_1 & 0 \\ 0 & t_2 \end{pmatrix}, \qquad M_L = \begin{pmatrix} r_1 & 0 \\ 0 & r_2 \end{pmatrix}. \tag{4.9}$$

The probability of obtaining the two cases can be calculated as in Eq.4.4 and are:

$$P(R) = \rho_{11} T_1 + \rho_{22} T_2, \quad P(L) = \rho_{11} R_1 + \rho_{22} R_2 \tag{4.10}$$

where ρ_{ij} are the elements of the DQD density matrix. At the same time the density matrix of the system must be updated, after the measurement, taking

into account the information of the measurement performed. Following Eq.4.5 we can write

$$\rho'_S = \frac{M_R \rho_S M_R^+}{Tr(\rho_S M_R^+ M_R)}, \quad \rho'_S = \frac{M_L \rho_S M_L^+}{Tr(\rho_S M_L^+ M_L)} \tag{4.11}$$

depending on the measurement outcome. Carrying on with the first case, for instance, we get:

$$\rho'_S = \frac{1}{P(R)} \begin{pmatrix} t_1 & 0 \\ 0 & t_2 \end{pmatrix} \begin{pmatrix} \rho_{11} & \rho_{12} \\ \rho_{12}^* & \rho_{22} \end{pmatrix} \begin{pmatrix} t_1^* & 0 \\ 0 & t_2^* \end{pmatrix} = \begin{pmatrix} \frac{T_1 \rho_{11}}{P(R)} & \frac{t_1 t_2^* \rho_{12}}{P(R)} \\ \frac{t_1^* t_2 \rho_{12}^*}{P(R)} & \frac{T_2 \rho_{22}}{P(R)} \end{pmatrix} \tag{4.12}$$

The result in Eq.4.12 can be interpreted as a quantum Bayes formula; we see that $\rho'_{11} P(R) = T_1 \rho_{11}$ is similar to $P(A|B)P(B) = P(B|A)P(A)$, indeed. However, the same rules can be derived in a more comprehensive manner developing the Bayesian formalism for selective quantum evolution of a qubit due to continuous measurement as in Ref.[38].
Moreover, it is not difficult to extend the previous statements for M electrons entering the DQD, which is a more realistic case and of physical interest. This is done by replacing the probabilities of transmission T_j and of reflection R_j by the binomial distribution

$$P(m, M|j) = \binom{M}{m} T_j^m (1 - T_j)^{M-m}, \tag{4.13}$$

which is the probability of measuring a current relative to m electrons on the total of M, under the condition that the electron of the DQD is in state $|j\rangle$ (j=1,2).
The measurements we have focused on, untill now, are strong measurements that heavly change the state of the system. In order to discuss the problem of weak measuring an observable is necessary to introduce a coupling parameter between system and ancilla.

4.2 QND measurements

Following the example discussed in the previous section, we want to measure the current in output from the QPC with small perturbation to the system S after each measurement. The measurement scheme was introduced by Jordan, Büttiker and Korotkov in Ref.[36] and is here schematised in Fig.4.1. we send a series of voltage kicks across the QPC, measuring the current through it. The voltage current denoted in Fig.4.1 helps to switch on and off the current. The currents across the QPC when the electron is in the sites 1 or 2 are I_1, I_2

respectivly. The typical measurement time necessary to distringuish between the two outcomes, which is the time for which the signal-to-noise ratio is close to one, is

$$T_M = \frac{4S_I}{(I_1 - I_2)^2}. \tag{4.14}$$

In the previous expression the term S_I denotes the detector shot noise power $S_I = eI(1-T)$ where with T we are referring to the trasparency [38]. The outcomes I_1,I_2 can be mapped onto a dimensionless variable $x = \pm 1$ as follows:

$$I = I_0 + x\frac{(I_1 - I_2)}{2} \tag{4.15}$$

Since we have introduced the kicking mechanism, it is possible to tune the interaction between the system and the ancilla and make the measurement in a weak form. In particular, if we denote with τ_V the kick duration, a weak coupling between QPC and DQD means that τ_V is smaller than T_M such that a single measurement cannot provide the full information to evaluate the flowing current (that is the position of the electron in the two-level system). However, as an advantage, it weakly perturbs the system S dynamics. We take the variable *x* to be normally distributed with variance $D = \frac{T_M}{\tau_V}$ and we denote with $P(x)$ the probability distribution for the outcome of x. In analogy with Eq.4.10 we can write

$$P(x) = \rho_{11}P_1(x) + \rho_{22}P_2(x), \tag{4.16}$$

where $P_j(x)$(j=1,2) is a Gaussian distribution (centered around -1,1). The measurement modifies the density matrix depending on the value of the observable measured similarly to Eq.4.12:

$$\begin{aligned}
\rho'_{11} &= \frac{\rho_{11}P_1(x)}{\rho_{11}P_1(x) + \rho_{22}P_2(x)} \\
\rho'_{12} &= \rho_{12}\sqrt{\frac{\rho'_{11}\rho'_{22}}{\rho_{11}\rho_{22}}}, \qquad \rho'_{21} = \rho'^{*}_{12} \\
\rho'_{22} &= \frac{\rho_{22}P_2(x)}{\rho_{11}P_1(x) + \rho_{22}P_2(x)}.
\end{aligned} \tag{4.17}$$

These equations define, again, a non unitary quantum map from density operator to density operator.

A single measurement, like the one described, does not give enough information to the experimentalist. Indeed, as demonstrated by Aharonov et al. in Ref.[7], when weak measurments are performed one can obtain strange values of the observable measured. For instance, they found $\langle \sigma_z \rangle = 100$ for a $1/2$-spin, which is obviously meaningless. They called this result a *strange weak value* and introduced the idea of the necessity of collecting the full information on the observable

that one want to measure, repeating the "experiment" several times. In the case of Kicked-QND measurements, usually one sends a huge number N of kicks, collecting a small amount of information at each step, and compose the N weak measurements to make an N-times stronger measurement. This is not our case, due to the fact that we want to calculate the Leggett-Garg's inequalities for a qubit and then we need two measurements at two fixed times. However, in the following we will show how to adapt this framework to fit it in our scheme.
It is useful to point out where is the *weakness* of the measurement studying the matrix update rules. From Eq.4.17 we get

$$\frac{\rho'_{11}}{\rho'_{22}} = \frac{\rho_{11}}{\rho_{22}} \frac{P_1(x)}{P_2(x)} = \frac{\rho_{11}}{\rho_{22}} e^{\frac{2x}{D}}. \tag{4.18}$$

This can be used to characterize the post-measurement density matrix writing it in another shape; let us denote with γ the ratio x/D and write

$$\rho'_{11}\rho_{22}e^{-\gamma} = \rho'_{22}\rho_{11}e^{\gamma} \rightarrow \rho'_{11} = \frac{\rho_{11}e^{\gamma}}{\rho_{11}e^{\gamma} + \rho_{22}e^{-\gamma}}. \tag{4.19}$$

Hence we obtain the following quantum-map from ρ_S to ρ'_S:

$$\rho'_S = \frac{1}{\rho_{11}e^{\gamma} + \rho_{22}e^{-\gamma}} \begin{pmatrix} \rho_{11}e^{\gamma} & \rho_{12} \\ \rho^*_{12} & \rho_{22}e^{-\gamma} \end{pmatrix} \tag{4.20}$$

This expression is much more significant than Eq.4.17. The quantity D, which is the variance of the dimensionless variable x, is easy tunable. This allow us to weaken the measurement until the post-measurement update in the density matrix is negligible. This is crucial in our argument if we want to study the Leggett-Garg's inequalities for a qubit, possibly during an annealing dynamics.
The last problem we have to face is then adapting this framework in the context of quantum annealing.

4.3 Weak Measurements and LGIs

The Kickend-QND measurements described in Ref.[36] are perfomed periodically on the same system during its evolution. This measurements allow one to collect enough information and evaluate the current flowing through the DQD.
In our scheme, instead, we need to perform two measurements at two fixed instants and calculate the correlation functions. Therefore, the idea is to take into account the same example, by which we mean the QPC interacting with the DQD, but using a different measurement pattern. We associate to the position of the electron in the DQD a spin degree of freedom. Let us say that if the

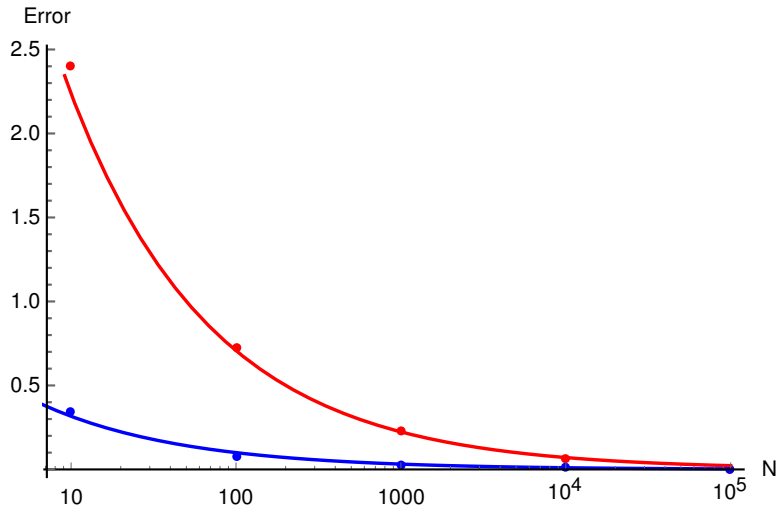

Figure 4.2: Log-linear plot of the errors on the residual energy and on K_3. We fix D=50 and evaluate σ_{K_3} and $\sigma_{\epsilon_{\text{res}}}$ for different values of N. The time difference t is fixed as $t = 3.3\ 1/\Gamma_x$. The errors obtained are normalized by the value of ϵ_{res} and K_3 obtained with $N = 10^5$. We show in red the error on K_3 and in blue the one on ϵ_{res}. The curves are guides for the eyes while the points are the ones simulated.

electron is on the site 1 it is denoted by $\sigma_z = 1$ and if it is on the site 2 it is denote by $\sigma_z = -1$. This is depicted in Fig.4.1. We set the Hamiltonian of the DQD as

$$H(s) = (1-s)\frac{\Gamma_x}{2}\sigma_x + s\frac{\Gamma_z}{2}\sigma_z \tag{4.21}$$

which we describe in more detail in chapter 6. We want to let the system evolve performing the quantum annealing and to measure the current at different times to evaluate the LGIs, as seen in chapter 3.
In the following we will denote with $I(t)$ the dimensionless variable x, to keep trace of the fact that we are measuring a current.
We may proceed in this way: let us prepare the system in the ground state of the Hamiltonian $H(0)$ and let the system evolve under $U = e^{-iH(t/t_f)t}$. Computationally this means solving the differential equation for the density matrix with a fourth-order Runge Kutta algorithm. At a fixed time t_1 let us suppose to perform a weak measurement, which means to extract a value of the current from the probability distribution 4.16. The system state changes following the Eq.4.20. The strenght of the interaction depends on the variance D of the current distribution and the measurement gives more or less depending on how weak is the interaction. Instead of performing a second weak measurement at time t_2 we can perform a projective one because we are only interested in the behavior of the system till that instant. This step leaves us with a value of the

product $I(t_1)I(t_2)$ which could be meaningless because the measurement can give strange weak values. The solution is to repeat the same evolution a large amount of times and evaluate the correlation function $\langle I(t_1)I(t_2)\rangle$ as the average of the different products obtained at each run. Considering this approach it is interesting to evaluate an uncertainty interval on the results of the simulations. We proceed computationally calculating the standard deviation of the residual energy ϵ_{res} and of the LG's function K_3. We perform the measurement at a given time t=3.3 in units of $1/\Gamma_x$, considering $\Gamma_x = 1$GHz and $t_f = 10\sqrt{2}$. These choices will be clear in the next chapter. In Fig.4.2, we show the trend of the uncertainty normalized dividing by the values of K_3 and ϵ_{res} obtained by an average on $N = 10^5$ runs. We see that the points follow the curves $\alpha/\sqrt{N}$ at fixed D=50, with different α. We can estimate that $\alpha = 1$ for the residual energy and $\alpha = \sqrt{50}$ for the function K_3. Therefore in the case of K_3 is necessary a greater number of repetitions to get the same confidence on the results with respect to ϵ_{res}. In our simulations we fix $N = 10^5$ so that we can be fairly sure that the results obtained converge.

The outcomes of this approch will be shown in chapter 6 after discussing analytically the properties of a single qubit following an annealing dynamics. Despite the power of this method one has to face the problem of the computational effort of repeting a large amount of times the same evolution. It will be necessary, then, to find a compromise between the precision of the results and the computational effort.

Chapter 5

Adiabatic master equations

In the following we describe the coupling of a quantum system to a thermal bath and develop the master equations suited to study the time evolution of the density matrix.
Adiabatic evolution in open quantum systems, that are systems coupled to an environment, is still an interesting topic and subject of several studies. In this regard, our concern is to a derive a master equation governing the evolution of a quantum system described by a time-dependent Hamiltonian. In this chapter we will trace the road to obtain a master equation in Lindblad form, while keeping track of the psysical approximations and time and energy scales. We will leave out most of the calculation details and tools developement for which the reader might refer to Ref.[33] and references therein.

A general system-bath Hamiltonian can be written as:

$$H(t) = H_S(t) + H_B + H_I, \tag{5.1}$$

where:

- $H_S(t)$ is the time-dependent system Hamiltonian. In the absence of the other terms, the free system evolution operator is

  $$U_S(t, t') = Te^{-i\int_{t'}^{t} d\tau H_S(\tau)}. \tag{5.2}$$

  where T is the time-ordering operator that orders the terms of the exponential series cronologically.

- H_B is the bath Hamiltonian and the corresponding evolution operator can be expressed as:
$$U_B(t,t') = e^{-iH_B(t-t')}. \tag{5.3}$$
- The last term, H_I describes the interaction between system and bath. Without loss of generality one can write it in the form:
$$H_I = g\sum_a A_a \otimes B_a, \tag{5.4}$$
where A_a and B_a are Hermitian and dimensionless operators, describing the system and the bath respectively, and g is a coupling costant.

If we denote with ρ the density operator of the system-bath ensemble, it has to satisfy the Von-Neumann equation ($\hbar = 1$):

$$i\frac{d\rho}{dt}(t) = [H(t), \rho(t)]. \tag{5.5}$$

It is more convenient to transform the operators in the Interaction picture (see appendix B). Hence, we can exploit the definition $U_0(t,t') = U_S(t,t')\otimes U_B(t,t')$, to obtain the following evolution operator, density matrix and interaction Hamiltonian:

- $\tilde{U}(t,0) = U_0^+(t,0)U(t,0)$
- $\tilde{\rho}(t) = U_0^+(t,0)\rho(t)U_0(t,0)$
- $\tilde{H}_I(t) = U_0^+(t,0)H_I(t)U_0(t,0)$

It can be seen, immediately, that $\tilde{U}(t,0)$ and $\tilde{\rho}$ have to satisfy the following differential equations:

$$\frac{d\tilde{U}}{dt}(t,0) = -i\tilde{H}_I(t)\tilde{U}(t,0), \quad \tilde{U}(0,0) = \mathbb{1}, \tag{5.6a}$$

$$\frac{d\tilde{\rho}}{dt}(t) = -i[\tilde{H}_I(t), \tilde{\rho}(t)], \quad \tilde{\rho}(0) = \mathbb{1}, \tag{5.6b}$$

5.1 Derivation of the master equation in Lindblad form

Equation 5.6b has as formal solution

$$\tilde{\rho}(t) = \tilde{\rho}(0) - i\int_0^t d\tau[\tilde{H}_I(\tau), \tilde{\rho}(\tau)]. \tag{5.7}$$

It is useful to substitute this expression back in 5.6b in order to obtain an equation for $\tilde{\rho}$ and trace over the bath degrees of freedom to obtain an equation for the reduced density matrix describing S:

$$\frac{d\tilde{\rho}_S}{dt}(t) = -iTr_B[\tilde{H}_I(t), \rho\tilde{(0)}] - Tr_B[\tilde{H}_I(t), \int_0^t d\tau[\tilde{H}_I(t-\tau), \tilde{\rho}(t-\tau)]]. \quad (5.8)$$

To simplify this equation one can recall the *Born approximation*. If we denote with $\chi(t)$ the density operator which describes the correlation between system and bath, we can express $\tilde{\rho}$ as $\tilde{\rho} = \tilde{\rho}_S(t) \otimes \tilde{\rho}_B + \chi(t)$. Therefore, neglecting $\chi(t)$, one has:

$$\frac{d\tilde{\rho}_S}{dt}(t) = g^2 \sum_{\alpha,\beta} \int_0^t d\tau[A_\beta(t-\tau)\tilde{\rho}_S(t-\tau), A_\alpha(t)]\mathcal{B}_{\alpha\beta}(t, t-\tau) + h.c. \quad (5.9)$$

The function $B_{\alpha\beta}(t, t-\tau)$ is a two-point correlation function defined as

$$\mathcal{B}_{\alpha\beta}(t, t-\tau) = \langle B_\alpha(t) B_\beta(t-\tau)\rangle = Tr[B_\alpha(t) B_\beta(t-\tau)\rho_B]. \quad (5.10)$$

We assume that it has a decaying behaviour with timescale τ_B. According to this, the choice of neglecting $\chi(t)$ is consistent. Furthermore it is also consistent with our idea of developing a master equation for adiabatic evolution of the system, indeed its state is close to the ground state at all times and "nearly pure" and, obviously, if $\tilde{\rho}_S$ is pure, then the correlation term χ(t) must vanish. In Eq.5.9 we have also supposed that $\langle B_\alpha\rangle = Tr[B_\alpha\tilde{\rho}_B(0)] = 0$ without loss of generality. In the previous approximation we need also to assume that the bath $\tilde{\rho}_B$ is stationary, hence the correlation function becomes homogeneous in time:

$$\mathcal{B}_{\alpha\beta}(t, t-\tau) = \langle B_\alpha(t) B_\beta(t-\tau)\rangle = \langle B_\alpha(\tau) B_\beta(0)\rangle = \langle B_\alpha(0) B_\beta(\tau)\rangle = \mathcal{B}_{\alpha\beta}(\tau, 0) \quad (5.11)$$

It is evident in 5.9 that the system density operators depends on the integration variable. A further approximation is to ignore the τ dependence in $\tilde{\rho}_S$ and extend the upper bound to infinity. This approximation is called *Markov approximation* and correspond to assume that the density operator has no memory of the previous state during the evolution. In conclusion, the equation of motion becomes:

$$\frac{d\tilde{\rho}_S}{dt}(t) = g^2 \sum_{\alpha,\beta} \int_0^\infty d\tau[A_\beta(t-\tau)\tilde{\rho}_S(t), A_\alpha(t)]\mathcal{B}_{\alpha\beta}(t, t-\tau) + h.c. + O(\tau_B^3 g^2) \quad (5.12)$$

We can apply the Markov approximation only if $\tau_\beta \ll 1/g$. However this final equation cannot resolve the dynamics of the system over a timescale shorter than τ_B.

In order to solve the master equation, we have to write all quantitites in a easier form to compute. Hence in the following we will try to express the integrals in term of a spectral density and simplify them taking advantage of the adiabatic evolution approximation.
First, let us introduce the spectral-density matrix

$$\Gamma_{\alpha\beta}(\omega) \equiv \int_0^\infty d\tau e^{i\omega\tau}\mathcal{B}_{\alpha\beta}(\tau). \tag{5.13}$$

This is a one-sided Fourier transform; it is convenient to replace it by a complete one as follows:

$$\Gamma_{\alpha\beta}(\omega) = \frac{1}{2}\gamma_{\alpha\beta}(\omega) + iS_{\alpha\beta}(\omega) \tag{5.14}$$

and one can show that $\gamma_{\alpha\beta}(\omega)$ and $S_{\alpha\beta}(\omega)$ are given by

$$\gamma_{\alpha\beta}(\omega) = \int_{-\infty}^\infty d\tau e^{i\omega\tau}\mathcal{B}_{\alpha\beta}(\tau) = \gamma^*_{\alpha\beta}(\omega), \tag{5.15a}$$

$$S_{\alpha\beta}(\omega) = \int_{-\infty}^\infty \frac{d\omega'}{2\pi}\gamma_{\alpha\beta}(\omega')P(\frac{1}{\omega-\omega'}) = S^*_{\alpha\beta}(\omega). \tag{5.15b}$$

To demonstrate the 5.14 we can start from the definition 5.13 and replace the correlation function $\mathcal{B}_{\alpha\beta}(\tau)$ with his Fourier tranform $\gamma_{\alpha\beta}(\omega)$. Therefore we obtain

$$\Gamma_{\alpha\beta}(\omega) = \int_0^\infty \int_{-\infty}^\infty \frac{d\tau d\omega}{2\pi} e^{i(\omega-\omega')}\gamma_{\alpha\beta}(\omega') \tag{5.16}$$

which gives the 5.14 using the following property:

$$\int_0^\infty e^{i(\omega-\omega')\tau} = \pi\delta(\omega-\omega') + iP(\frac{1}{\omega-\omega'}). \tag{5.17}$$

If we assume that the bath is in thermal equilibrium as well as stationary, then it follows that the correlation function $\mathcal{B}_{\alpha\beta}(\tau)$ satisfies the Kubo-Martin-Schwinger condition:

$$\langle B_a(\tau)B_b(0)\rangle = \langle B_b(0)B_a(\tau+i\beta)\rangle, \tag{5.18}$$

where β is the inverse temperature $\beta = 1/k_BT$. In addition, if the correlation function is analytic for $\tau \in [-i\beta, 0]$, then it can be shown that the Fourier transform $\gamma_{ab}(\omega)$ satisfies the, so called, detailed balance condition:

$$\gamma_{ab}(-\omega) = e^{-\beta\omega}\gamma_{ab}(\omega). \tag{5.19}$$

In the following we will replace the correlation function with its Fourier transform; we will also make use of the adiabatic approximation to rewrite the master equation.

Let us suppose that the system is evolving in the fully adiabatic limit (App.D). The system evolution operators can be written as

$$U_S(t,t') = U_s^{ad}(t,t') + O(\frac{h}{\Delta^2 t_f}) \tag{5.20a}$$

$$U_S^{ad}(t,t') = \sum_a |\epsilon_a(t)\rangle \langle\epsilon_a(t)| e^{-i\mu_a(t,t')}, \tag{5.20b}$$

where t_f is the total evolution time and Δ is the minimum ground state energy gap. The operator in 5.20b describes an ideal adiabatic evolution which evolves the eigenstate $|\epsilon_a(t)\rangle$ in the same eigenstate at a later time $|\epsilon_a(t')\rangle$. During the evolution the system acquires a geometric phase

$$\mu_a(t,t') = \int_{t'}^{t} d\tau[\epsilon_a(\tau) - \phi_a(\tau)] \tag{5.21}$$

which is known as Berry phase (Appendix C).
To achieve our goal of arriving to a master equation expressed in terms of the spectral density matrix, our idea is to replace the system operator $A_\beta(t-\tau) = U_S^+(t-\tau)A_\beta U_S(t-\tau)$ with an appropriate adiabatic approximation. First, let us note that

$$U_S(t-\tau,0) = U_S(t-\tau,t)U_S(t,0) = U_S^+(t,t-\tau)U_S(t,0). \tag{5.22}$$

Now we can replace $U_S(t,0)$ with his adiabatic approximation $U_S^{ad}(t,0)$ and then $U_S^+(t,t-\tau)$ with $e^{iH_s(t)\tau}$; this second statement is justified by the fact that the bath correlation make the integral vanish in a very short time τ_B. Therefore we can write:

$$U_S(t-\tau,0) \approx e^{iH_S(t)\tau}U_S^{ad}(t,0). \tag{5.23}$$

The next step is to insert this expression in the right-hand side of the 5.12 together with using the spectral densisty function instead of the correlation function $\mathcal{B}_{\alpha\beta(\tau)}$. The operator $A_\beta(t-\tau)$ becomes

$$\begin{aligned} A_\beta(t-\tau) =& U_S^+(t-\tau,0)A_\beta U_S(t-\tau,0) = \\ =& U_S^{ad+}(t,0)e^{-iH_S(t)\tau}A_\beta e^{iH_S(t)\tau}U_S^{ad}(t,0) = \\ =& \sum_{a,b} |\epsilon_a(0)\rangle \langle\epsilon_a(t)| e^{i\omega_{ba}(t)\tau}e^{-i\mu_{ba}(t,0)}A_\beta |\epsilon_b(t)\rangle \langle\epsilon_b(0)| = \\ =& \sum_{a,b} e^{-i\mu_{ba}(t,0)} \langle\epsilon_a(t)| A_\beta |\epsilon_b(t)\rangle \Pi_{ab}(0)e^{i\omega_{ba}(t,0)\tau}. \end{aligned} \tag{5.24}$$

where $\mu_{ba}(t,0) = \mu_b(t,0) - \mu_a(t,0)$, $\omega_{ba}(t) = \epsilon_b(t) - \epsilon_a(t)$ and $\Pi_{ab}(t) = |\epsilon_a(t)\rangle \langle\epsilon_b(t)|$. Hence we have

$$\begin{aligned} &\int_0^\infty A_\beta(t-\tau)\tilde{\rho}_S(t)A_\alpha(t)\mathcal{B}_{\alpha\beta}(\tau) \approx \\ &\approx \sum_{a,b} e^{-i\mu_{ba}(t,0)} \langle\epsilon_a(t)| A_\beta |\epsilon_b(t)\rangle \Pi_{ab}(0) \int_0^\infty d\tau e^{i\omega_{ba}(t,0)\tau}\mathcal{B}_{\alpha\beta}(\tau). \end{aligned} \tag{5.25}$$

We have a similar expression also for the other term and we can use these and the spectral density matrix to arrive at the following *one-sided adiabatic interaction picture master equation*:

$$\frac{d\tilde{\rho}_S}{dt} = g^2 \sum_{a,b,\alpha,\beta} e^{-i\mu_{ba}(t)} \Gamma_{\alpha\beta}(\omega_{ba}(t)) A_{\beta ab}(t) [\Pi_{ab}(0)\tilde{\rho}_S(t), A_\alpha(t)] + h.c. \quad (5.26)$$

where $A_{\beta ab}(t) = \langle \epsilon_a(t)| A_\beta |\epsilon_b(t)\rangle$. Starting from this expression we can transform the master equation back into the Schrödinger picture. However, let us note first that we can use the adiabatic approximation for $A_\alpha(t)$ as well as for $A_\beta(t-\tau)$. If this is done, we obtain the *double-sided adiabatic interaction picture master equation* that it is convenient to switch in the Schrödinger picture. In the end, we get the following expression:

$$\frac{d\rho_S}{dt} = -i[H_S(t), \rho_S(t)] + g^2 \sum_{a,b,\alpha,\beta} \Gamma_{\alpha\beta}(\omega_{ba}(t)) [L_{ab,\beta}(t)\rho_S(t), A_\alpha] + h.c. \quad (5.27)$$

with the short notation $L_{ab,\beta}(t) \equiv A_{\alpha ab}(t) |\epsilon_a(t)\rangle \langle \epsilon_b(t)| = L^+_{ba,\alpha}$.
The master equation we have found so far is not in the Lindlbad form, which we strictly need as it guarantees the positivity of the density matrix at any time during the evolution, hence we have to exploit an additional approximation.
Previously we have introduced the Markov approximation neglecting the τ dependence of $\tilde{\rho}_S$ and extending the integral in dτ from t to ∞. If we had used the adiabatic approximation before taking the limit ($t \to \infty$), we would have got the following expression:

$$\begin{aligned} &\int_0^t d\tau A_\beta \tilde{\rho}_S(t) A_\alpha(t) \mathcal{B}_{\alpha\beta}(\tau) \approx \\ &\approx \int_0^t d\tau \sum_{abcdc} e^{-i[\mu_{ba}(t,0)+\mu_{dc}(t,0)]} |\epsilon_a(0)\rangle \langle \epsilon_a(t)| A_\beta |\epsilon_b(t)\rangle \times \\ &\times \langle \epsilon_b(0)| \tilde{\rho}_S(t) |\epsilon_c(0)\rangle \langle \epsilon_c(t)| A_\alpha |\epsilon_d(t)\rangle \langle \epsilon_d(0)| e^{i\omega_{ba}(t)\tau} \mathcal{B}_{\alpha\beta}(\tau). \end{aligned} \quad (5.28)$$

Sending $t \to \infty$, we can say that the terms for which the phase factor $\mu_{ba}(t,0) + \mu_{dc}(t,0) = \int_0^t d\tau[\omega_{dc}(\tau) + \omega_{ba}(\tau) - (\phi_d(\tau) - \phi_c(\tau)) + (\phi_b(\tau) - \phi_a(\tau))]$ vanishes are the ones that contribute more to the integral in 5.28 enforcing the energy conservation conditions: $a = d, b = c$ or $a = b, c = d$. This result, known as *Rotating Wave Approximation* (RWA), allows us to proceed in the derivation of the master equation and, transforming it back to the Schrödinger's picture, we

get the *Schrödinger's picture adiabatic master equation in Lindblad form*:

$$\begin{aligned}\frac{d\rho_S}{dt} &= i[H_S(t) + H_{LS}(t), \rho_S(t)]+ \\ &+ \sum_{a\neq b,\alpha,\beta} \gamma_{\alpha\beta}(\omega_{ba}(t))\Big[L_{ab,\beta}(t)\rho_S(t)L^+_{ab,\alpha}(t) - \frac{1}{2}\{L_{ab,\alpha}(t)^+ L_{ab,\beta}(t), \rho_S(t)\}\Big]+ \\ &+ \sum_{a,b,\alpha,\beta} \gamma_{\alpha\beta}(0)\Big[L_{aa,\beta}(t)\rho_S(t)L^+_{bb,\alpha}(t) - \frac{1}{2}\{L_{aa,\alpha}(t)^+ L_{bb,\beta}(t), \rho_S(t)\}\Big],\end{aligned} \tag{5.29}$$

where the term H_{LS} is said Hermitian Lamb shift and has the following form:

$$H_{LS}(t) = \sum_{\alpha,\beta}\Big[\sum_{a\neq b} L_{ab,\beta}(t)L^+_{ab,\alpha}(t)S_{\alpha\beta}(\omega_{ba}(t)) + \sum_{a,b} L_{aa,\beta}(t)L^+_{bb,\alpha}(t)S_{\alpha\beta}(0)\Big]. \tag{5.30}$$

The operatators $L_{ab,\beta}$ are called *Lindblad operators*. In the previous expression we have included the factor g^2 in the Fourier transform $\gamma_{\alpha\beta}(\omega_{ba})$. This Lindblad form for our master equation guarantees the positivity of the density matrix, indeed from the Bochner's theorem the Fourier transform of the bath correlation functions is positive since the bath correlations are positive functions.
The Lindblad equation is usually written in the generic form

$$\frac{d\rho_S}{dt} = -i[H, \rho_S(t)] + \mathcal{D}(t)[\rho_S(t)]. \tag{5.31}$$

where $H = H_S + H_{LS}$. It is possible to transform 5.29 in 5.31, replacing all the sums over the eingenvalues with sums over their differences:

$$\sum_{a,b} \to \sum_{\omega=\epsilon_b-\epsilon_a} \Longrightarrow L_{ab,\beta} \to L_{\omega,\beta} = \sum_{\omega} |\epsilon_a(t)\rangle \langle\epsilon_a(t)| A_\beta |\epsilon_b(t)\rangle \langle\epsilon_b(t)| \tag{5.32}$$

In conclusion, Eq.5.29 can be expressed as 5.31 where $\mathcal{D}$ and H_{LS} take the following form:

$$\mathcal{D}(t) = \sum_{\alpha,\beta,\omega} \gamma_{\alpha\beta}(\omega)\Big[L_{\omega,\beta}(t)\rho_S(t)L^+_{\omega,\alpha}(t) - \frac{1}{2}\{L^+_{\omega,\alpha}(t)L_-\omega,\beta(t), \rho_S(t)\}\Big] \tag{5.33a}$$

$$H_{LS} = \sum_{\alpha,\beta,\omega} S_{\alpha\beta}(\omega)L^+_{\omega,\alpha}(t)L_{\omega,\beta}(t). \tag{5.33b}$$

5.2 Approximations and time scales

In the previous section we have derived a master equation in Lindblad form. In the following we will introduce the relations that must be satisfied by the time scales and the coupling constants to justify the assumptions above.
The first approximation is the so called *Born approximation*. In the weak coupling limit for the interaction between the system and the bath, we said that we could decompose the density matrix $\tilde{\rho}$ as $\tilde{\rho} = \tilde{\rho}_S(t) \otimes \tilde{\rho}_B + \chi(t)$ and neglect $\chi(t)$. We have not given an answer about the magnitude of the coupling constant. If we define the minimum ground state energy gap as Δ_{min}:

$$\Delta_{\text{min}} = \min_{t\in[0,t_f]} [\epsilon_1(t) - \epsilon_0(t)] \tag{5.34}$$

where $\epsilon_0(t)$ and $\epsilon_1(t)$ are the ground and first excited state energies of $H_S(t)$, we require that

$$\frac{g^2\tau_B}{\Delta_{\text{min}}} \ll 1. \tag{5.35}$$

In this inequality we see the coupling constant g (let us remember that the interaction between system and bath has been written as $H_I = g\sum_a A_a \otimes B_a$) and the coherence time τ_B of the bath correlation function $\mathcal{B}_{\alpha\beta}(t, t-\tau)$. This yeld us to the second approximation: the *Markov Approximation*.
In appendix B of Ref.[33] an upper bound associated with the markovian assumption is derived which involves the replacement of $\tilde{\rho}_S(t-\tau)$ by $\tilde{\rho}_S(t)$ and the extension of the upper integration limit to infinity. This bound goes to zero with an appropriate choice of the correlation time τ_B which must be smaller than the system relaxation time $1/g$:

$$g\tau_B \ll 1. \tag{5.36}$$

Correlated with the relaxation time of the system is also the *Rotating Wave Approximation*. In the RWA, rapidly oscillating terms are neglected, ensuring that the quantum master equation is in Lindblad form. This is valid, again, if the time scale of the oscillations is much shorter than the relaxation time $1/\text{g}$.
Furthermore, there are two additional time scales we have to concern about which refer to the adiabatic evolution of the system. As shown in appendix D adiabatic conditions require:

$$\max_{s\in[0,1]} \frac{|\langle\epsilon_k(s)|\,\partial_s H\,|\epsilon_{k'}(s)\rangle|}{t_f\Delta_{kk'}^2} \ll 1 \rightarrow \frac{h}{t_f\Delta_{\text{min}}^2} \ll 1 \tag{5.37}$$

where $s = \frac{t}{t_f}, h = \max_{s\in[0,1]} |\langle\epsilon_k(s)|\,\partial_s H\,|\epsilon_{k'}(s\rangle)|$, $\Delta_{kk'}^2 = |\epsilon_k(s) - \epsilon_{k'}(s)|^2$ and $\tau, k(s)$ are replaced by $t_f, \epsilon_k(s)$. This condition must be satisfied during all the evolution

and furthermore we require the change in the eigenbasis to be small on the time scale of the bath τ_B. Then, we must also have that

$$\frac{h\tau_B}{t_f} \ll 1. \tag{5.38}$$

In conclusion all the time scale condition can be reassumed by the following inequalities;

$$g\tau_B \ll \min\Big(1, \frac{\Delta_{\min}}{g}\Big) \tag{5.39a}$$

$$\frac{h\tau_B}{\Delta_{\min} t_f} \ll \min\Big(\Delta_{\min}\tau_B, \frac{1}{\Delta_{\min}\tau_B}\Big) \tag{5.39b}$$

Provided that these condition are satisfied we are sure that the master equation we have written before is justified and that it describes the system-bath dynamics neglecting only terms that are higher orders in our approximations.

Chapter 6

Single qubit dynamics

In this section, we are going to describe the evolution of a single qubit in the presence of decoherence using the master equation in the Lindblad form developed in the previous chapter.
First of all, we have to choose the type of the interaction between the system and the bath in the Hamiltonian $H(t) = H_S(t) + H_B + H_I$. We assume that the system is coupled to a thermal bath of harmonic oscillators described by the Hamiltonian

$$H_B = \sum_{k=1}^{\infty} \omega_k b_k^+ b_k, \tag{6.1}$$

where b_k^+ and b_k are, respectively raising and lowering operators for the k-th oscillator with frequency ω_k. The interaction between the system and the bath can be expressed as

$$H_I = \sum_{i=1}^{N} \sigma_z^i \otimes B_i \tag{6.2}$$

where N is, in general, the number of considered qubits. The operators B_i are defined by

$$B_i = \sum_k g_k^i (b_k^+ + b_k), \tag{6.3}$$

where g_k^i are the constants that couple the i-th spin with the k-th oscillator. In this work we consider that all the coupling constants are equal to g and that the bath is in thermal equilibrium at inverse temperature $\beta = 1/k_B T$ and described by an ohmic spectral density:

$$\gamma(\omega) = 2\pi\eta \frac{g^2 \omega e^{-\frac{|\omega|}{\omega_c}}}{1 - e^{-\beta\omega}}. \tag{6.4}$$

Here we set a frequency cutoff ω_c that is the maximum phonon energy. η is a positive coupling constant wth dimensions of time squared [39].
In order to study the behavior of the system during quantum annealing, following Ref.[39] we start with the description of the qubit dynamics in two particular cases:

$$\begin{aligned} &\text{Pure dephasing case: } H_S = \frac{\Gamma_z}{2}\sigma_z \text{ and } H_I = g\sigma_z \otimes B, \\ &\text{Full decoherence case: } H_S = \frac{\Gamma_x}{2}\sigma_x \text{ and } H_I = g\sigma_z \otimes B. \end{aligned} \tag{6.5}$$

Afterwards we will describe the annealing dynamics by means of the hamiltonian

$$H_S = (1-s)\frac{\Gamma_x}{2}\sigma_x + s\frac{\Gamma_z\sigma_z}{2} \tag{6.6}$$

and calculate the Leggett-Garg's inequalities in the absence and in the presence of interaction with the thermal bath.

6.1 Pure dephasing

We first decribe the case listed: $H_S = \frac{\Gamma_z}{2}\sigma_z$ and $H_I = g\sigma_z \otimes B$. The eigenvector and the eigenvalues of H_S are, respectively, $|\downarrow\rangle, |\uparrow\rangle$ and $-\frac{\Gamma_z}{2}, +\frac{\Gamma_z}{2}$. Here we denoted with $|\downarrow\rangle$ ($|\uparrow\rangle$) the state with spin down (up) but we may use also the computational basis notation $|0\rangle$ ($|1\rangle$). The Lindblad operators in Eq.5.32 are all zero except for $L_{0,z} = \sigma_z$ because H_S and H_I commute

$$[H_S, H_I] = 0 \tag{6.7}$$

and so they have the same eigenvectors.
Furthermore the term H_{LS} in Eq.5.31 is $\propto \mathbb{1}$ and the master equation for the single qubit becomes:

$$\frac{d}{dt}\rho(t) = -i[H_S, \rho(t)] + \gamma(0)[L_{0,z}\rho(t)L^+_{z,0} - \frac{1}{2}\{L^+_{0,z}L_{0,z}, \rho(t)\}] \tag{6.8}$$

This equation can be solved analytically giving the following populations and coherences of the density matrix

$$\rho_{00}(t) = \rho_{00}(0), \tag{6.9a}$$

$$\rho_{01}(t) = \rho_{01}(0)e^{-\frac{t}{T_2^c} - i\Gamma_z t}. \tag{6.9b}$$

The term T_2^c is the decoherence time in the computational basis. We see that the off-diagonal elements decay with characteristic time scale T_2^c, while the diagonal terms remain unaltered (thermalization time $T_1 \to \infty$). This is due to the fact that H_S and H_I commute hence the population of the eigenstates remain fixed.

6.2 Full dechoerence

In this section we are going to analyse the case with $H_S = \frac{\Gamma_x}{2}\sigma_x$ and $H_I = g\sigma_z \otimes B$. The eigenvectors of the Hamiltonian can be written in the logic base as:

$$|\epsilon_\pm\rangle = \frac{1}{\sqrt{2}}(|0\rangle \pm |1\rangle), \tag{6.10}$$

where the $|0\rangle, |1\rangle$ are the eigenvectors of σ_z. These two eigenstates are associated with the eigenvalues $\pm\Gamma_x/2$ respectively. There are two non-zero Lindblad operators which we denote as:

$$\begin{aligned} L_{\Gamma_x} &= |\epsilon_-\rangle \langle\epsilon_+|, \\ L_{-\Gamma_x} &= |\epsilon_+\rangle \langle\epsilon_-|. \end{aligned} \tag{6.11}$$

With some algebra we can write the term $H_{LS} = S(-\Gamma_x)|\epsilon_-\rangle\langle\epsilon_-| + S(\Gamma_x)|\epsilon_+\rangle\langle\epsilon_+|$ and hence the Lindblad equation for the density matrix of the qubit:

$$\frac{d}{dt}\rho_{--} = -\gamma(-\Gamma_x)\rho_{--}(t) + \gamma\Gamma_x\rho_{++}(t), \tag{6.12a}$$

$$\frac{d}{dt}\rho_{-+} = \left[-i[S(-\Gamma_x) - S(\Gamma_x) - \Gamma_x] - \frac{1}{2}\gamma(-\Gamma_x)(1 + e^{\beta\Gamma_x})\right]\rho_{-+}. \tag{6.12b}$$

These equations can be solved analytically using the condition 5.19 and they give the following results:

$$\rho_{--}(t) = [\rho_{--}(0) - P_{Gibbs}(-)]e^{-t/T_1^{(e)}} + P_{Gibbs}(-), \tag{6.13a}$$

$$\rho_{-+}(t) = 2\rho_{-+}(0)e^{-i[S(-\Gamma_x) - S(\Gamma_x) - \Gamma_x]t}e^{-t/T_2^{(e)}}. \tag{6.13b}$$

where $P_{Gibbs}(\pm) = \frac{1}{Z}e^{\mp\beta\Gamma_x/2}$ and the partition function $Z = e^{\beta\Gamma_x/2} + e^{-\beta\Gamma_x/2}$. In this expressions we have used $T_1^{(e)}$ and $T_2^{(e)}$ where the superscript *e* signals that we are working in the energy eigenbasis. The relaxation time $T_1^{(e)}$ is given by

$$T_1^{(e)} = \frac{1}{\gamma(\Gamma_x)(1 + e^{-\beta\Gamma_x})}, \tag{6.14}$$

instead the decoherence time is $T_2^{(e)} = 2T_1^{(e)}$. The off-diagonal terms approach to zero with a time scale determined by $T_2^{(e)}$, while the population converge to the population of the Gibbs states in time $T_1^{(e)}$.

6.3 Annealing schedule

We are now ready to consider the annealing dynamics of the single qubit described by the following Hamiltonian:

$$H(s) = (1-s)\frac{\Gamma_x}{2}\sigma_x + s\frac{\Gamma_z}{2}\sigma_z. \tag{6.15}$$

Here $s = t/t_f$, $s \in [0,1]$ and t_f is the annealing time. The system-bath interaction is schematised according to Eq.6.2 and the Hamiltonian H(s) interpolates between the "Full Dechoerence" and the "Pure Dephasing" case. The eigenvalues change during the dynamics according to the expression $\epsilon_\pm(s) = \frac{1}{2}\sqrt{(1-s)^2\Gamma_x^2 + s^2\Gamma_x^2}$. We define the instantaneous energy gap $\Delta(s)$ so that $\epsilon_\pm(s) = \pm\Delta(s)/2$. The energy gap is minimum in $s = \frac{1}{1+\Gamma^2}$ where values $\Delta_{\text{min}} = \frac{\Gamma_x\Gamma_z}{\sqrt{\Gamma_x^2+\Gamma_z^2}}$, with Γ we are denoting the ratio $\Gamma = \Gamma_z/\Gamma_x$. It is useful defining a dimensionless instantaneous gap

$$\lambda(s) = \frac{\Delta(s)}{\Gamma_x} = \sqrt{(1-s)^2 + s^2\Gamma^2} \tag{6.16}$$

so that $\lambda_{\text{min}} = \frac{\Gamma}{1+\Gamma^2}$. Furthermore we may obtain the istantaneous eigenvectors with some algebra and get the following expressions:

$$|\epsilon_+(s)\rangle = \frac{1}{c_+(s)}\left[\frac{s\Gamma - \lambda(s)}{1-s}|0\rangle + |1\rangle\right], \tag{6.17a}$$

$$|\epsilon_-(s)\rangle = \frac{1}{c_-(s)}\left[\frac{s\Gamma + \lambda(s)}{1-s}|0\rangle + |1\rangle\right]. \tag{6.17b}$$

The terms $c_+(s)$ and $c_-(s)$ are appropriate constants, at fixed s, which normalize the eigenvectors. We know that the annealing time must satisfy the adiabatic condition

$$\max_{s\in[0,1]} \frac{|\langle k(s)|\,\partial_s H\,|k'(s)\rangle|}{t_f\Delta_{kk'}^2} \ll 1 \rightarrow \frac{h}{t_f\Delta_{min}^2} \ll 1, \tag{6.18}$$

derived in appendix D. We might demonstrate that $h = \frac{\Gamma_x^2}{2}\sqrt{1+\Gamma^2}$, hence the previous inequalities becomes:

$$\frac{\frac{1}{2}\sqrt{1+\Gamma^2}\Gamma_x^2}{t_f^2\Delta_{\text{min}}} \ll 1. \tag{6.19}$$

Here we can use the dimensionless istantaneous energy gap to write the adiabatic condition as

$$t_f\Gamma_x \gg \frac{\Gamma}{2\lambda_{\text{min}}^3}. \tag{6.20}$$

As done in section 6.2 we have to find the Lindblad operators. Since in Eq.5.32 we have to sum over the differences of the energy eigenvalues ω, we observe that here we have $\omega = 0, \pm\Delta(s)$. Hence,

$$L_{0,z} = \frac{s\Gamma}{\lambda(s)}\Big[\,|\epsilon_-\rangle\langle\epsilon_-| - |\epsilon_+\rangle\langle\epsilon_+|\,\Big], \tag{6.21a}$$

$$L_{\pm\Delta,z} = -\frac{1-s}{\lambda(s)}\,|\epsilon_\mp\rangle\langle\epsilon_\pm|\,. \tag{6.21b}$$

The index z is the analogous of the index β in Eq.5.32, however since there is only a qubit coupled to the bath, according to H_I, we can drop such subscript. Starting from these definition we must write the Eq.5.31 explicitly. Therefore, let us start from $\frac{d\rho(s)}{dt}$; it can be expressed in function of the dimensionless time s as follows:

$$\frac{d\rho(s)}{dt} = \frac{1}{t_f}\frac{d\rho(s)}{ds}. \tag{6.22}$$

Since we must evaluate separately the differential equation for each density matrix element. Let us start from the expression

$$\frac{d}{ds}\langle\epsilon_\pm|\,\rho\,|\epsilon_\pm\rangle = \partial_s(\langle\epsilon_\pm|)\rho\,|\epsilon_\pm\rangle + \langle\epsilon_\pm|\,\partial_s\rho\,|\epsilon_\pm\rangle + \langle\epsilon_\pm|\,\rho\,\partial_s(|\epsilon_\pm\rangle), \tag{6.23}$$

hence the left-hand side of Eq.5.31 becomes

$$\langle\epsilon_\pm|\,\frac{d\rho}{ds}\,|\epsilon_\pm\rangle = \left[\frac{d}{ds}\rho_{\pm\pm} - \partial_s(\langle\epsilon_\pm|)\rho\right]|\epsilon_\pm\rangle - \langle\epsilon_\pm|\,\rho\,\partial_s(|\epsilon_\pm\rangle). \tag{6.24}$$

Perfoming the derivatives in Eq.6.24, after some algebra, we obtain the result

$$\langle\epsilon_\pm|\,\frac{d\rho}{ds}\,|\epsilon_\pm\rangle = \frac{d\rho_{\pm\pm}}{ds} + \frac{\Gamma}{2\lambda^2(s)}\Big[\rho_{\pm\mp}(s) + \rho_{\mp\pm}\Big]. \tag{6.25}$$

The equation for the ground state population is:

$$\begin{aligned}\frac{d\rho_{--}}{ds} - \frac{\Gamma}{2\lambda^2(s)}\Big[\rho_{-+} + \rho_{+-}\Big] = &-it_f\,\langle\epsilon_-|\,[H_{LS} + H_S, \rho(s)]\,|\epsilon_-\rangle + \\ &+ t_f\,\langle\epsilon_-|\,\mathcal{D}(t)[\rho(s)]\,|\epsilon_-\rangle\,.\end{aligned} \tag{6.26}$$

From Eq.5.33a and Eq.5.33b it is straightforward to obtain $\mathcal{D}[\rho(s)]$ and H_{LS} using Eq.6.21. Eventually, we get the following differential equation:

$$\frac{d\rho_{--}(s)}{ds} = \frac{\Gamma}{2\lambda^2(s)}[\rho_{-+}(s) + \rho_{+-}(s)] + [\mathcal{F}_+(s)\rho_{++}(s) - \mathcal{F}_-(s)\rho_{--}(s)], \tag{6.27}$$

where $\mathcal{F}_{\pm} = t_f \frac{(1-s)^2}{\lambda^2(s)} \gamma(\pm\Delta(s))$. In a similar way we could derive the equation for ρ_{+-} which is the one we miss for a complete description of the evolution of the system, because $\rho_{++} = 1 - \rho_{--}$ and $\rho_{-+} = \rho^*_{+-}$. Introducing the following functions:

$$\Omega(s) = t_f \Delta(s) + t_f \frac{(1-s)^2}{\lambda^2(s)} [S(\Delta(s)) - S(-\Delta(s))], \tag{6.28a}$$

$$\Sigma(s) = t_f \Big\{ 2\gamma(0) \Big[\frac{\Gamma s}{\lambda}\Big]^2 + \frac{1}{2} \Big[\gamma(\Delta(s)) + \gamma(-\Delta(s))\Big] \frac{(1-s)^2}{\lambda^2(s)} \Big\}, \tag{6.28b}$$

we may write

$$\frac{d\rho_{+-}}{ds} = \frac{\Gamma}{2\lambda^2(s)} [\rho_{--}(s) - \rho_{++}(s)] - [i\Omega(s) + \Sigma(s)]\rho_{+-}(s). \tag{6.29}$$

In this equation, the term involving $\Sigma(s)$ is responsible for the exponential decay of the off-diagonal terms on a time scale $t_f/\Sigma(s)$.For s=0 and s=1, the expected decay time should be T_2^e and T_2^c respectively, that denotes that the Hamiltonian H_S interpolates between the two Hamiltonians in Eq.6.5 as well as the Lindblad operators.
Since the functions $\mathcal{F}, \Omega$ and Σ have a non trivial dependence from the annealing time t_f, the ground state population also depends on the time t_f. In order to solve the annealing dynamics we proceed numerically assuming that the spectral density is equal to the one in Eq.6.4. Considering $\Gamma_x = \Gamma_z = 1$GHz we choose $t_f = 10\sqrt{2}$ in units of $1/\Gamma_x$ so that the condition in Eq.6.20 is satisfied as in Ref.[33]. The time evolution is perfomed with the fourth-order Runge Kutta method to solve the differential equation for the density matrix. In the case of closed-system evolution, that is neglecting the interaction with the thermal bath, we obtain that the ground state population oscillate due to non-adiabatic transitions and approaches to 1 at the annealing time.
This is depicted in red in Fig.6.1. If we turn on the coupling to the thermal bath, the qubit evolves as the curve in orange in Fig.6.1. It is evident that the population of the ground state depends on the interaction with the bath. Indeed, it influences the system trying to populate the energy levels following the Boltzman distribution. Of course increasing the final time may be beneficial for the annealing dinamycs but at the same time it could cause the quantum adiabatic algorithm to perform worse, because relaxation effects may dominate. This is shown in Fig.6.2 where we observe that, in the case of unitary evolution, the fidelity remains equal to one increasing the annealing time while, if the system is interacting with the thermal bath, it decreases after reaching a maximum value at a certain t_f. A stronger interaction causes a faster reduction of the ground state population with respect to the annealing time, hence its maximum is lower

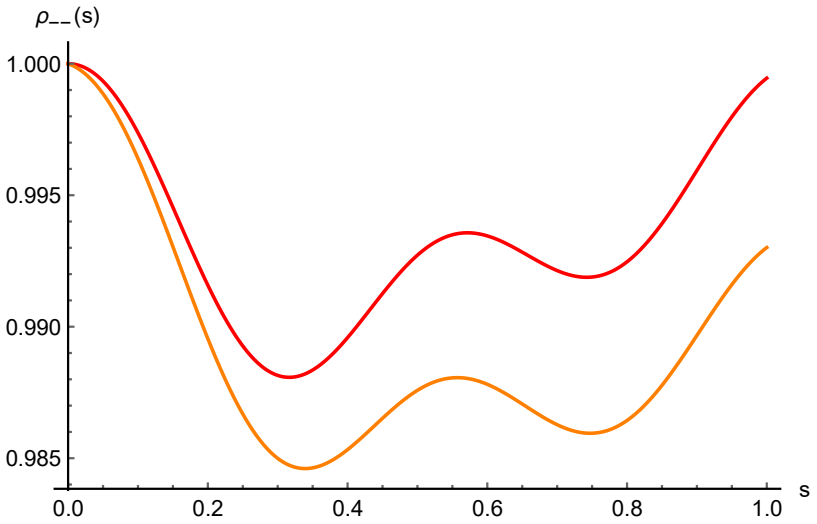

Figure 6.1: Ground state population of a single spin during the annealing dynamics with and without coupling to a thermal bath (orange,red). Here we set the annealing time t_f equal to $10\sqrt{2}$ in units of $1/\Gamma_x$ so that the adiabatic condition is satisfied. We see that the ground state population fluctuate due to unitary nonadiabatic transitions. In the case of coupling to a thermal bath we set $\beta = 1/2.23$, $\eta g^2 = 10^{-4}$ and $\omega_c = 25$, it is evident that the oscillation is damped by the bath.

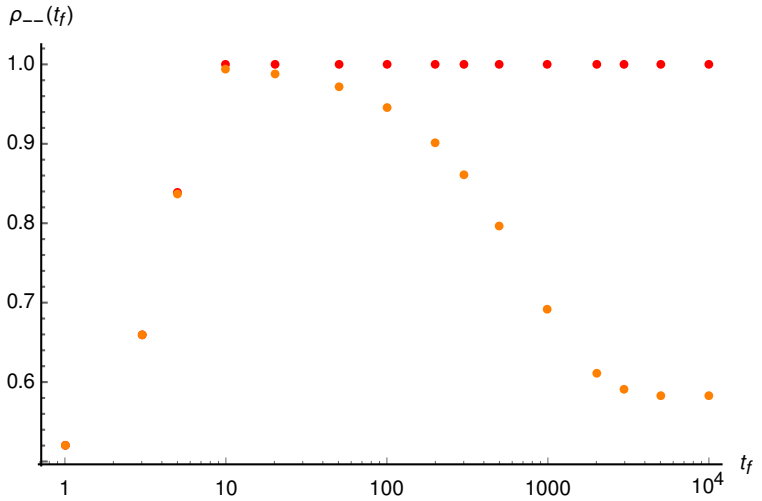

Figure 6.2: Ground state population of a system, consisting of a single qubit, during the annealing dynamics, with and without coupling to a thermal bath (orange,red). Here we set the annealing time t_f equal to $10\sqrt{2}$ in units of $1/\Gamma_x$ so that the adiabatic condition is satisfied. We see that the ground state population decreases with t_f in the case of interaction, approaching eventually to $\rho_{gs} \approx 0.61$ which is the population of the ground state according to the Boltzman distribution. We set $\beta = 1/2.23$, $\eta g^2 = 10^{-4}$ and $\omega_c = 25$.

in magnitude and it reaches its equilibrium value for smaller t_f. The equilibrium value is, of course, given by the Boltzman distribution and it is $\rho_{gs} \approx 0.61$ in this special case.
However, what we are interested in is whether or not the evolution of the system is quantum till the annealing time. Indeed we would verify that systems which make use of the quantum annealing are actually perfoming quantum evolutions. For this reason, in the next section we will use the formalism developed in chapter 4 and we will calculate and discuss the Leggett-Garg's inequalities for the system described in this section.

6.4 LGIs with weak measurements

System-bath interaction causes the thermalization of the system in a certain time, which reflects in a lost of fidelity.
The fidelity $\rho_{--}(t_f)$ as well as the residual energy ϵ_{res} are reliable control parameters for the annealing, but do not provide any information on the nature of the evolution. On the other hand the LGIs may be used as witness of the quantum coherence of a system but their calculation could be detrimental for the annealing dynamics. With this in mind, we need to evaluate how much the weak measurements developed in chapter 4 still influence the system.
In Fig.6.3 we show the residual energy as a function of D which is the variance of the gaussian distributions in Eq.4.16. We remind the reader that, since it represents the width of the distributions, D can be considered also as a parameter that describes the strenght of the measurement. The large is D the weaker is the interaction. In Fig.6.3 we observe three curves per points corresponding to three different times at which a single measurement per run has been performed. It is evident that projective measurements, which are the ones corresponding to $D \to 0$, strongly perturb the system; indeed the residual energy is very large, giving evidence that the annealing dynamics has not been successful. Weakening the measurements, the residual energy approaches the value of the unperturbed case, which is $\epsilon_{\text{res}} = 5.49 \cdot 10^{-4}$, eventually reaching it for $D \approx 10^3$.
However the case $D \approx 10^3$ is still interesting from the theoretical point of view but meaningless from an experimental point of view, corresponding to a situation where the interaction is so weak to be practically null and difficult to manage by an experimentalist. Therefore let us point out that already from $D = 10$ the influence of the measurement is small enough to be fairly sure that the annealing dynamics is hardly perturbed. At the same time, the choice of a lower value of D allows an easier implementation of the method discussed in chapter 4 both from a theoretical and from an experimental point of view. Indeed, the large is the variance D, that is the uncertainty of the measurement, the greater is the num-

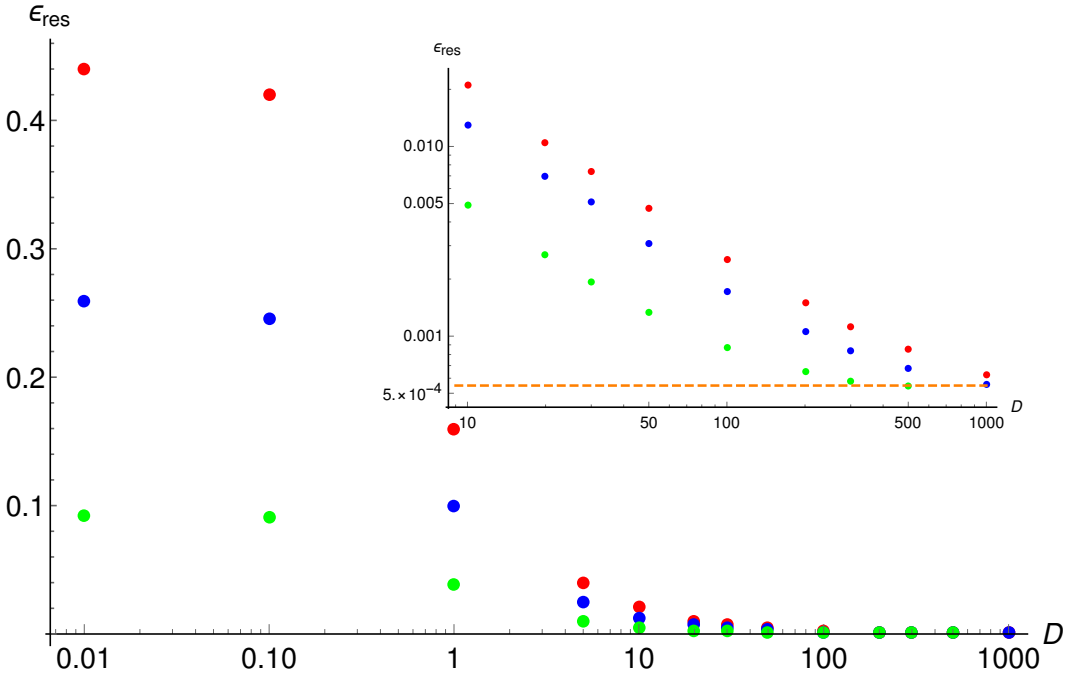

Figure 6.3: Log-linear plot of the residual energy of the system as a function of the variance D and of the measurement time t. We set $t_f = 10\sqrt{2}$; a single measrurement has been performed per run at times 0.3 t_f, 0.5 t_f and 0.7 t_f (red, blue, green).

- Red, 0.3 t_f,
- Blue, 0.5 t_f,
- Green, 0.7 t_f.

We observe that the residual energy decreases eventually going to $5.49 \cdot 10^{-4}$ which is the residual energy of the system in the absence of interaction. The inset shows the trend in the interval $D \in [10, 10^3]$ in bilogarithmic scales highlighting the value $5.49 \cdot 10^{-4}$ with a dashed orange line.

ber of repetitions needed to collect enough information, and calculate the LGIs with a given confidence. For instance, in Fig.4.2 we have shown the error on the residual energy and on the function K_3 at fixed D=50. Let us start describing the way we proceed to simulate the annealing dynamics. Our time-dependent Hamiltonian is

$$H_S(s) = (1-s)H_0 + sH_I = (1-s)\frac{\Gamma_x}{2}\sigma_x + s\frac{\Gamma_z}{2}\sigma_z, \tag{6.30}$$

we start the annealing schedule with the qubit in the ground state of H_0 and we evolve it solving the differential equation for the density matrix with the fourth-order Runge-Kutta method. We showed in chapter 5 that the density matrix obeys the differential equation

$$\frac{d\rho_S}{dt} = -i[H, \rho_S(t)] + \mathcal{D}(t)[\rho_S(t)]. \tag{6.31}$$

where the term $\mathcal{D}(t)[\rho_S(t)]$ is due to the interaction with the thermal bath and $H = H_S + H_{LS}$. $H_L S$ is given by Eq.5.33b. During the evolution we calculate the LGIs, evaluating the correlation functions $\langle Q_\alpha Q_\beta \rangle$ at different times.
In our example Q_α is a current flowing through a quantum point contact, therefore in the following we will denote it with $I(t)$; we remind the reader that measuring the current flowing across a QPC dependent on a DQD is equivalent to measuring the observable σ_z. Indeed, the current is dichotomic. i.e. it can assume only two values depending on the position of the electron in the DQD, and we may associate to it a spin degree of freedom (see chapter 4).
Since we do not care about the evolution after the second measurement we can perform a weak measurement at time t_α and a projective one at time t_β, $t_\alpha < t_\beta$. The weak measurement at time t_α modifies the density matrix according to the update rule

$$\rho'_S = \frac{1}{\rho_{11}e^{\gamma} + \rho_{22}e^{-\gamma}} \begin{pmatrix} \rho_{11}e^{\gamma} & \rho_{12} \\ \rho_{12}^* & \rho_{22}e^{-\gamma} \end{pmatrix} \tag{6.32}$$

which describes neglegible changes for appropriate choices of D in $\gamma = I(t_\alpha)/D$. At time t_β we can perform a strong measurement and evaluate the product $I(t_\alpha)I(t_\beta)$. Weak measurements may give strange values, as pointed out before. With this in mind, in order to collect enough information and obtain a reasonable result, we must repeat this evolution N times and average the different outcomes of $I(t_\alpha)I(t_\beta)$. In the following we will take into account D=50 and we will repeat our measurement $N = 10^5$ times for each choice of the times t_α and t_β. The simulation may be carried out by a code written in Fortran language which executes the Runge-Kutta method and solve the differential equation with and without the system-bath coupling.

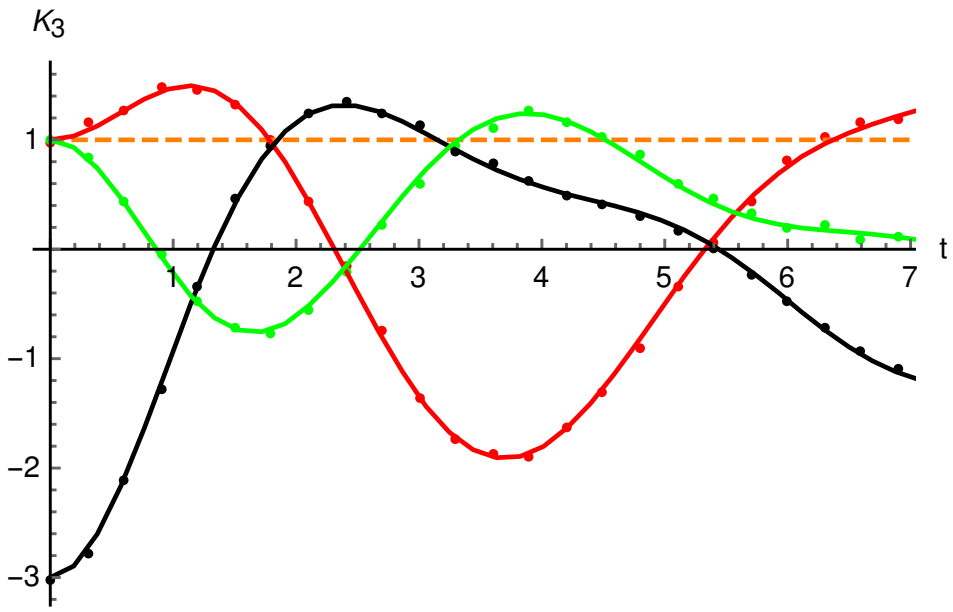

Figure 6.4: Plot of the Leggett-Garg's functions during the annealing dynamics of a qubit, without coupling to a thermal bath. The curves are guides for the eyes, being the ones obtained performing projective measurements. The points are the values calculated with our method, considering D=50 and N=10^5. The different curves are depicted with different colours: K_3 in red, K_3' in black and K_{perm} in green. The orange line highlights the bound of the LGI. The LG's functions ar plotted as function of the difference of the times at which the measurements have been perfomed: $t_2 - t_1 = t_3 - t_2 = t$. The time t goes from 0 to $t_f/2$ so that it scans the whole evolution.

In order to compare with the existing literature, Ref.[39], we choose the parameters as the previous example, that are $\Gamma_x = 1\text{GHz} = \Gamma_z$ and $t_f = 10\sqrt{2}$ in units of $1/\Gamma_x$. First, we can evaluate the LGIs for the closed system. In Fig.6.4 we show the LG's functions. The lines are the results obtained performing projective measurements and serve as guide for the eyes. The points are the results of our approach. Here we must highlight that the Leggett-Garg's inequalities are calculated without perturbing the system during its annealing dynamics. We can use them to assert that the system is following a quantum dynamics and, in general, as an evidence of the quantum nature of the evolution. In this case at the end of the annealing dynamics the function K_3 is above the bound $K_3 = 1$ ensuring us that the dynamics is quantum. Of course this is a trivial observation because we are not taking into account any source of dechoerence. However it is useful to be compared with the following results.
Let us now fix the inverse temperature $\beta = 10$ in units of Γ_x and let us con-

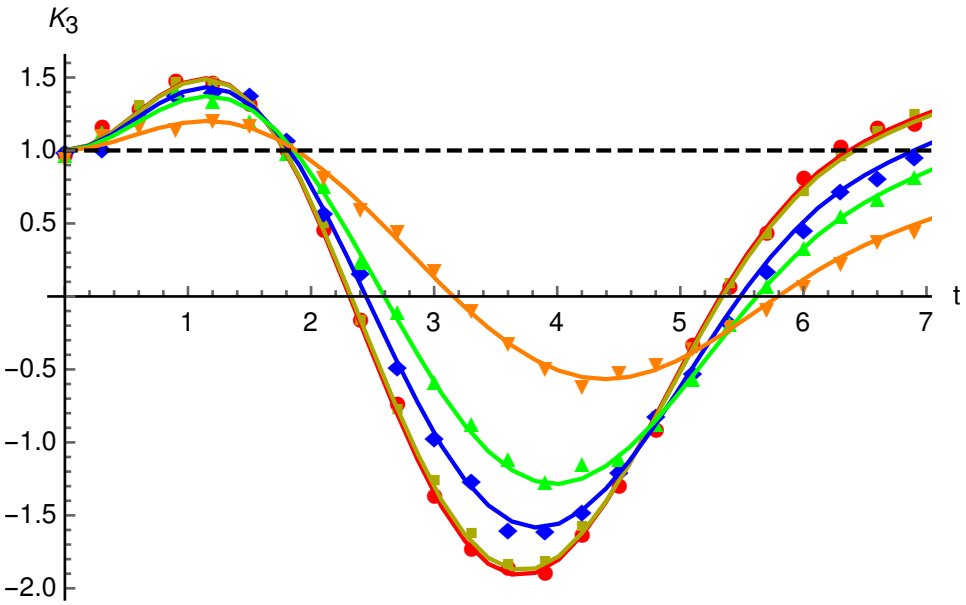

Figure 6.5: Plot of the Leggett-Garg's function K_s during the annealing dynamics with different coupling constant to a thermal bath. The curves are guides for the eyes, being the ones obtained performing projective measurements. The points are the values calculated with our method, considering $\beta = 10$,D=50 and N=10^5.

- Red, $\eta g^2 = 0$,
- olive, $\eta g^2 = 10^{-3}$,
- blue, $\eta g^2 = 10^{-2}$,
- green, $\eta g^2 = 2 \times 10^{-2}$,
- orange, $\eta g^2 = 5 \times 10^{-2}$.

The black line highlights the bound of the LGIs. The LG's functions ar plotted as function of the difference of the times at which the measurements have been perfomed: $t_2 - t_1 = t_3 - t_2 = t$. The time t goes from 0 to $t_f/2$ so that it scans the whole evolution.

sider different values of the coupling strenght, i.e. g. As before we fix a cut-off frequency $\omega_c = 25$. From Fig.6.4 we get that the only function beyond the quantum to classical bound at times approximately equal to $t_f/2$ is K_3, hence in the following we will take into account only that function.
Switching on the interaction between the system and the environment we obtain different Leggett-Garg's functions as shown in Fig.6.5. Here we plot only the K_3 for different values of the coupling between the system and the bath. The points obtained with our method follow the curves calculated through projective measurement and present a different behavior depending on the constant ηg^2. The different curves are depicted with different colours: we observe that the red and the blue ones, that correspond to $\eta g^2 = 0$ and $\eta g^2 = 10^{-3}$,almost overlap, therefore we can assert that the coupling is too weak to influence the system during its annealing dynamics. Increasing the interaction the function K_3 decreases, eventually falling below the limit and ensuring us that the evolution of the system is no more quantum. We expect that the quantum behavior lasts less increasing temperature, because classical properties should be destroyed faster when the system is coupled to a "hot" environment. For this reason we show the behavior of the LG's function K_3 at fixed coupling but for different values of the inverse temperature. We set $\eta g^2 = 10^{-3}$ so that, for $\beta = 10$, K_3 is beyond the bound at t=t_f, and we study the evolution of the system for different values of β. From Fig.6.6, it is evident that the temperature plays a key role in the detrimental effect of the thermal bath. For low temperatures the quantum behavior persists during the whole evolution even in the presence of coupling with the environment. However increasing temperature the time during which the system shows quantum features decreases eventually going to zero for very high temperatures.
However using a master equation written in Lindblad form contraints us to take into account only the weak coupling limit. Then the results shown for very high temperatures might be beyond our approximation and they should be considered with attention.

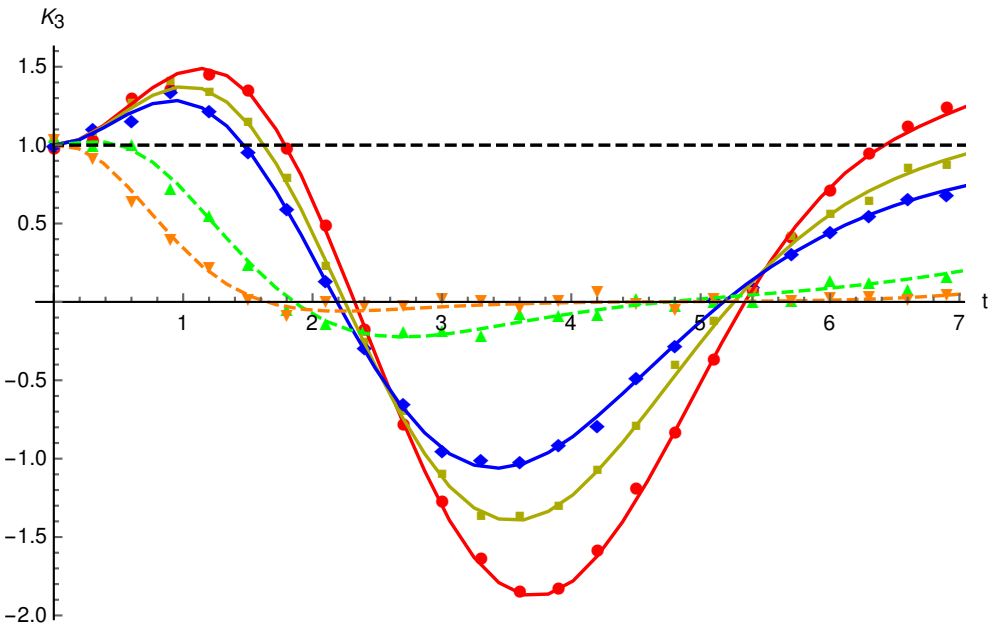

Figure 6.6: Plot of the Leggett-Garg's function K_s during the annealing dynamics with different coupling constant to a thermal bath. The curves are guides for the eyes, being the ones obtained performing projective measurements. The points are the values calculated with our method, considering D=50 and N=10^5.

- Red, $\beta = 10$,
- olive, $\beta = 0.1$,
- blue, $\beta = 0.05$,
- green, $\beta = 0.01$,
- orange, $\beta = 0.005$.

The black line highlights the bound of the LGIs. The LG's functions ar plotted as function of the difference of the times at which the measurements have been perfomed: $t_2 - t_1 = t_3 - t_2 = t$. The time t goes from 0 to $t_f/2$ so that it scans the whole evolution.

Conclusions

In this work we discuss the problem of the quantum annealing of a single qubit in the presence of dissipation due to a thermal bath of harmonic oscillators at inverse temperature β.
We focus on the research of a quantum coherence estimator, developing the formalism of the Leggett-Garg's inequalities and evaluating them to check the behavior of the system under investigation.
We provide a new method to derive the Leggett-Garg's inequalities without perturbing the system with projective measurement and we conclude that the LGIs might be used as witness of quantum coherence. Although our scheme of measurement needs a heavy computational effort, we show that it is possible to find a compromise between the number of simulation needed and the strenght of the interaction between measurement device and system.
The system described is very simple, but we do not exclude the possibilty of extending this way of reasoning for more complicated ensambles. A system of N (> 1) spins ordered in a Ising chain might be an interesting topic of research for next studies.
In conclusion we may ask ourselves if we have found an answer to the question proposed at the beginning. Actually we have provided a method to evaluate the LGIs which gives us information about the "quantumness" of the system under investigation. In principle, one may use it to check the behavior of a quantum annealer if it is possible to measure the LGIs along the adiabatic dynamics.
On the other hand, we have not provided yet a general approach to evaluate the evolution of every sort of system.
Since the newest quantum annealer are composed of hundreds of qubits, it is necessary to study and design, starting from what we have done, a more powerful tool to investigate their behavior.

Appendices

Appendix A

Higher order Leggett-Garg's inequalities

In this appendix we derive the correlation function C_{ij} for a large ensamble of qubits and discuss the violation of Leggett-Garg's inequalities. We take into account a system of N qubits described by the Hamiltonian $H = \Gamma_x J_x$ where J_x is the x-component of the total angular momentum. The first step to obtain the correlation functions is to choose the dichotomic variable; for example we may consider $Q_m = 1 - 2\delta_{m,-j}$, so that it is -1 when the z-component of the total angular momentum m is equal to -j and $+1$ otherwise. The choice is arbitrary and the reader can refer to [25] for more examples.
Moreover, for every quantum system evolving in time under an evolution operator U, the correlation functions can be expressed as follows (Ref.[28]):

$$C_{ab} = \sum_l \sum_m Q_l Q_m Tr(\Pi_m U_{ab} \Pi_l U_{0a} \rho(t_0) U_{0a}^+ \Pi_l U_{ab}^+). \tag{A.1}$$

Here we are using Π_m for the projector onto the eigenstate of J_z with eigenvalue m, and we are denoting with U_{ab} the evolution operator from time t_a to time t_b. The $\rho(t_0)$, indeed, is the density matrix of the system at time t_0.

We set the initial state of the system equal to $\rho = |j\rangle \langle j|$ where with $|j\rangle$ we are denoting the eigenstate of the z-component of the total angular momentum J_z with eigenvalue j. Calculating the correlation function C_{ab} we perform the trace on the J_z base at fixed J^2 because the evolution cannot change its value.

$$C_{ab} = \sum_l \sum_m \sum_k Q_l Q_m \langle k| \Pi_m U_{ab} \Pi_l U_{0a} |j\rangle \langle j| U_{0a}^+ \Pi_l U_{ab}^+ |k\rangle . \tag{A.2}$$

Firstly, we can observe that $\langle k| \Pi_m = \langle k|m\rangle \langle m| = \delta_{k,m} \langle m|$ and we can simplify the expression above:

$$C_{ab} = \sum_l \sum_m Q_l Q_m \langle m| U_{ab} \Pi_l U_{0a} |j\rangle \langle j| U_{0a}^+ \Pi_l U_{ab}^+ |m\rangle . \tag{A.3}$$

Secondly, we can also explicit the projectors and put the equation in the following form:

$$C_{ab} = \sum_l \sum_m Q_m Q_l |\langle m| U_{ab} |l\rangle|^2 |\langle l| U_{0a} |j\rangle|^2. \tag{A.4}$$

As written before, our system evolves accorrding to the operator $U = e^{-i\Gamma_x J_x t}$ ($\hbar = 1$), therefore we have to calculate the quantity:

$$\langle m| e^{-i\Gamma_x J_x (t_\beta - t_\alpha)} |l\rangle . \tag{A.5}$$

With this in mind, we can exploit the Wigner D-matrices writing the rotation around the x-axis in terms of the Euler's angles:

$$e^{-i\Gamma_x J_x (t_b - t_a)} = e^{-iJ_z\alpha} e^{-iJ_y\beta} e^{-iJ_z\gamma}. \tag{A.6}$$

Since what we are insterested in is the absolute square of the matrix element of the evolution, we can ignore the rotations around the z axis that provide only a phase factor. Therefore, the matrix element reads

$$|\langle m| U_{ab} |l\rangle|^2 = (d^j_{m,l})^2(\beta), \tag{A.7}$$

where $d^j_{m,l}$ is the reduced Wigner D-matrix and β is the rotation angle around the z axis, dependent on $t_b - t_a$. To obtain the rotation angle we have to compare the rotation matrices $e^{-i\Gamma_x J_x (t_b - t_a)}$ and $e^{-iJ_z\alpha} e^{-iJ_y\beta} e^{-iJ_z\gamma}$. They must describe the same rotation. Doing so, we can demonstrate that

$$\cos\beta = \cos\Gamma_x (t_b - t_a). \tag{A.8}$$

Finally, we write the correlation function in a more useful and intuitive form:

$$C_{ab} = \sum_m \sum_l Q_m Q_l \left(d^j_{m,l}(\beta_1)\right)^2 \left(d^j_{l,-j}(\beta_2)\right)^2, \tag{A.9}$$

where the reduced Wigner D-matrices are tabulated. We used the "Mathematica" software to do these calculations.
For the case $J = \frac{1}{2}$, we can check the result obtained using the ones in section 3.2. The correlation function C_{ab} becomes:

$$C_{ab} = \sum_{m,l=\pm\frac{1}{2}} Q_m Q_l \left(d^{\frac{1}{2}}_{m,l}(\beta_1)\right)^2 \left(d^{\frac{1}{2}}_{l,-\frac{1}{2}}(\beta_2)\right)^2. \tag{A.10}$$

Here, $d^{\frac{1}{2}}_{\frac{1}{2},\frac{1}{2}}(\beta) = \cos\frac{\beta}{2}$ and $d^{\frac{1}{2}}_{\frac{1}{2},-\frac{1}{2}}(\beta) = \sin\frac{\beta}{2}$, so, remembering $Q_m = 1 - 2\delta_{m,-\frac{1}{2}}$, the expression above reads

$$\begin{aligned} C_{ab} = & \cos\frac{\beta_1}{2}^2 \sin\frac{\beta_2}{2}^2 - \sin\frac{\beta_1}{2}^2 \cos\frac{\beta_2}{2}^2 + \\ & - \sin\frac{\beta_1}{2}^2 \sin\frac{\beta_2}{2}^2 + \cos\frac{\beta_1}{2}^2 \cos\frac{\beta_2}{2}^2 = \\ & = \cos\beta_1 = cos[\Gamma_x (t_b - t_a)]. \end{aligned} \tag{A.11}$$

The correlation function is equal to the one found for a qubit described by the Hamiltonian $H = \frac{\Gamma_x \sigma_x}{2}$ in chapter 3.

More interesting results can be provided studying the cases of $J = 1$ and $J = \frac{3}{2}$. We do not report the analytic expression of the correlation and we show their behavior in Fig A.1 and Fig.A.2. The times at which the measurements are performed have been chosen as in section 3.2: the first time is $t_1 = \pi$ and $t_{i+1} - t_i = t$. Then, the plots show the curves in function of the time difference between two subsequent measurements. We see that only for certain values of t the Leggett-Garg's inequalities are violated (a function is beyond the bounds) and there is not the chance for a complete detection of the non-classical properties of the system because K_3 and K_3' are no more complementary as in the case of a single qubit.
One could suggest that exist higer-order Leggett-Garg's functions that could satisfy the above-mentioned property, which is that at least a function takes values above the bound at every time. However, one can observe that, despite the trivial case of the single qubit which already satisfies that property for the lowest order in n of K_n, it is not true for systems with a total angular momentum larger than $1/2$. For instance we can show the case of $J = 1$, calculating all the possible Leggett-Garg's functions of the fourth-order and plotting them. Without reporting the analytic expressions of all the different quantities, Fig.A.3 shows their behavior in time, where the convention for the time measurement is always the same (i.e. $t_1 = \pi$,$t_{i+1} - t - i = t$).
Observing Fig.A.3, one can notice that the bounds are not always violated despite the fact that we are taking into account all the possibile time permutations. This can be shown for all the orders of the inequalities and for all the systems except for the simple qubit, as we said above. With this in mind, we can say that the study of the Leggett-Garg's inequalities of order higher than the third seems not to provide further information with respect to K_3,K_3' and $K_{3\mathsf{perm}}$.

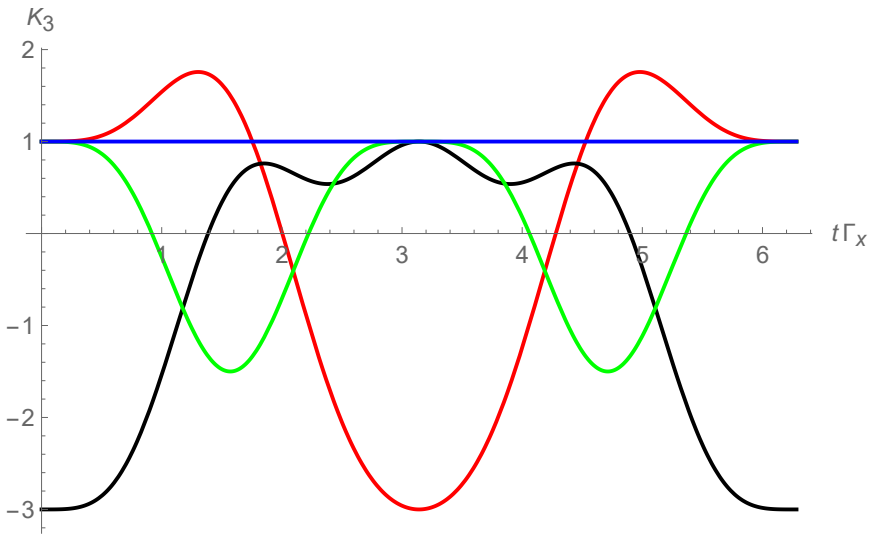

Figure A.1: Plot of the Leggett-Garg's functions K_3,K_3' and K_{3perm} in function of the time difference between two measurements for J=1. K_3 in red, K_3' in black and K_{3perm} in green.

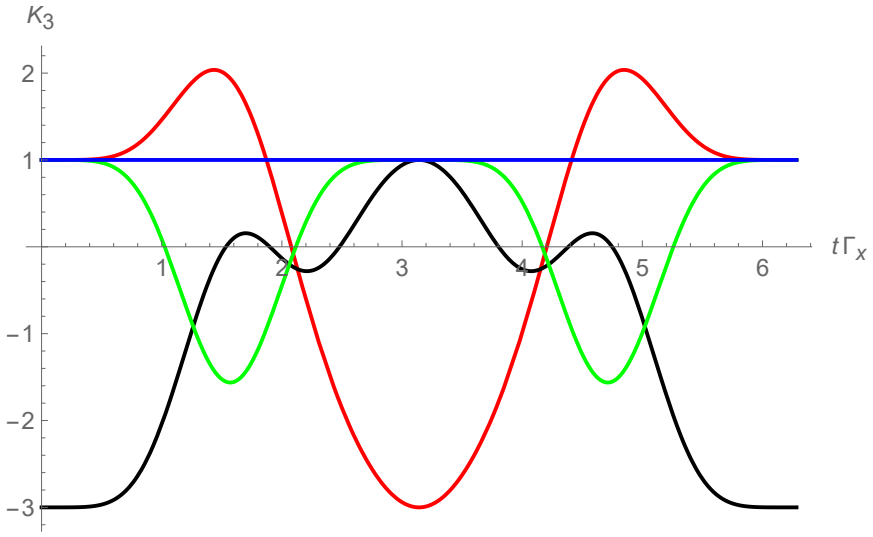

Figure A.2: Plot of the Leggett-Garg's functions K_3,K_3' and K_{3perm} in function of the time difference between two measurements for $J = \frac{3}{2}$. K_3 in red, K_3' in black and K_{3perm} in green.

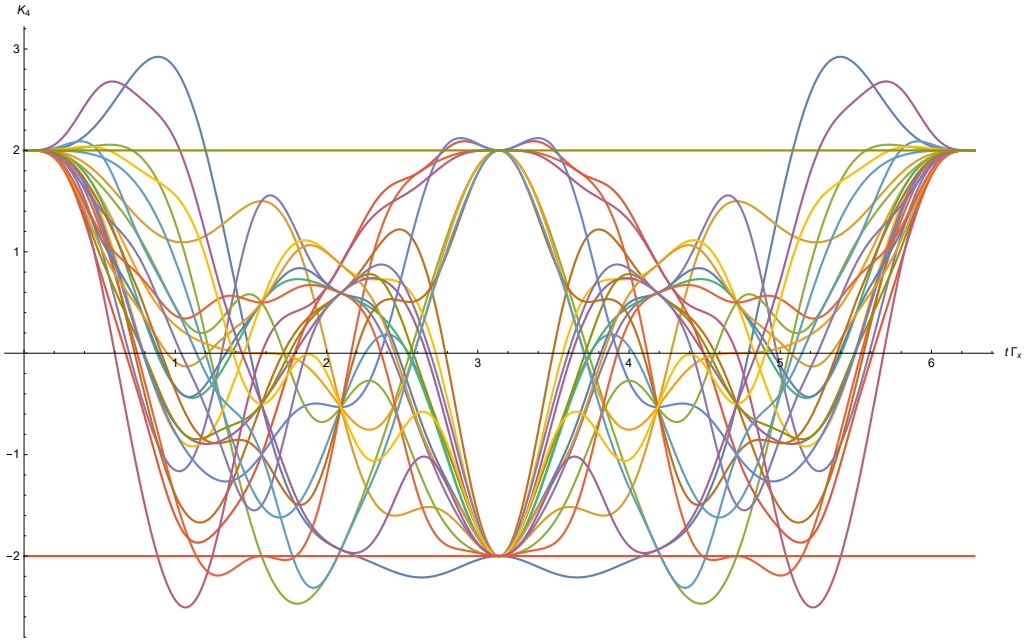

Figure A.3: All the possible functions obtained from K_4 by permutation of time indices, for J=1. The two horizontal lines mark the bounds for the macroscopic realism of the system.

Appendix B

Schrödinger, Heisenberg and Interaction picture

Following [31], in this appendix we will briefly recall the different pictures of the quantum mechanics.
According to the postulates of the quantum mechanics, the dynamic evolution of a state has to satisfy the Schrödinger equation:

$$i\hbar\frac{\partial\left|\psi\right\rangle(t)}{\partial t}=\hat{H}\left|\psi\right\rangle(t). \tag{B.1}$$

Every observable is associated with a hermitian operator whose mean value is the only physically meaningful quantity. Hence what we are interested in is the value of

$$\langle A\rangle=\langle\psi|\,A\,|\psi\rangle \tag{B.2}$$

in time, where A is a generic observable.
The time evolution of $< A >$ is usually described fixing the operator $\hat{A}$ in time, and considering a time dependent state $|\psi\rangle$ whose time dependence is determined by the equation above.
However, the same evolution can be fixed, even changing the time dependences of $|psi\rangle$ and $\hat{A}$. Hence one can describe the same evolution exploiting different pictures that we call the: Schrödinger picture, Heisenberg picture and Interaction picture.
If $|\psi\rangle$ and $\hat{A}$ are the state vector and an operator associated to an observable A at time t=0, we set:

$$\begin{aligned}|\psi\rangle&=\hat{W}(t)\,|\psi\rangle\\ \hat{A}(t)&=\hat{V}^{+}(t)\hat{A}\hat{V}(t)\end{aligned} \tag{B.3}$$

where both $\hat{W}(t)$ and $\hat{V}(t)$ are supposed unitary. The expectation value of $\hat{A}$ can be expressed as follows:

$$\langle \hat{A} \rangle(t) = \langle \psi | \hat{W}^{+}(t)\hat{V}^{+}(t)\hat{A}\hat{V}(t)\hat{W}(t) | \psi \rangle \tag{B.4}$$

with $\hat{U}(t) = \hat{V}(t)\hat{W}(t)$. The three different pictures we have talked about, correspond to various choices of $\hat{W}$ and $\hat{V}$ such that the operator $\hat{U}(t)$ satisfies the equation

$$i\hbar \frac{d\hat{U}(t)}{dt} = \hat{H}\hat{U}(t) \tag{B.5}$$

with initial condition $\hat{U}(0) = \mathbb{1}$. In the following we will analyse the different descriptions of the Quantum Mechanics.

- **Schrödinger picture**.
  This is equivalent to the coiches

$$\begin{aligned} \hat{W}(t) &= \hat{U}(t) \\ \hat{V}(t) &= \mathbb{1}. \end{aligned} \tag{B.6}$$

  Due to this claim the operators result time indipendent $\hat{A}_S(t) = \hat{A}$, hence the Hamiltonian $\hat{H}_s = \hat{H}$ and the state vector obeys to the following equation

$$i\hbar \frac{\partial |\psi\rangle_S}{\partial t}(t) = \hat{H}_S(t) |\psi\rangle_S (t) \tag{B.7}$$

- **Heisenberg picture**.
  The operators are set as:

$$\begin{aligned} \hat{W}(t) &= \mathbb{1} \\ \hat{V}(t) &= \hat{U}(t). \end{aligned} \tag{B.8}$$

  In this case the state vector is time indipendent $|\psi\rangle_H = |\psi\rangle = |\psi\rangle(0)$ and the operators follow the rule

$$i\hbar \frac{d\hat{A}_H}{dt}(t) = [\hat{A}_H(t), \hat{H}_H(t)]. \tag{B.9}$$

  This equation is called "Heisenberg equation" and can be easly deduced from the B.5, toghether with the initial condition $\hat{A}_H(0) = \hat{A}$.

- **Dirac or Interaction picture**.
  Let us suppose that $\hat{H}$ is the sum of two terms, hence it has the form: $\hat{H} = \hat{H}_0 + \hat{H}_1$. If one sets, with $\hat{V}(0) = \mathbb{1}$,

$$i\hbar \frac{d\hat{V}}{\partial t}(t) = \hat{H}_0 \hat{V}(t), \tag{B.10}$$

from B.5 we obtain:

$$\begin{aligned} 0 &= (\hat{H}_0 + \hat{H}_1)\hat{V}(t)\hat{W}(t) - i\hbar\frac{d\hat{V}}{dt}(t)\hat{W}(t) - i\hbar\hat{V}(t)\frac{\partial\hat{W}}{\partial t}(t) = \\ &= \hat{H}_1\hat{V}(t)\hat{W}(t) - i\hbar\hat{V}(t)\frac{d\hat{W}}{dt}(t) \end{aligned} \tag{B.11}$$

which becomes, multipling to the right side by $\hat{V}^+(t)$,

$$i\hbar\frac{d\hat{W}}{dt}(t) = \hat{H}_{1I}(t)\hat{W}(t). \tag{B.12}$$

with $\hat{W}(0) = \mathbb{1}$. Therefore, from B.10 and B.12, we come to the evolution equations for operators and state vectors:

$$\frac{d\hat{A}_I(t)}{dt} = \frac{\partial\hat{A}_I(t)}{\partial t} + \frac{1}{i\hbar}[\hat{A}_I(t), \hat{H}_{0I}(t)] \tag{B.13a}$$

$$i\hbar\frac{\partial\left|\psi\right\rangle_I}{\partial t}(t) = \hat{H}_{0I}(t)\left|\psi\right\rangle_I(t) \tag{B.13b}$$

Appendix C

Berry phase

The adiabatic approximation says that: if the time scale over which a Hamiltonian changes is long compared to $\hbar/\Delta^2$ (where Δ is the minimum energy gap between the eigenvalues of the spectrum of the system), a system beginning at time t_i in an istantaneous eigenstate $\psi_n(\vec{x}, t_i)$, will remain in this same eigenstate at all later times but develops a simple dynamical phase factor [32] (for a demonstration of the above mentioned theorem we remind the reader to appendix D):

$$e^{i\phi} = e^{-i\int_{t_i}^{t_f} dt E_n(t)}. \tag{C.1}$$

Where $E_n(t)$ e $\psi_n(\vec{x}, t)$ are the instantaneous eigenvectors and the eigenvalues of the Hamiltonian and satisfy the equation:

$$H(t)\psi_n(\vec{x}, t) = E_n(t)\psi_n(\vec{x}, t). \tag{C.2}$$

We know that, generally, it is possible to modify the global phase of a state vector without changing the system dynamics, although one may observe that this is not always true. In particular, when the final state ($t = t_f$) matches with the inital state ($t = t_i$) after an adiabatic evolution, a phase factior occurs: $e^{i\gamma_n}$ where

$$\gamma_n = i \oint dR_i \left\langle \psi_n(\vec{R_i}) \right| \vec{\nabla}_{R_i} \left| \psi_n(\vec{R_i}) \right\rangle. \tag{C.3}$$

Here, with $R_i(t)$ for $i = 1, 2, \ldots, k$, we mean a set of time dependent parameters, by which the Hamiltonian depends itself. This factor was studied by Berry, in 1984, and takes his name. We can derive this phase factor starting from the Schrödinger equation for a state $\psi(t)$ with $H = (R_i(t))$.

$$i\frac{d}{dt}\psi(t) = H(R_i(t))\psi(t) \tag{C.4}$$

Since the adiabatic approximation is satisfied, the state $\psi(t)$ can be expressed in function of the instantaneous eigenstate $\psi_n(t)$.

$$\psi(t) = \psi_n(t) e^{-i\int_{t_i}^{t_f} E_n(t)dt} e^{i\gamma_n} \tag{C.5}$$

Substituing the expression of $\psi(t)$ in the Schrödinger equation we obtain an equation for the phase factor γ_n

$$\dot{\gamma_n}(t) = i \int d^3\vec{x} \sum_i \psi_n^*(\vec{x}, R_i(t)) \vec{\nabla}_{R_i} \psi_n(\vec{x}, R_i(t)) \dot{R}_i(t), \tag{C.6}$$

which can be simplified recalling the vector $\vec{R}(t) = \begin{pmatrix} R_1(t) \\ R_2(t) \\ \vdots \\ R_k(t) \end{pmatrix}$ and changing $\psi_n(\vec{x}, R_i(t))$ in the ket notation $\left|n; \vec{R}(t)\right\rangle$

$$\dot{\gamma}_n = i \left\langle n; \vec{R}(t) \right| \vec{\nabla}_{\vec{R}} \left| n; \vec{R}(t) \right\rangle . \tag{C.7}$$

Berry realized that this phase is an observable when $R(t_f) \equiv R(t_i)$, that is when the system follows a cyclic evolution along a closed curve C in the parameters space. The gained geometric phase is called Berry phase and is written as:

$$\gamma_n = i \oint d\vec{R} \left\langle n; \vec{R}(t) \right| \vec{\nabla}_{\vec{R}} \left| n; \vec{R}(t) \right\rangle \tag{C.8}$$

The vector $\vec{A}_n(\vec{R}) = i \left\langle n; \vec{R}(t) \right| \vec{\nabla}_{\vec{R}} \left| n; \vec{R}(t) \right\rangle$ is called Berry connection and acts as a potential vector. The closed path integral of this field can be used to define the Berry curvature, according to the Stokes theorem: $\vec{B}_n = \vec{\nabla}_{\vec{R}} \times \vec{A}_n$. We observe that $\vec{\nabla}_R \vec{B}_n = 0$, hence as for the magnetic field $\vec{A}_n$ it can be redefined by a gauge transformation. This gauge choice implies that γ_n cannot be deleted by a redefinition of the phase factor of the inital state, and that comparing $\left|n; \vec{R}(t_f)\right\rangle$ and $\left|n; \vec{R}(t_i)\right\rangle$ we can obtain information about the acquired phase. Explicitly, we can see that modifying the inital state, sending $\left|n; \vec{R}(t)\right\rangle$ in $\left|n; \vec{R}(t)\right\rangle e^{i\phi_n}$, the Berry connection changes of the quantity $\vec{\nabla}_{\vec{R}} \phi_n$, which however do not touch γ_n:

$$\begin{aligned} \vec{A}_n \to \vec{A'}_n &= i \left\langle n; \vec{R}(t) \right| e^{-i\phi_n} \vec{\nabla}_{\vec{R}} e^{i\phi_n} \left| n; \vec{R}(t) \right\rangle \\ &= - \left\langle n; \vec{R}(t) \right| \vec{\nabla}_{\vec{R}} \phi_n \left| n; \vec{R}(t) \right\rangle + \vec{A}_n(\vec{R}) \\ &= \vec{A}_n(\vec{R}) - \vec{\nabla}_{\vec{R}} \phi_n \end{aligned} \tag{C.9}$$

It can be proved that the soruces of the Berry curvature $\vec{B}_n$ (if any) are the degeneration points of the energy, which results different from zero when the integration surface contains these field sources. Neglecting the exact derivation, one can obtain:

$$\vec{B}_n = -\mathrm{Im} \sum_{m \neq n} \frac{\left\langle n; \vec{R}(t) \right| \vec{\nabla}_{\vec{R}} H \left| m; \vec{R}(t) \right\rangle \left\langle m; \vec{R}(t) \right| \vec{\nabla}_{\vec{R}} H \left| n; \vec{R}(t) \right\rangle}{(E_m - E_n)^2} \quad \text{(C.10)}$$

Appendix D

The adiabatic theorem

Approaching the resolution of the dynamics of a system described by a time-dependent Hamiltonian one can follow several ways. Instead of requiring that the Hamiltonian change is small, which is done in perturbation theory, one can assume that the evolution is *slow enough*, say adiabatic. Defining how slowly the system must evolve and be aware of possible transitions between the eigenstates of the Hamiltonian, are the main problems of the adiabatic theory. In the following we will present a brief review of the adiabatic theorem in order to prove the adiabatic condition on the evolution time of the system.
Let us consider the Hamiltonian H depending, in general, by a multi-variate parameter s function of the time t, $s(t)$. We denote with $\{E_n(t)\}$ the instantaneous eigenvalues of H which correspond to the eigenvectors $\{|n(t)\rangle\}$. Let us assume the eigenvalues to be non-degenerate and discrete for sake of simplicity. A general wave function in the Hilbert space $\mathcal{H}$ at time t may be written as

$$|\psi(t)\rangle = \sum_n a_n(t)\,|n(t)\rangle \tag{D.1}$$

and it is determined by the Schrödinger's equation:

$$i\frac{d}{dt}\,|\psi(t)\rangle = H\,|\psi(t)\rangle\,, \tag{D.2}$$

where we set $\hbar = 1$. If we insert D.1 in D.2 we obtain:

$$i\Big(\sum_n \dot{a}_n(t)\,|n(t)\rangle + a_n\frac{d}{dt}\,|n(t)\rangle\Big) = \sum_n a_n E_n(t)\,|n(t)\rangle\,. \tag{D.3}$$

Projecting both sides on the vector $|k(t)\rangle$ we may get the equation for the coefficient a_k:

$$\dot{a}_k(t) = -ia_k E_k(t) - \sum_n a_n\,\langle k(t)|\,\frac{d}{dt}\,|n(t)\rangle\,. \tag{D.4}$$

With the useful definition $a_n(t) = c_n(t)e^{-i\int_0^t dt' E_m(t')}$ the first term on the right-hand side can be added to the second:

$$\dot{c}_k(t) = -\sum_n c_n(t)e^{-i\int_0^t E_n(t')dt'} e^{i\int_0^t E_k(t')dt'} \langle k(t)| \frac{d}{dt} |n(t)\rangle . \tag{D.5}$$

This equation can be also written as follows:

$$\dot{c}_k(t) = -c_k \langle k(t)| \frac{d}{dt} |k(t)\rangle - \sum_{n\neq k} c_n(t)e^{i\int_0^t (E_k(t')-E_n(t'))dt'} \langle k(t)| \frac{d}{dt} |n(t)\rangle . \tag{D.6}$$

With some algebra one can show that the scalar product $\langle k(t)| \frac{d}{dt} |k(t)\rangle$ reads:

$$\langle k(t)| \frac{d}{dt} |k(t)\rangle = \frac{\langle k(t)| \frac{dH}{dt} |n(t)\rangle}{E_n(t) - E_k(t)}. \tag{D.7}$$

Let us remind that H depends on a parameter s, hence

$$\frac{dH}{dt} = \frac{dH(s)}{ds}\frac{ds}{dt} = \dot{s}\frac{dH(s)}{ds} \tag{D.8}$$

We denote with the name *fully adiabatic limit* the case $\dot{s} \to 0$ which yelds to:

$$\dot{c}_k = -c_k \langle k(t)| \frac{d}{dt} |k(t)\rangle . \tag{D.9}$$

In this case the equation is easly integrable and if $|k(t)\rangle$ is the initial state of the system, the system remain in this state gaining only a phase factor. The solution of the equation is the following:

$$a_k(t) = a_k(0)e^{i\gamma_k(t)}e^{-i\int_0^t E_k(t')dt'}, \quad \gamma_k(t) = i\int_0^t \langle k(t')| \frac{d}{dt} |k(t')\rangle \, dt', \tag{D.10}$$

where $\gamma_k(t)$ is real and is the ,so called, Berry phase C.
However, discussing the case of the annealing dynamics we need to keep track of the adiabatic evolution, hence we need to solve the problem out of the fully adiabatic limit.
Let us take into account the term in $\dot{s}$ and let us write Eq.D.6 using $\dot{s} = \frac{1}{\tau}$ (hence, the fully adiabatic limit corresponds to $\tau \to \infty$).

$$\frac{d}{ds}c_k(s) = -c_k \langle k(s)| \frac{d}{ds} |k(s)\rangle - \sum_{n\neq k} c_n(s)\frac{\langle k(s)| \frac{dH}{ds} |n(s)\rangle}{E_n(s) - E_k(s)} e^{-i\tau\int_0^s (E_n(s')-E_k(s'))ds'}. \tag{D.11}$$

Introducing, again, the phase $\gamma_k(s)$ the previous equation can be written as:

$$\frac{d}{ds}c_k(s) = -\sum_{n\neq k} c_n(s)e^{i(\gamma_n(s)-\gamma_k(s))}\frac{\langle k(s)|\,\frac{dH}{ds}\,|n(s)\rangle}{E_n(s)-E_k(s)}e^{-i\tau\int_0^s(E_n(s')-E_k(s'))ds'}. \tag{D.12}$$

We can now integrate the following equation:

$$c_k(0) + \sum_{n\neq k}\int_0^{\tilde{s}} c_k(0)e^{i(\gamma_n(s)-\gamma_k(s))}\frac{\langle k(s)|\,\frac{dH}{ds}\,|n(s)\rangle}{\Delta_{nk}(s)}e^{-i\tau\int_0^s(\Delta_{nk}(s'))ds'} \tag{D.13}$$

where $\Delta_{nk}(s) = E_n(s) - E_k(s)$. To simplify the calculation of the integral we can assume that the initial state is the fundamental state; in this case the only term that remain is the one for n=0 and

$$\begin{aligned} c_k(\tilde{s}) &= \frac{i}{\tau}\Big[A_k(0)e^{i(\gamma_0(0)-\gamma_k(0))} - A_k(\tilde{s})e^{i(\gamma_0(\tilde{s})-\gamma_k(\tilde{s}))}e^{i\tau\int_0^s\Delta_{k0}(s')ds'}\Big] = \\ &= \frac{i}{\tau}A_k(0) - A_k(\tilde{s})e^{i(\gamma_0(\tilde{s})-\gamma_k(\tilde{s}))}e^{i\tau\int_0^s\Delta_{k0}(s')ds'} \end{aligned} \tag{D.14}$$

with $A_k(\tilde{s}) = \frac{\langle k(\tilde{s})|\frac{dH}{ds}|n(\tilde{s})\rangle}{\Delta_{nk}}$. The Berry phases can be neglected for τ large enough; the other phase factor is strongly fluctuating so gives a vanish average. Therefore, a first approximation for the solution can be

$$c_k(s) = \frac{i}{\tau}A_k(0) + o(\frac{1}{\tau^2}). \tag{D.15}$$

Asserting that the evolution of the system must be adiabatic means that the system must remain in the inital state, that is every contribute c_k with $k \neq 0$ must be neglegible. Therefore we have the adiabatic condition:

$$\frac{|A_k(0)|}{\tau} \ll 1 \rightarrow \frac{|\langle k(\tilde{s})|\frac{dH}{ds}\,|n(\tilde{s})\rangle}{\Delta_{nk}^2} \ll 1. \tag{D.16}$$

This condition must be satisfied during the whole evolution and it is evident that the energy gap must never be vanishing.
This means that when a system goes across a quantum state transition the condition cannot be satisfied. To generalize the previos condition starting from every eigenstate of the Hamiltonian H, we can write:

$$\underset{s\in[0,1]}{max}\frac{|\langle k(s)|\,\partial_s H\,|k'(s)\rangle|}{\tau\Delta_{kk'}^2} \ll 1 \rightarrow \frac{h}{\tau\Delta_{min}^2} \ll 1 \tag{D.17}$$

where $h = |\langle k(s)|\,\partial_s H\,|k'(s)\rangle|$.

Bibliography

[1] A. Yu. Kitaev, A. H. Shen, and M. N. Vyalyi. Classical and Quantum Computation. American Mathematical Society, 2001.

[2] P.W. Shor, Algorithm for quantum computation: Discrete log and factoring, FOCS'35, 1994, pp. 124-134.

[3] Michael A. Nielsen , Isaac L. Chuang, Quantum Computation and Quantum Information: 10th Anniversary Edition, Cambridge University Press, New York, NY, 2011

[4] R. Landauer, Irreversibillty and heat generation in the computing process, IBM J. Res. Develop. 3 (1961), 183-191.

[5] S. Kirkpatrick, C. D. Gelatt, and M. P. Vecchi, Optimization by simulated annealing, Science 220.4598 (1983), pp. 671–680.

[6] Farhi, E., J. Goldstone, S. Gutmann, and M. Sipser (2000),Quantum Computation by Adiabatic Evolution, arXiv.org:quant-ph/0001106.

[7] Aharonov, D., W. van Dam, J. Kempe, Z. Landau, S. Lloyd,and O. Regev (2007), SIAM J. Comput. 37 (1), 166.

[8] R. Harris et al. Quantum annealing with manufactured spins, Nature473 (7346 2011), pp. 194–198.

[9] Arnab Das and Bikas K. Chakrabarti, Colloquium: Quantum annealing and analog quantum computation, Rev. Mod. Phys., Vol 80,2008

[10] Zener, C. 1932, Proceedings of the Royal Society of London A: Mathematical, Physical and Engineering Sciences, 137, 696

[11] E. Schrödinger, Die gegenwärtige Situation in der Quantenmechanik, Naturwissenschaften 23, 807 (1935).

[12] A. J. Leggett, J. Phys.: Cond. Mat. 14, R415 (2002).

[13] A. J. Leggett and A. Garg, Quantum mechanics versus macroscopic realism: Is the flux there when nobody looks?, Phys. Rev. Lett. 54, 857 (1985).

[14] C. Emary, N. Lambert, and F. Nori, Rep. Prog. Phys. 77, 016001 (2014).

[15] O. J. E. Maroney, Detectability, Invasiveness and the Quantum Three Box Paradox, arXiv:1207.3114 (2012).

[16] A. Palacios-Laloy, F. Mallet, F. Nguyen, P. Bertet, D. Vion, D. Esteve, and A. N. Korotkov, Experimental violation of a Bell's inequality in time with weak measurement, Nat. Phys. 6, 442 (2010).

[17] M. E. Goggin, M. P. Almeida, M. Barbieri, B. P. Lanyon, J. L. O'Brien, A. G. White, and G. J. Pryde, Violation of the Leggett-Garg inequality with weak measurements of photons, Proc. Natl. Acad. Sci. USA 108, 1256 (2011).

[18] G. C. Knee, S. Simmons, E. M. Gauger, J. J. Morton, H. Riemann, N. V. Abrosimov, P. Becker, H.-J. Pohl, K. M. Itoh, M. L. Thewalt, G. A. D. Briggs, and S. C. Benjamin, Violation of a Leggett-Garg inequality with ideal non-invasive measurements, Nat. Commun. 3, 606 (2012).

[19] J. P. Groen, D. Rist'e, L. Tornberg, J. Cramer, P. C. de Groot, T. Picot, G. Johansson, and L. DiCarlo, Partial-Measurement Backaction and Nonclassical Weak Values in a Superconducting Circuit, Phys. Rev. Lett. 111, 090506 (2013).

[20] V. Athalye, S. S. Roy, and T. S. Mahesh, Investigation of the Leggett-Garg Inequality for Precessing Nuclear Spins, Phys. Rev. Lett. 107, 130402 (2011).

[21] G. Waldherr, P. Neumann, S. F. Huelga, F. Jelezko, and J. Wrachtrup, Violation of a Temporal Bell Inequality for Single Spins in a Diamond Defect Center, Phys. Rev. Lett. 107, 090401 (2011).

[22] T. Fritz, Quantum correlations in the temporal ClauserHorneShimonyHolt (CHSH) scenario, New J. Phys. 12, 083055 (2010).

[23] S. Jansen, M. B. Ruskai, and R. Seiler, Bounds for the adiabatic approximation with applications to quantum computation,Journal of Mathematical Physics 48.10 (2007), p. 102111.

[24] S. F. Huelga, T. W. Marshall, and E. Santos, Proposed test for realist theories using Rydberg atoms coupled to a high-Q resonator, Phys. Rev. A 52, R2497 (1995).

[25] Neill Lambert, Kamanasish Debnath, Anton Frisk Kockum, George C. Knee, William J. Munro, Franco Nori, Leggett-Garg inequality violations with a large ensemble of qubits, Rev. A 94, 012105 (2016).

[26] Experimental violation of the Leggett-Garg inequality in a 3-level system, Hemant Katiyar, Aharon Brodutch, Dawei Lu and Raymond Laflamme, New Journal of Physics, Volume 19, February 2017.

[27] A scheme for efficient quantum computation with linear optics, Knill E., R. Laflamme, and G. J. Milburn,Nature 409, 46–52 (04 January 2001).

[28] Costantino Budroni and Clive Emary, Temporal quantum correlations and Leggett-Garg inequalities in multi-level systems, Phys. Rev. Lett. 113, 050401 (2014).

[29] Pieter Kok, W. J. Munro, Kae Nemoto, T. C. Ralph, Jonathan P. Dowling, and G. J. Milburn, Linear optical quantum computing with photonic qubits, Rev. Mod. Phys. 79, 135 (2007).

[30] Tommaso Zanca, Landau-Zener processes in out-of-equilibrium quantum physics, PhD Thesis at S.I.S.S, International School for Advanced Studies, Physics Area/Condensed Matter.

[31] P. Caldirola, R. Cirelli, and G. M. Prosperi, Introduzione alla fisica teorica, UTET, Milano, 1984

[32] B. R. Holstein, The adiabatic theorem and Berry's Phase, Am. J. Phys., Vol. 57, No 12 (1989)

[33] T. Albash, S. Boixo, D. A. Lidar, and P. Zanardi. Quantum adiabatic Markovian master equations. New Journal of Physics 14.12 (2012), p. 123016.

[34] Quantum nondemolition measurement with a kicked qubit, Andrew N. Jordan and Marcus Büttiker, Phys. Rev. B 71, 125333 (2005).

[35] Andrew N. Jordan and Alexander N. Korotkov, Quibt feedback and control with kicked quantum non demolition measurements: A quantum Bayesian analysis. Phys. Rev. B 74, 085307 (2006).

[36] Andrew N. Jordan, Alexander N. Korotkov and Markus Büttiker, Leggett-Garg Inequality with a Kicked Quantum Pump, Phys. Rev. Lett. 97, 026805 (2006).

[37] Weak Values and the Leggett-Garg inequality in Solid-State Qubits, Nathan S. Williams and Andrew N. Jordan, Phys. Rev. Lett. 100,026804 (2008).

[38] Alexander N. Korotkov, Selective quantum evolution of a qubit state due to continuous measurement, Phys. Rev. B, Volume 63, 115403 (2001).

[39] Tameem Albash and Daniel A. Lidar, Decoherence in adiabatic quantum computation, Phys. Rev. A 91, 062320 (2015).

[40] Adiabatic Quantum Computing, Tameem Albash, Daniel A. Lidar, arXiv preprint arXiv:1611.04471, 2016.

[41] Hardware-efficient variational quantum eigensolver for small molecules and quantum magnets, Kandala, Abhinav, et al., Nature 549.7671 (2017): 242-246.

[42] Assessing the quantumness of a damped two-level system, Friedenberger A., Lutz E.,Physical Review A, 95(2), 022101, (2017).

[43] Pedagogical review of quantum measurement theory with an emphasis on weak measurements, Svensson B. E., Quanta, 2(1), 18-49 (2013).

[44] Leggett-Garg inequality for qubits coupled to thermal environment,Łobejko, Marcin, Jerzy Łuczka, and Jerzy Dajka, Physical Review A 91.4 (2015): 042113.

[45] Optimization using quantum mechanics: quantum annealing through adiabatic evolution, Santoro Giuseppe E. and Erio Tosatti, Journal of Physics A: Mathematical and General 39.36 (2006): R393.